



Universidade do Minho
Escola de Medicina

Diana Alves Afonso

**THE IMPACT OF CHOROID PLEXUS DERIVED FACTORS IN THE
SUBVENTRICULAR ZONE NEURAL PROGENITOR CELLS NICHE**

Dissertação de Mestrado

Mestrado em Ciências da Saúde

Trabalho efetuado sob a orientação do:

Prof. Doutor João Carlos Sousa

e da:

Prof. Doutora Fernanda Marques

Outubro de 2016

DECLARAÇÃO

Nome: Diana Alves Afonso

Endereço eletrónico: dianafonso_17@hotmail.com

Telefone: 936845708

Número do Cartão de Cidadão: 14396751

Título da dissertação:

The impact of choroid plexus derived factors in the subventricular zone neural progenitor cells niche

Orientadores:

Prof. Doutor João Carlos Sousa

Prof. Doutora Fernanda Marques

Ano de conclusão: 2016

Designação do Mestrado:

Ciências da Saúde

É AUTORIZADA A REPRODUÇÃO INTEGRAL DESTA DISSERTAÇÃO APENAS PARA EFEITOS DE INVESTIGAÇÃO, MEDIANTE DECLARAÇÃO ESCRITA DO INTERESSADO, QUE A TAL SE COMPROMETE.

Universidade do Minho, 31 de Outubro de 2016

Assinatura:

Funding

This work has been funded by the Bial Foundation under the grant number 217/12.



Cofinanciado por:



*“O que dá o verdadeiro sentido ao encontro é a busca e que
é preciso andar muito para alcançar o que está perto”*

José Saramago

Aos meus pais e irmão

Agradecimentos

O trabalho realizado ao longo desta tese foi o esforço conjunto de muitas pessoas a quem gostaria de deixar umas pequenas palavras de agradecimento.

Gostaria de começar por agradecer ao João. Obrigada por teres sido meu orientador, pelos conselhos e pelas críticas que me fizeram crescer não só de forma profissional, mas também pessoal. Obrigada também por me ensinares que a melhor maneira de lidar com as adversidades é fazê-lo com um sorriso na cara.

À Fernanda, obrigada pela tua orientação e disponibilidade constantes. Obrigada pelas sugestões, discussões e apoio dado ao longo deste ano que foram essenciais para me guiar neste trajeto. Levo comigo tudo o que me ensinaste e todos os conhecimentos que me transmitiste.

À Ana, porque “Rocky e a amiga” já diz bastante, mas não o suficiente, obrigada por teres sempre tempo para ajudar ou para descontraír. Fico feliz de acabar esta tese sabendo que levo daqui alguém com quem vou poder contar.

À Catarina, mini chefe, obrigada pela ajuda indispensável que foste ao longo desta tese, pelas discussões e pelo que me ensinaste. Obrigada também, pelos momentos de descontração e boa disposição proporcionadas em conjunto com os nossos companheiros de mesa, Marco e Dinis.

Ao António Salgado, ao Fábio e à Bárbara pela ajuda que foram com a cultura de células. À Ana Pereira e ao Luís Jacinto pelo que me ensinaram.

Ao Master Gang, por partilharmos juntos as graças e desgraças deste ano. Um especial obrigado à Joana e à Sara pelo apoio e por perceberem que “sometimes you just need to dance it out”.

Aos meus Nerds bioquímicos, Ângela, Augusto, Carla, Cristina, Daniela, Liliana e Patrícia por provarem que mesmo à distância e com pouca compatibilidade de agenda conseguiram apoiar-me sempre. É muito bom ter amigos como vocês!

À Ariana e à Rita um pedido de desculpas por todas as vezes que troquei a vossa companhia pela de outros mamíferos menos evoluídos filogeneticamente.

Aos meus pais, ao Filipe e à minha família porque sem eles nada disto era possível. Obrigada que mesmo não compreendendo tenham aceitado todos os meus momentos de ausência. Vocês sabem que só o fiz para dar o meu melhor porque foi isso que vocês me ensinaram a fazer.

The impact of choroid plexus derived factors in the subventricular zone neural progenitor cells niche

Abstract

Neurogenesis is the complex process of generating new neurons from their progenitor cells. It occurs both in developmental stages and in adulthood (in the latter case mainly in two brain areas, the subventricular zone (SVZ) and the subgranular zone). Neural stem cells (NSCs) and their progeny are regulated by a proper balance of intrinsic and extrinsic factors. One source of extrinsic factors is the choroid plexuses (CPs), located inside the cerebral ventricles. CPs play active roles in barrier function, secretion and as major regulator of the cerebrospinal fluid (CSF) composition. The SVZ neurogenic niche and the lateral ventricles are in close proximity and NSCs project their apical process into the lateral ventricles being under direct influence of CSF signaling. Thereby, it is plausible to assume that CP, through the modulation of CSF composition, can impact neurogenesis at embryonic and adult SVZ.

Thus, the aim of this master thesis was to provide new insights on how molecules secreted by the CP affect the SVZ neurogenic niche. For this purpose, we selected two candidate proteins to study their hypothetical effect in SVZ cells: amphiregulin (AREG) and insulin growth factor binding protein 2 (IGFBP2), both known to be secreted by the CP towards the CSF. For this we used two *in vitro* techniques, a clonal assay and a differentiation assay, allowing us to study the impact of these proteins in proliferation and differentiation of human neuro progenitor cells. We also evaluated the effects of each protein in the SVZ of adult rats in terms of proliferation, cell cycle index and formation of new immature neurons. Moreover, as an additional aim, we intended to analyze the CP in key milestones of development to determine the temporal changes in the CP transcriptome and then correlate it with developmental changes known to occur in the SVZ cell population. For the transcriptome analysis, we extracted RNA from CP of animals in postnatal day 1, 4, 7, 10 and 60 and sequenced it by RNA-Seq.

Our results indicate that AREG increases cell proliferation associated with a superior number of cells reentering the cell cycle and increases the number of newborn neurons. Regarding the experiments performed with IGFBP2 they indicate that this protein can increase proliferation rate and the number of cells reentering the cell cycle. This is accompanied with an augment in the number of newly born neuroblasts.

In summary, the data presented here provides novel insights for two factors, secreted by the CP, that are playing a role in the modulation of SVZ neurogenic niche.

Impacto de fatores secretados pelo plexo coroide no nicho de células neuroprogenitoras da região subventricular

Resumo

A neurogênese é um processo complexo que leva à formação de novos neurónios a partir de células progenitoras. Este processo acontece tanto em estadios de desenvolvimento embrionário como no estado adulto (neste caso ocorre maioritariamente em duas áreas do cérebro, a região subventricular e a região subgranular). As células neuronais estaminais e a sua descendência são reguladas pelo balanço adequado de fatores intrínsecos e extrínsecos. Uma das fontes de fatores extrínsecos é o plexo coroide, localizado no interior dos ventrículos cerebrais. O plexo coroide tem um papel ativo em funções de barreira e secreção, bem como na modulação da composição do líquido cefalo-raquidiano (LCR). O nicho neurogénico da região subventricular e os ventrículos laterais são estruturas próximas e as células neuronais estaminais projetam o seu processo apical para o ventrículo lateral, estando desta forma sob a influência direta da sinalização do LCR. Assim, é plausível assumir que o plexo coróide, através da modulação da composição do LCR, consegue modular a neurogênese na região subventricular tanto no estado embrionário como no adulto.

Desta forma, nesta tese de mestrado foi objetivo explorar de que forma moléculas secretadas pelo plexo coroide afetam o nicho neurogénico da região subventricular. Para tal, seleccionámos duas proteínas para estudar o seu potencial impacto nas células da região subventricular: a anfiregulina (AREG) e a proteína de ligação 2 ao fator de crescimento insulina (IGFBP2), ambas secretadas pelo plexo coróide para o LCR. Para este estudo aplicamos duas técnicas *in vitro*, um ensaio clonal e um ensaio de diferenciação, que nos permitiram avaliar o efeito das proteínas na proliferação e diferenciação de células neuronais progenitoras humanas. Avaliamos também, *in vivo*, o efeito de cada proteína na região subventricular de ratos adultos em termos de proliferação, índice do ciclo celular e formação de novos neurónios imaturos. Como outro objetivo do trabalho propusemo-nos ainda a analisar as alterações temporais do transcriptoma do plexo coróide em alturas específicas do desenvolvimento, para posteriormente as correlacionar com alterações que ocorrem na população de células da SVZ. Para a análise do transcriptoma, extraímos RNA do CP de animais no dia pós-natal 1, 4, 7, 10 e 60 e sequenciámo-lo por RNA-Seq.

Os nossos resultados indicam que a AREG aumenta a proliferação celular, com um aumento no número de células a reentrarem no ciclo celular, aumentando também o número de novos neurónios imaturos.

Resultados similares foram observados quando testámos os efeitos da IGFBP2, uma vez que observámos um aumento da proliferação acompanhado de um número superior de células a reentrarem no ciclo celular e no número de novos neuroblastos.

Em suma, os dados apresentados aqui demonstram o papel desempenhado por dois fatores secretados pelo plexo coróide na modulação do nicho neurogénico da região subventricular.

Table of contents

Funding.....	iii
Abstract.....	ix
Resumo.....	xi
Table of contents.....	xiii
List of abbreviations.....	xvii
List of figures.....	xix
List of tables.....	xxi
1. Introduction	1
1.1. Neurogenesis.....	3
1.2. Embryonic neural stem cells.....	3
1.2.1. The VZ microenvironment.....	4
1.2.2. Cellular features of RGCs	5
1.2.3. Extrinsic regulation of embryonic VZ-SVZ	6
1.3. Adult neurogenesis.....	8
1.3.1. Adult SVZ	9
1.3.2. Cellular composition and structural organization of the aSVZ	9
Type E cells	10
Type B cells	11
Type C cells	11
Type A cells	12
1.3.3. Extrinsic regulation of the adult SVZ	12
1.4. Functional relevance of neurogenesis	14
1.5. Choroid plexus	14

1.5.1.	Choroid plexus-CSF impact in embryonic neurogenesis	16
1.5.2.	Choroid plexus-CSF impact in adult SVZ	17
2.	Aims.....	19
3.	Materials and methods.....	23
3.1.	Ethics statement	25
3.2.	Animals	25
3.3.	Study the impact of CP-derived proteins in human neural progenitor cells.	25
3.3.1.	Clonal assay	26
3.3.2.	Differentiation assay	26
3.3.3.	Immunocytochemistry for BrdU and β III-Tubulin.....	27
3.4.	Study the impact of CP-derived proteins in the SVZ cell population	27
3.4.1.	Surgeries.....	28
3.4.2.	BrdU and proteins administration.....	28
3.4.3.	BrdU, Ki67 and Doublecortin immunohistochemistry.....	29
3.4.4.	Confocal imaging and quantitative analysis.....	30
3.5.	Transcriptome analysis of CP in different stages of development.....	31
3.5.1.	CP collection	31
3.5.2.	RNA extraction and quality analysis	31
3.5.3.	Library preparation	32
3.5.4.	RNA sequencing	33
3.5.5.	Data analysis and interpretation	33
3.6.	Statistical analysis.....	33
4.	Results	35
4.1.	Impact of AREG in neurogenesis.....	37
4.1.1.	Does AREG impact the growth of hNPCs?.....	37

4.1.1.1.	Clonal assay	37
4.1.1.2.	Differentiation assay.....	38
4.1.2.	Does AREG have an effect in the adult rat SVZ?	40
4.1.2.1.	Analysis of cell proliferation rates along the SVZ.....	40
4.1.2.2.	Analysis of cell cycle index along the SVZ.....	44
4.1.2.3.	Analysis of new neuroblasts in the SVZ	45
4.2.	Impact of IGFBP2 in neurogenesis.....	47
4.2.1.	IGFBP2 can impact growth of hNPCs?	47
4.2.1.1.	Clonal assay	47
4.2.1.2.	Differentiation assay.....	48
4.2.2.	IGFBP2 impact in SVZ neurogenesis	50
4.2.2.1.	Effects of IGFBP2 in cell proliferation in the SVZ.....	50
4.2.2.2.	Effects of IGFBP2 in cell cycle index	54
4.2.2.3.	Effects of IGFBP2 in the number of newly formed neuroblasts at the SVZ	55
4.3.	Analysis of CPs transcriptome in key developmental stages.....	57
4.3.1.	RNA quality control	57
4.3.2.	cDNA library quality control.....	58
4.3.3.	Quality control of RNA seq data: MultiQC report.....	59
4.3.3.1.	Per base sequence quality.....	59
4.3.3.2.	Per sequence quality score.....	60
4.3.3.3.	Per base N content	61
5.	Discussion	63
5.1.	Amphiregulin impact in the neural stem cells modulation.....	66
5.1.1.	AREG enhances proliferation.....	66
5.1.2.	AREG induces cell cycle reentry in proliferating cells of the SVZ	68

5.1.3.	AREG increase the number of immature neurons	68
5.2.	IGFBP2 impact in neural stem cells modulation	69
5.2.1.	IGFBP2 enhances cells proliferation	70
5.2.2.	IGFBP2 alters cell cycle index at the SVZ.....	71
5.2.3.	IGFBP2 increases the number of newborn neurons	71
5.3.	Choroid plexus transcriptome analysis in key milestones of development	72
6.	Conclusion and future perspectives	73
7.	References	79
8.	Supplementary information	91

List of abbreviations

A

aCSF- Artificial cerebrospinal fluid

AREG- Amphiregulin

Ascl1- achaete-scute complex homolog 1

aSVZ- Adult subventricular zone

B

BDNF- Brain derived neurotrophic factor

bHLH- Basic helix loop helix

BLBP- Brain lipid binding protein

BMPs- Bone morphogenic proteins

BrdU- 5-bromo-2'-deoxyuridine

C

cDNA- Complementary deoxyribonucleic acid

CNS- Central nervous system

CPs- Choroid plexuses

CSF- Cerebrospinal fluid

D

DAPI- 4',6-diamidino-2-phenylindole

DCX- Doublecortin

Dlx2- Distal-less homeobox

E

EGF- Epidermal growth factor

EGFR- Epidermal growth factor receptor

ERK- Extracellular signal-regulated kinases

E_x- Embryonic day x

F

FACS- Fluorescence-activated cell sorting

FBS- Foetal bovine serum

FGF- Fibroblast growth factor

FITC- Fluorescein isothiocyanate

G

GDNF- Glial cell derived neurotrophic factor

GFAP- Glial fibrillary acidic protein

GLAST- Glutamate aspartate transport

H

HCl- Hydrochlorid acid

I

ICV- Intracerebroventricular injection

IGFs- Insulin growth factors

IGFBP2- Insulin growth factor binding protein 2

IGFR- Insulin growth factor receptor

IL- Interleukin

IPCs- Intermediate progenitor cells

J

JNK- c-Jun N-terminal kinases

L

LVs- Lateral ventricles

M

MAP- Microtubule associated protein

MAPK- Mitogen activated protein kinase

N

NECs- Neuroepithelial cells

Ngn- Neurogenin

NICD- Notch intracellular domain

NPC- Neural progenitor cells

NSCs- Neural stem cells

NT- Neurotrophin

O

OBs- Olfactory bulbs

P

PBS- Phosphate buffered saline

PBS-T- Phosphate buffered saline-Triton

PCR- Polymerase chain reaction

PEDF- Pigment epithelium derived factor

PFA- Paraformaldehyde

Pi3K- Phosphoinositide 3-kinase

Prom1- Prominin 1

PSA-NCAM- polysialylated neural cell adhesion molecule

P_x- Postnatal day

Q

qNSCs- Quiescent neural stem cells

R

RGCs- Radial glial cells

RMS- Rostral migratory stream

RNA- Ribonucleic acid

RQI- RNA quality index

RT- Room temperature

RT-PCR- Real time- polymerase chain reaction

S

SEM- Standard error of the mean

SDF- Stromal derived factor

Shh- Sonic hedgehog

SVZ- Subventricular zone

T

TAPs- Transit amplifying cells

TGF- Transforming growth factor

TNF- Tumor necrosis factor

V

VZ- Ventricular zone

List of figures

Figure 1: Representation of the cellular components of the embryonic neurogenic niche.....	4
Figure 2: Embryonic origin of neural stem cells of adult subventricular zone.....	9
Figure 3: The structural and cellular organization of the adult subventricular zone.....	10
Figure 4: Structural organization of the choroid plexus.....	15
Figure 5: Schematic representation of clonal assay.....	26
Figure 6: Schematic representation of differentiation assay.....	26
Figure 7: Schematic representation of protein administration procedure and postmortem analysis....	29
Figure 8: Division of the subventricular zone along the dorsal-ventral axes.....	31
Figure 9: Schematic representation of total RNA extraction protocol using SPLIT RNA Extraction Kit..	32
Figure 10: Clonal assay in hNPCs exposed to AREG.....	37
Figure 11: Differentiation assay in hNPCs exposed to AREG.....	39
Figure 12: BrdU ⁺ cells in the rostral migratory stream (RMS), dorsolateral and ventral areas of the subventricular zone of animals injected with 25, 100 or 200ng/mL of AREG.....	41
Figure 13: Ki67 ⁺ cells of animals injected with 200ng/mL of AREG in the rostral migratory stream (RMS), dorsolateral and ventral areas of the subventricular zone.....	43
Figure 14: Cell cycle index analysis of animals injected with 200ng/mL of AREG in the rostral migratory stream (RMS), dorsolateral and ventral areas of the subventricular zone.....	44
Figure 15: DCX ⁺ BrdU ⁺ cells in the rostral migratory stream (RMS), dorsolateral and ventral areas of the subventricular zone of animals injected with 25, 100 or 200ng/mL of AREG.....	46
Figure 16: Clonal assay in hNPCs exposed to IGFBP2.....	48
Figure 17: Differentiation assay in hNPCs exposed to IGFBP2.....	49

Figure 18: BrdU ⁺ cells in the rostral migratory stream (RMS), dorsolateral and ventral areas of the subventricular zone of animals injected with 25, 100 or 200 ng/mL of IGFBP2.	51
Figure 19: Ki67 ⁺ cells of animals injected with 200ng/mL of IGFBP2 in the rostral migratory stream (RMS), dorsolateral and ventral areas of the subventricular zone.....	53
Figure 20: Cell cycle index of animals injected with 200ng/mL of IGFBP2 in rostral migratory stream (RMS), dorsolateral and ventral areas of the subventricular zone.....	54
Figure 21: DCX ⁺ BrdU ⁺ cells in the rostral migratory stream (RMS), dorsolateral and ventral areas of the subventricular zone of animals injected with 25, 100 or 200ng/mL of IGFBP2.	56
Figure 22: Summary of the quality control of the multiplexed cDNA library.....	60
Figure 23: Per base sequence quality. Provides an overview of the quality values of all sequenced bases in each sample file.	59
Figure 24: Per sequence quality score. Plot of the average quality of a read according to the distribution of this average quality.	61
Figure 25: Per base N content. This graph represents the percentage of base calls at each position for which an N was identified.	62
Figure 26: Representation of hypothetical temporal alterations of the CPs transcriptome and its effects in the SVZ cellular dynamics.	77

List of tables

Table 1: Signaling pathways involved in the modulation of the aSVZ.....	13
Table 2: Factors involved in the modulation of the aSVZ.	13
Table 3: Summary of the CP transcriptome analysis performed by array or high throughput sequencing.	16
Table 4: List of primary and secondary antibodies used for the immunocytochemistry	27
Table 5: List of primary and secondary antibodies used for the immunohistochemistry.	30
Table 6: Statistical analysis of the clonal assay with AREG.	38
Table 7: Statistical analysis of the differentiation assay of cells exposed to AREG.....	40
Table 8: Statistical analysis of BrdU ⁺ cells in the subventricular zone of animals injected with AREG... ..	42
Table 9: Statistical analysis of Ki67 ⁺ cells in the subventricular zone areas of animals injected with AREG.	44
Table 10: Statistical analysis of the cell cycle index in the subventricular zone of animals injected with AREG.	45
Table 11: Satatistical analysis of DCX ⁺ BrdU ⁺ cells in the subventricular zone of animals injected with AREG.	47
Table 12: Statistical analysis of the clonal assay with IGFBP2.	48
Table 13: Statistical analysis of the differentiation assay with IGFBP2.	50
Table 14: Statistical analysis of BrdU ⁺ cells in the subventricular zone of animals injected with IGFBP2.	52
Table 15: Statistical analysis of Ki67 ⁺ cells in the subventricular zone of animals injected with IGFBP2.	54
Table 16: Statistical analysis of cell cycle index in the subventricular zone of animals injected with IGFBP2.	55

Table 17: Statistical analysis of DCX+BrdU+ cells in the subventricular zone of animals injected with IGFBP2.	57
Table 18: Concentration and quality of the extracted RNA assessed with the RNA StdSenses Analysis Kit.	58
Table S 1: Post hoc test for the statistical analysis of clonal assay with AREG.....	93
Table S 2: Post hoc test for the statistical analysis of differentiation assay with AREG.	94
Table S 3: Post hoc tests for the Statistical analysis of BrdU+ cells in the subventricular zone of animals injected with AREG.	95
Table S 4: Post hoc tests for the Statistical analysis of DCX+BrdU+ cells in the subventricular zone of animals injected with AREG.	96
Table S 5: Post hoc test for the statistical analysis of clonal assay with IGFBP2.....	97
Table S 6: Post hoc test for the statistical analysis of differentiation assay with IGFBP2.	98
Table S 7: Post hoc tests for the Statistical analysis of BrdU+ cells in the subventricular zone of animals injected with IGFBP2.	99
Table S 8: Post hoc tests for the Statistical analysis of DCX+BrdU+ cells in the subventricular zone of animals injected with IGFBP2.	100

1. Introduction

1.1. Neurogenesis

Neurogenesis encompasses the set of events that leads to the formation of new neurons from their stem or progenitor cells. This process includes cell division, production of migratory precursors, differentiation, and lastly, integration of functional neurons into existing circuits. It occurs massively during embryonic development to construct the nervous system and it persists throughout adulthood in restricted areas. For over a century it was thought that the capacity to generate new neurons was restricted to embryonic development, and that no new neurons were added to the adult mammalian brain¹. Even though, some suggestions regarding the existence of dividing cells in the postnatal brain were raised². Nevertheless, the first evidence of adult neurogenesis was only published in 1958 reporting the existence of mitosis in the lateral wall of brain ventricles of young mice³. After that many evidences of adult neurogenesis on the adult mammalian brain were communicated^{4,5}. Currently, the major efforts on this field relay on sorting the molecular mechanisms involved in the formation and integration of new neurons, and in unraveling the heterogeneity of the neurogenic niches. Due to the scope of this thesis we will next make a summary of the major aspects of both embryonic and adult neurogenesis at the lateral walls of the brain ventricles. In the next sections we will give an overview on the neurogenesis in the embryonic and in the adult brain

1.2. Embryonic neural stem cells

The embryonic central nervous system (CNS) contains two distinct proliferative areas where the stem/progenitor cells are retained⁶. The first to be generated is the ventricular zone (VZ); it is constituted of neuroepithelial cells (NECs) with stem cell properties that appear approximately at embryonic day 8 (E8) and from which all the mature cells of the embryonic and adult CNS will be generated⁶. After a period of symmetric division of the NECs, a second proliferative area appears, the subventricular zone (SVZ), generated by the asymmetric division of the progenitor cells from the VZ that migrate basally⁷. The cells that compose the embryonic SVZ are known as intermediate progenitors (IPCs) or basal progenitors and produce neurons or glia by symmetric division⁷ (Figure 1).

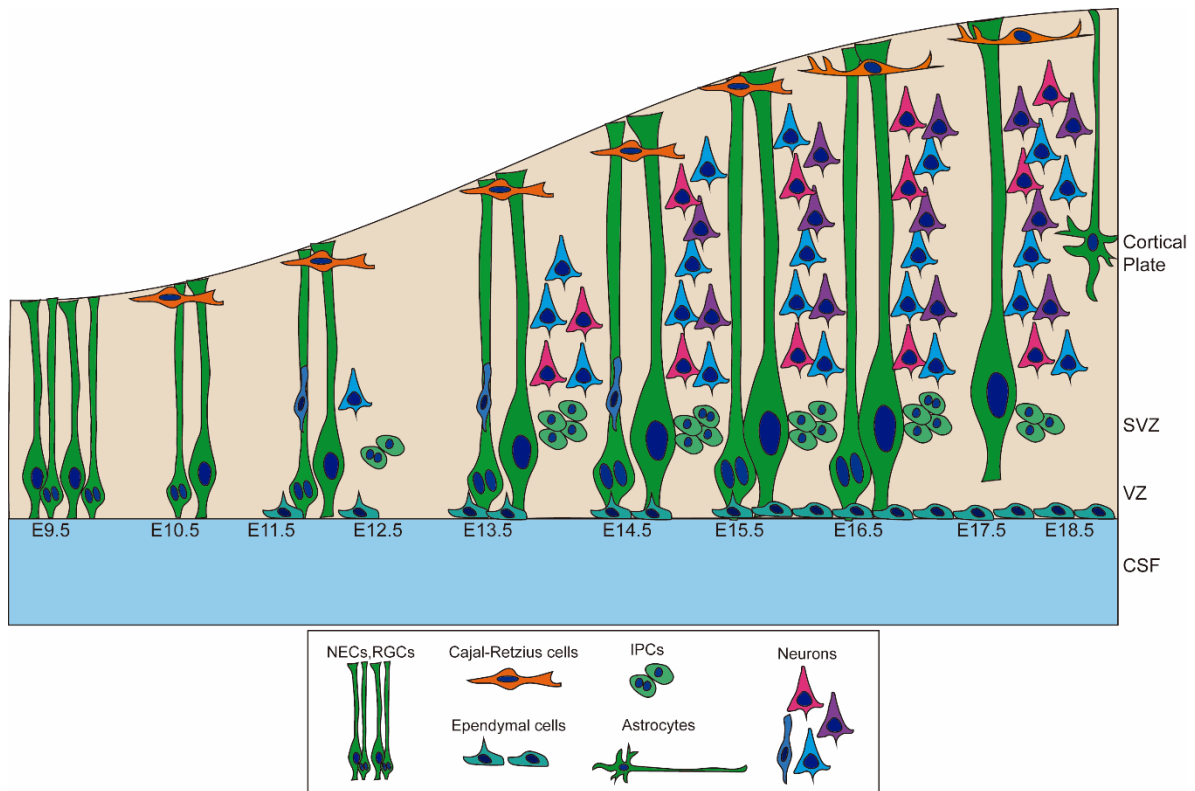


Figure 1: Representation of the cellular components of the embryonic neurogenic niche. Appearance and ontogenic maturation of the embryonic niche components derived from neuroepithelial cells. SVZ, subventricular zone; VZ, ventricular zone; NECs, neuroepithelial cells; RGCs, radial glia cells; IPCs, intermedia progenitor cells; CSF, cerebrospinal fluid.

The VZ microenvironment

When neural induction happens, the walls of the neural tube are composed of a monolayer of NECs. These cells are multipotent, radially elongated and present epithelial features: apical-basal polarity and lateral connections through tight and adherent junctions. During cell cycle, the nuclei of the NECs migrates up and down through the apical-basal axis, being located at the apical side in mitosis and basally during S phase. This phenomenon is called interkinetic nuclear migration and gives a pseudostratified appearance to the neuroepithelium layer⁸.

The NECs are highly proliferative at the anterior end of the central canal, where they divide fast and symmetrically to expand the precursor structure of the future brain. Due to this foundational process, the lumen of the developing brain starts to be surrounded by several layers, and the progenitor cells are located in the innermost apical layer, the VZ⁸.

At the onset of neurogenesis, between E10-E12 in the mice, NECs transform into radial glial cells (RGCs)⁹. This transition from NECs to RGCs is characterized by the downregulation of Golgi derived apical

trafficking and loss of tight junctions. Moreover, the cells initiate the expression of astroglial markers (glutamate aspartate transporter [GLAST], glial fibrillary acidic protein [GFAP], and brain lipid binding protein [BLBP])¹⁰. The mechanisms involved in this transition are not fully elucidated, however some candidate molecules involved in the process were identified. For instance, it was reported that Hes1 and Hes5 deficient mice present normal NECs at E8 but impaired RGCs differentiation at E9.5¹¹. Another study, demonstrated a transient expression of fibroblast growth factor (*Fgf10*) by NECs coincident with this transition period, where targeted deletion of *Fgf10* causes a delay in the transition¹².

1.2.2. Cellular features of RGCs

As mentioned above, RGCs are characterized by the expression of astroglial markers. However, these cells also share epithelial features with the NECs, such as the expression of the intermediate filament protein nestin, interkinetic nuclear migration and the presence of adherent junctions.

Adherent junctions consist of cadherins and catenins that connect the intracellular network of actin and are present at basal to apical and at the subapical membrane of RGCs, mediating cell-cell adhesion¹⁰. Newborn neurogenic cells downregulate cadherins, a process mediated by proneural genes, allowing cells to withdraw their apical endfoot and migrate away from the ventricle. Abscission of the apical endfoot is characterized not only by the downregulation of cadherins but also by the loss of ciliary proteins and cell cycle exit, which in turn leads to cell differentiation¹⁰.

The apical plasma membrane of NECs and RGCs faces the ventricular surface of the developing brain¹⁰. As described with further detail in section 1.5, brain ventricles are filled with cerebrospinal fluid (CSF) that contains signaling molecules produced by the choroid plexus (CP)¹³. These molecules include, FGFs, insulin growth factors (IGFs), retinoic acid, bone morphogenic proteins (BMPs), sonic hedgehog (Shh) and Wnt, molecules that have already been described as playing a role in brain development, and its effects are likely to be mediated by receptors at the apical membrane¹⁴⁻¹⁶. Interestingly, both NECs and RGCs extend their primary cilium into the brain ventricles, receiving signals from the molecules present at the CSF^{14,15,17}. The primary cilium also plays an essential role in the maintenance of NECs and RGCs polarity¹⁸.

On the other hand, the basal process of RGCs, besides serving as a scaffold for migrating newborn neurons, plays an important role in the maintenance of RGCs proliferation, since active transportation and translation of cyclin D2, a regulator of G₁-S phase, induces asymmetric division of RGCs^{10,19}.

One other particular feature of both NECs and RGCs is their complex mitotic behavior, the interkinetic nuclear migration²⁰. It is hypothesized that this process regulates neurogenesis exposing RGCs nucleus to signals present along the apical-basal gradient, specifically to Notch, that can regulate proliferation^{21,22} or block cell differentiation^{23,24}.

In vitro and *in vivo* data suggest that RGCs divide asymmetrically to produce another RGCs and a neuron or IPCs^{25,26}. This IPCs accumulate above the VZ producing a second germinal zone, the SVZ⁸. The expansion of the SVZ, constituted of IPCs and RGCs, is thought to cause the majority of cerebral cortex expansion. In accordance, a Cre/loxP fate mapping study using the promoter of BLBP, a marker of RGCs, revealed that all neuronal populations of the CNS derived from BLBP expressing progenitor cells²⁷. Moreover, the transition of RGCs to neurogenic state is spatiotemporal dynamic, since RGCs from the ganglionic eminence achieve earlier their neurogenic stage when compared with their counterparts in neocortex²⁷. This dynamic is tightly regulated by the combination of intrinsic and extrinsic factors that provide unique signaling to the different regions of the VZ-SVZ. Next we will summarize the impact of different factors on the embryonic VZ-SVZ.

1.2.3. Extrinsic regulation of embryonic VZ-SVZ

The neurogenic niche is the term used to describe the highly complex environment that supports NECs and RGCs and their progeny. This is a dynamic microenvironment composed of several cells and factors that together provide signals that determine the fate of these cells. This microenvironment guides the neurogenic niche through its structural and functional changes observed from embryonic development into adulthood^{8,10}.

During embryonic development the progenitor cells receive diffusible signals from different sources, including ventricular fluid, blood vessels, meninges and components that mediate cell to cell and cell-extracellular matrix interactions (ECM). These molecules form gradients within the brain and can signal far from their source. As a result, progenitor cells located in different positions of the CNS experience a unique combination of signals that might induce a region specific behavior. Growth factors are particular examples of these molecules, and represent a group of major key factors involved in the regulation of stem cells proliferation and differentiation²⁰. We will next summarize existing evidence of the role of the most relevant growth factors in VZ-SVZ stem cells modulation during embryonic development.

BMPs, members of the transforming growth factor- β (TGF- β) family, are implicated in neuronal development given that it was shown that BMP is present at the VZ and triggers neuronal differentiation. Specifically, BMP4 treatment increased the number of microtubule associated protein 2 (MAP-2) and TUJ-1 positive cells within the VZ²⁸. Another report, shows that BMP7 regulates cortical neurogenesis through two independent sources, i.e. the meninges and the CP²⁹. In particular, it was hypothesized that the secretion of BMP7 by the CP will impact proliferation and neurogenin 2 expression (*Ngn2*, a proneural gene)²⁹.

Fgf2 is expressed by microglia in the embryonic brain and plays a crucial role in the regulation of cortical development⁸. *Fgf2* and FGF receptors (FGFR) are transiently expressed along the pseudostratified epithelium during early neurogenesis³⁰. 5-bromo-2'-deoxyuridine (BrdU) studies in embryos that received a FGF2 injection in brain ventricles suggests that this growth factor increases the number of proliferating cells without affecting its cell cycle³¹. Moreover, mice that lost function of all FGFR at E12.5 lead to a faster production of neurons causing a severe loss of RGCs and early end of neurogenesis³⁰. Associated with FGFR loss of function it was observed a decreased in the production of NICD (active Notch), *Notch1* mRNA and the Notch downstream gene *Hes1*, together with a upregulation of *Ngn2*, *Dll1* and *Mash1*³⁰. These results indicate cooperation between FGFR and Notch signaling to regulate RGCs self-renewal.

The Notch pathway is essential in the modulation of both embryonic and adult neurogenesis. Activation of this signaling pathway has the ability to induce self-renewal by inhibiting neuronal differentiation through lateral inhibition, and by promoting symmetric division to promote expansion of the stem cells pool^{32,33}.

Insulin and insulin like peptides are involved in the regulation of growth and maintenance of stem cells in several organisms, including *Drosophila melanogaster*, *Caenorhaditis elegans* and *Danio Rerio*³⁴. Similar to the findings on invertebrates and zebrafish, IGF signaling is involved in the modulation of mammalian stem cells. IGF1 regulates cell proliferation at the VZ during cortical neurogenesis by the modulation of the cell cycle length, decreasing specifically the length of G₁ phase³⁵. Another member of the insulin family involved in the modulation of the embryonic VZ-SVZ is IGF2. This growth factor is expressed by the CP and secreted into the CSF in an age dependent manner, presenting different expression levels in rat CSF at the following ages: E13, E15, E17, E19, E21, P0, adult. It binds to the IGF1 receptor (IGF1R) present at the apical domain of neural stem cells (NSCs) promoting progenitor cells¹⁵.

The Wnt signaling pathway plays a critical role in the regulation of proliferation and differentiation in the developing brain. During early neurogenesis, Wnt ligands promote symmetric division of RGCs causing a

delay in IPCs formation. Conversely, at later neurogenic stages, Wnt promotes IPCs formation and differentiation through the upregulation of its downstream target N-myc^{36,37}.

Other members of the complex microenvironment that modulates the fate of RGCs and their progeny are Shh ligands. A crosstalk between Shh and Notch signaling has been shown to promote symmetric division of RGCs to extend their pool³⁸. Moreover, Shh signaling has been shown to promote RGCs proliferation and expansion of GABAergic neurons³⁹.

Despite the fact that we focused our attention on summarizing the modulation of the embryonic SVZ by extrinsic factors, there are several intrinsic factors that also control their behavior. These intrinsic factors comprehend transcription factors and cell cycle components that modulate processes as epigenetic modifications and post translational modifications¹⁰. Given the scope of this thesis, we will not refer here to the specific embryonic intrinsic factors regulating neurogenesis, or their role in this process.

1.3. Adult neurogenesis

Active neurogenesis in the adult mammalian brain occurs at a much slower rate when compared to embryonic neurogenesis and it is constrained to specific brain areas: the subgranular zone of the dentate gyrus, which produces neurons to the granular zone of the hippocampus, and the adult SVZ (aSVZ)⁴⁰. The aSVZ, considered the major neurogenic niche in the adult mammalian brain, underlies the lateral walls of the lateral ventricles and, under physiological conditions, it produces neurons that integrate existing circuits of the olfactory bulbs (OBs). It is suggested that the NSCs of the aSVZ are derived from RGCs. A Cre-lox technique that specifically and permanently labeled RGCs revealed that at postnatal day 0 (P0), the aSVZ is mainly composed of RGCs and few immature neurons, however the number of RGCs at this region decreases with time and it correlated with an increase in GFAP⁺ cells (P6). Moreover, a technique that specifically labels RGCs progeny revealed that infected RGCs produce GFAP⁺ aSVZ astrocytes, indicating that NSCs of the aSVZ derive from RGCs⁴¹. What mediates this embryonic to adult change in the cell phenotype of NSCs at the aSVZ is unknown. In the context of the present thesis, in the next sections, we will only explore the aSVZ niche.

1.3.1. Adult SVZ

A large population of multipotent cells with self-renewing capacities is present in the aSVZ lining the CSF-filled ventricles of the adult mammalian brain. This region is typically seen as a thin layer of proliferative cells separated of the lateral ventricles by a layer of ependymal cells. However, NSCs are not exclusively restricted to the lateral ventricles, being also found in the rostral migratory stream (RMS)⁴², subcallosal zone⁴³ and in the ventral third ventricle⁴⁴.

The embryonic origin of NSCs from the aSVZ, determined by a Cre-lox model, revealed that these cells are derived from telencephalic neuroepithelium, specifically from the medial ganglionic eminence, lateral ganglionic eminence, and cerebral cortex⁴⁵. Moreover, depending on their embryonic origin, NSCs will have different positions in the aSVZ, specifically NSCs derived from the cortex and lateral ganglionic eminence settle in the ventral aSVZ, while stem cells derived from the medial ganglionic eminence are located in the dorsolateral aSVZ⁴⁵ (Figure 2).

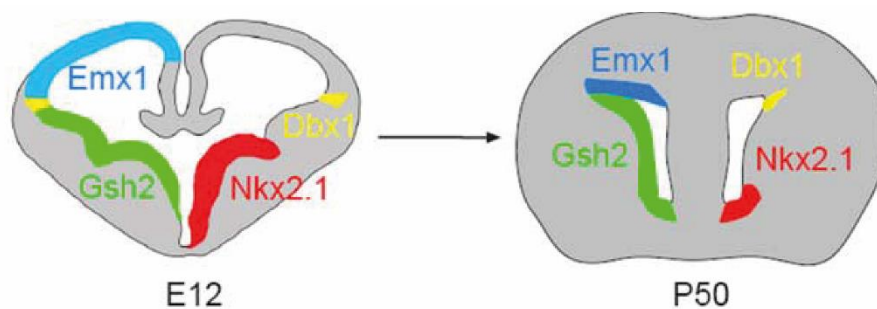


Figure 2: Embryonic origin of neural stem cells of adult subventricular zone. Contributions of the different regions of the embryonic ventricular zone to the adult subventricular zone. Emx1-Cre was used to label cerebral cortex, Gsh2-Cre to label lateral and medial ganglionic eminence, Nkx2.1-Cre used to label medial ganglionic eminence and Dbx1-Cre to label corticostriatal sulcus. Adapted from Young *et al.* 2007⁴⁵.

1.3.2. Cellular composition and structural organization of the aSVZ

The aSVZ is composed mainly of three cell types (type A, B and C) that are differently distributed into three layers, below an ependymal cell layer (type E cells)⁴⁰ (Figure 3). Quiescent type B cells (that may be further sub-divided into type B1 and type B2 cells), or progenitor cells, when activated, divide asymmetrically, giving rise to another type B cell and a type C or transit-amplifying cell (TAPs). These TAPs cells undergo rapid divisions producing neuroblasts (type A cells) or glia (astrocytes or

oligodendrocytes). Neuroblasts are immature neurons that migrate along the RMS through chains of astrocytes and vasculature towards the OBs. We will next describe with further detail these cell types.

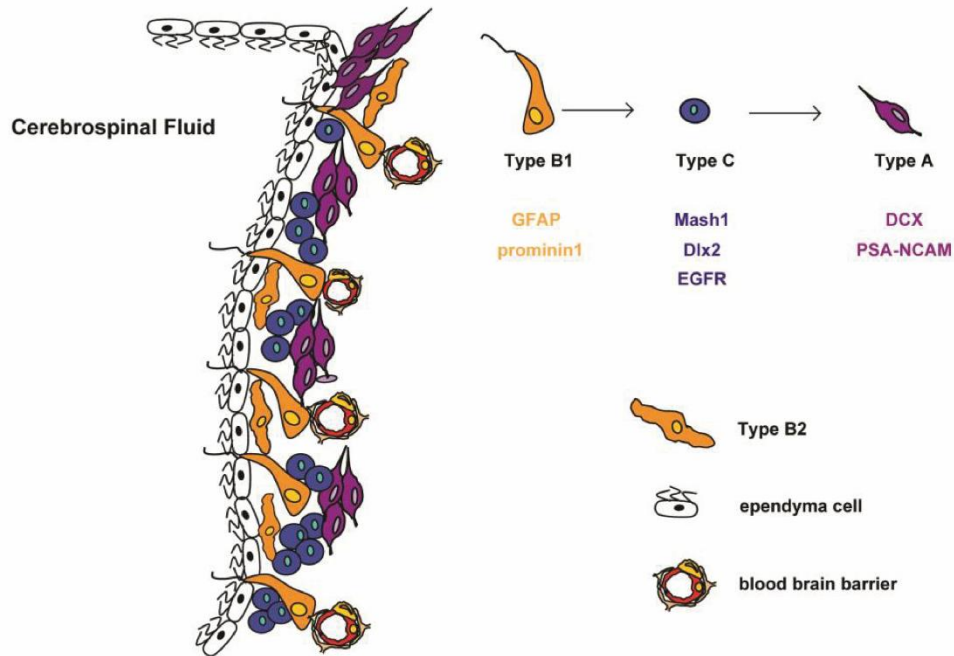


Figure 3: The structural and cellular organization of the adult subventricular zone. The adult subventricular zone, located below an ependymal layer is composed of mainly three cell types (Type B, C and A). Type B or progenitor cells, that project their apical process into the brain ventricles, give rise to type C cells or transit amplifying cells, that express molecular markers such as Mash1 (a basic helix loop helix transcription factor) or Dlx2. These C cells divide into neuroblasts (type A) that express proteins associated with neuronal migration and adhesion (DCX and PSA-NCAM). The adult subventricular zone also contains type B2 cells and blood vessels from the blood brain barrier. Adapted from Falcão et al. 2012¹⁶.

Type E cells

A monolayer composed of ependymal cells separates the aSVZ cells from the lateral ventricles. Two types of ependymal cells are present at this monolayer, E1 and E2 cells. E1 cells are multiciliate, and are organized in a pinwheel like structure around the apical process of type B1 cells. E2 cells are biciliated cells characterized by extraordinary complex bodies and constitute less than 5% of cells on the ventricular surface⁴⁶. These two cells, located within all regions of the ventricle, show no evidence of proliferation⁴⁶ and are commonly marked with the S100 β marker⁴⁷.

Type B cells

In 1997 Doetsch and colleagues first identified GFAP expressing-astrocytic cells as the stem cells of aSVZ⁴⁸. Entitled type B cells, these can be divided into two sub-types: B1 cells, which are located in close contact to the ependymal layer and considered to be the NSCs of the adult brain; and B2 cells, characterized by a highly branched morphology which are located deeper in the brain parenchyma⁴⁸. As mentioned above (section 1.3), type B1 cells are thought to be the direct successors of RGCs⁴¹, presenting a radial morphology⁴⁹ and the expression of the astrocytic markers GFAP, GLAST and BLBP⁵⁰. Moreover, B1 cells express *Id1* transcription factor, which is responsible for the self-renewing capacity of this cell type⁵¹. The main features that recognize B1 cells as the NSCs are based on the following evidences: i) they are structurally similar to their ancestors, that also extend an apical process into the brain ventricle; ii) they express prominin1 (Prom1 or CD133) and nestin, which are markers of NSCs; and iii) they are multipotent cells giving rise to neurons and glial cells. aSVZ NSCs extend their apical processes through the center of the pinwheel structures formed by the ependymal cells and directly contact with the CSF present in the lateral ventricles being exposed to signals present in this fluid^{46,52,53}. On the other hand, their basal processes extend into the perivascular niche, which also represents an important source of signals to the aSVZ⁸. These cells exist as quiescent NSCs or in an activated state NSCs. A recent study revealed that quiescent NSCs are largely dormant, rarely form colonies *in vitro* and do not express nestin. However, when activated, B1 cells upregulate nestin and epidermal growth factor receptor (EGFR) expression, becoming highly proliferative⁵⁴. Moreover, this study revealed that quiescent NSCs can be prospectively isolated as GFAP⁺CD133⁺ and activated NSCs can be isolated as GFAP⁺CD133⁺EGFR⁺⁵⁴.

Type C cells

Type C cells, or TAPs, present throughout the aSVZ and characterized by their abundant free ribosomes, deeply invaginated nucleus and absence of intermediate filaments, were first identified by electron microscopy⁴⁸. These cells express distal-less homeobox 2 (*Dlx2*)⁵⁵, implicated in the development of GABAergic neurons and oligodendrocytes during embryonic development. They also express achaete-scute complex homolog 1 (*Asc1* or *Mash1*), a basic helix loop helix (bHLH) transcription factor described as essential for neuronal differentiation during embryogenesis⁴⁰. These cells are the most frequently labeled after injection of a proliferation marker, such as BrdU, constituting the largest pool of dividing cells in adult SVZ. Type C cells express EGFR⁵⁶. Injection of exogenous EGF into the brain ventricle

significantly increased cell proliferation at the SVZ associated with an increase in the number of newborn astrocytes at the OB and reduction of neurogenesis⁵⁷, indicating multipotency of C cells that can be prompted by EGF. *In vitro* studies suggest that TAPs give rise to multipotent neurospheres when stimulated with EGF, supporting the idea that these cells can be reprogrammed in response to EGF⁵⁵.

Type A cells

Derived from the TAP cells, neuroblasts or type A cells are the immature neurons that express doublecortin (DCX) and polysialylated neural cell adhesion molecule (PSA-NCAM), two proteins associated with neuronal migration⁵⁶. Neuroblasts are not homogeneous and express a variety of different markers. The pattern of markers expressed by these cells is associated with their site of origin at the SVZ and will determine the type of interneurons that will integrate different layers of the OB⁵⁸. During migration through the RMS, type A cells continue to divide and initiate the maturation process⁵⁹. When approaching OBs the proliferation rate of these cells significantly decreases and the cell cycle length is enhanced⁵⁹.

1.3.3. Extrinsic regulation of the adult SVZ

The stability of the aSVZ cell population is maintained due to the tight balance of intrinsic and extrinsic factors that control NSCs proliferation and self-renewal or differentiation into neuroblasts or glial cells. Next, we will briefly summarize the regulation of the aSVZ by extrinsic factors. Although not being the scope of this thesis, intrinsic factors also play a relevant role in the modulation of this neurogenic niche⁴⁰. Several extrinsic factors that regulate SVZ population comprehend growth and trophic factors, hormones, cytokines, morphogens and neurotransmitters. FGF2 and EGF are the principal mitogens used in the *in vitro* culture of SVZ NSCs. Receptors for these growth factors are expressed in the aSVZ and mice with the ablation of the gene for Fgf2 or for TGF- α (an EGF receptor ligand), present impaired neurogenesis in the aSVZ⁴⁰. Ciliary neurotrophic factor, is the example of another factor involved in the modulation of the aSVZ, given that its ventricular infusion increases proliferation. Other factors have been involved in the regulation of aSVZ. Brain derived neurotrophic factor (BDNF), is implicated in aSVZ proliferation and neurogenesis at the OBs. Several other growth factors and signaling pathways are described as participating in the modulation of neurogenesis and are summarized in table 1 and 2^{40,60}. These signaling molecules have their origin in diverse sources, mostly from neurons, NSCs, ependymal cells, blood vessels, microglia and the CP-CSF system⁶⁰. Furthermore, neurotransmitters released by neurons are key

members of the SVZ niche, with different neurotransmitters playing different roles⁶⁰. For instance, serotonin induces NSCs proliferation while dopamine can either increase or decrease proliferation. A key component of the microenvironment that surrounds the neurogenic niche is the CP-CSF system¹⁶. Further information on this system, and its influence in the SVZ will be provided below (Section 1.5).

Table 1: Signaling pathways involved in the modulation of the aSVZ.

Signaling pathways	Role
Shh	Maintenance of B1 cells; Regulator of aSVZ regional identity Shh
Wnt	Act on different aSVZ lineage throughout canonical and noncanonical pathways
Notch	Control NSCs maintenance and asymmetric division

Table 2: Factors involved in the modulation of the aSVZ.

Source	Factor	Effect
Ependymal cells	Noggin (BMP antagonist)	Inhibits or promotes neurogenesis
	Pigment epithelium derived factor (PEDF)	Promotes self-renewal of NSCs
Fractones (ECM extensions)	FGF2	Promotes proliferation of NSCs
	BMP4, BMP7	Inhibit neurogenesis
Microglia	NT3, GDNF, FGF2, BDNF and cytokines	Enhance neurogenesis
	IL-1 α , IL-1 β , IL-1 and TNF- α , β	Decrease differentiation and proliferation of NSCs
Vascular endothelial cells	PEDF	NSCs self-renewal
	NT3	NSCs maintenance
	SDF1	Neuronal migration
Choroid plexus-CSF	SLIT1/2	Neuronal migration
	Amphiregulin	Mitogen
	IGF2	Mitogen, NSCs self-renewal
	CSF flow	Neuronal migration
Neurons	Serotonin	NSCs proliferation
	ChAT ⁺	proliferation
	Nitric oxide	Effect on proliferation on a dose dependent manner

1.4. Functional relevance of neurogenesis

Under physiological conditions the major function of aSVZ NSCs is the production of new neurons to the OBs, promoting plasticity of the existing circuitry by making new synaptic contacts with mature neurons⁵⁶. Behavioral studies propose that adult neurogenesis is important for memory consolidation dependent on the OBs⁶¹. New OB interneurons play important roles in short-term memory and flexible olfactory associative learning.

Under pathological or challenging conditions, adult SVZ neurogenesis seems to play diverse roles dependent on the condition. For instance, in rodent ischemia models enhanced neurogenesis occurs in both adult neurogenic niches. Specifically, in the SVZ after ischemic stroke, cells migrate to the injury site expressing markers of resident neurons. In the case of neurodegenerative diseases, for example Alzheimer's disease models based on amyloid precursor protein, present reduced neurogenesis⁶². Also, Parkinson models based on the overexpression of wild-type human synuclein present reduced survival of new neurons on both neurogenic niches, while expression of mutant α -synuclein inhibited cell proliferation. CNS response to inflammation is often related with neurodegenerative diseases and brain injury⁶². For instance, endotoxin induced inflammation leads to a down-regulation of adult neurogenesis, restored by anti-inflammatory treatments⁶². Studies that examined the role of immune system in the regulation of adult neurogenesis suggest that different mechanisms of the immune response might have a different impact on adult neurogenesis⁶². Taking these evidences into account NSCs provide a source of potential endogenous therapies to several CNS disorders.

1.5. Choroid plexus

The choroid plexuses are folded epithelial structures residing at the brain ventricles. They are a highly vascularized secretory structure that develops from different locations along the dorsal axis of the neural tube⁶³. There are four CPs in the mammalian brain, being the CP of the fourth ventricle the first to be formed, followed by the CPs of the lateral ventricles and later the one lining the third ventricle⁶³. The structure of the CPs consists of a monolayer of epithelial cells surrounding a stromal core. Neighboring epithelial cells are bounded together by tight junctions, forming the blood-CSF barrier that prevents the free passage of molecules from the systemic circulation into the CSF⁸ (Figure 4). The stroma of this structure is highly vascularized, consisting of pericytes, connective tissue and blood vessels⁶³. Contrarily to blood vessels from brain parenchyma that are connected by tight junctions to form the blood-brain

barrier, these are fenestrated and leaky⁶³. CPs have dual embryonic origin, being the stromal cells originated from the mesoderm and the epithelial cells having origin from the ectoderm⁸.

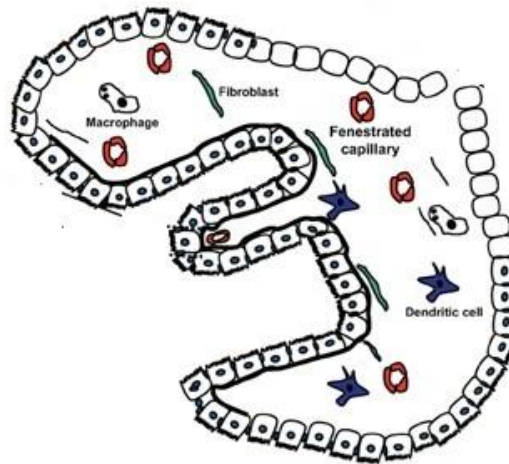


Figure 4: Structural organization of the choroid plexus. The choroid plexuses are a monolayer of epithelial cells that surround a stromal core. The epithelial cells are bounded by tight junctions, preventing the free passage of molecules from the systemic circulation into the CSF. The stroma of the choroid plexuses is highly vascularized and contains fenestrated capillaries, macrophages dendritic cells and fibroblasts. Adapted from Falcão *et al.* 2012¹⁶.

Functionally, the CPs display several roles: i) regulation and protection of brain environment, acting as the blood-CSF barrier; ii) secretion and modulation of CSF composition through protein secretion by their epithelial cells; iii) removal of brain metabolites and waste via CSF renewal; and, iv) during embryonic development it creates an expansive pressure through the secretion of CSF¹⁶.

The production and secretion of molecules by the CPs varies in a time dependent manner and it is regionally different, i.e. the pattern of expression is different among the four CPs, which contributes to the dynamic signaling gradients across the brain^{64,65}.

Table 3 summarizes the several CP transcriptome analyses performed both in rat and mouse that revealed the expression of several factors by the CP that influence neurogenesis at the SVZ both during embryonic development and adulthood.

Table 3: Summary of the CP transcriptome analysis performed by array or high throughput sequencing.

Species	Age	Sample	Type	GEO accession
<i>Rattus norvegicus</i>	E15	LV- CP epithelial cells	Expression profiling by high throughput sequencing	GSE44072
<i>Rattus norvegicus</i>	E19, P2, adult	LV-CP	Expression profiling by array	GSE44056
<i>Mus musculus</i>	E15, 10 weeks	LV-CP epithelial cells	Expression profiling by array	GSE33009
<i>Mus musculus</i>	E18.5	Fourth and LV-CP	Expression profiling by high throughput sequencing	GSE66312
<i>Mus musculus</i>	8-9 weeks	CP from all ventricles	Expression profiling by array	GSE23714
<i>Mus musculus</i>	8 weeks and 72 weeks	LV-CP	Expression profiling by array	GSE82308

1.5.1. Choroid plexus-CSF impact in embryonic neurogenesis

As mentioned before, embryonic progenitor cells, that line the ventricular surface, project their apical process into lateral brain ventricles, being in direct contact with the CSF. This apical process contains receptors that receive signals from the CSF. Therefore, being the CP the major responsible for the regulation of CSF production and for the modification of its composition, either by alterations in the transference of molecules from blood into CSF or by variations in the secretion of molecules produced by the CP, it is expected that the dynamic CSF composition will somehow have an impact on neurogenesis. In fact, an *in vitro* study revealed that CSF alone was capable of maintaining the viability and proliferation of cortical cells⁶⁶. Additionally, this study demonstrated that CSF isolated from different ages affected differently the growth of cortical cultures⁶⁶. Similar results were observed when rat neurospheres were exposed to CSF isolated from different embryonic ages; specifically, cells cultured with CSF collected from E17 proliferated more when compared with neurospheres exposed to CSF from E19¹⁵. Moreover, a proteome analysis of embryonic CSF revealed the presence of 423 proteins in E12.5 CSF, 318 in E14.5 and 382 in E17.5 of which only 137 proteins were common among the three ages, highlighting the dynamic range in CSF composition⁶⁷. IGF2 constitutes an example of these molecules that vary in a time depend manner in the CSF, present in different ages of embryonic CSF, but at different levels. Moreover, some of the proliferative effects of the CSF in the SVZ can be attributed to this CP-secreted protein, that

establishes its effects through IGF1R present at the apical process of RGC^{15,68}. Nevertheless, CSF has a milieu of signaling molecules with the ability to influence neurogenesis, for example, Shh, FGF, retinoic acid and leukemia inhibitory factor constitute some of the molecules with confirmed presence in embryonic CSF and described as capable of modulating neurogenesis. Hence, the proper balance of CSF composition is essential for the correct interaction of multiple signaling activities that reach the embryonic SVZ. *In vivo* studies of CSF composition manipulation support the idea that CSF regulation has an impact on neurogenesis. For example, intraventricular injection in rat and mice embryos of recombinant IGF1 resulted in increased cell proliferation⁶⁹. Another experiment, revealed that removal of *Fgf2* from chick embryonic CSF lead to a decrease in cell proliferation and increase in neuronal differentiation⁷⁰.

Taking this into account, the CPs, via modulation of CSF composition, are potential regulators of embryonic NSCs. However, until now little is known on how these molecules are regulated and secreted by the CPs. The improvement of region and time specific deletion techniques will provide new strategies to target CP-derived molecules and study its effect on neurogenesis. For example, deletion of Shh from the 4th ventricle-CP resulted in a decrease of proliferation and an impair in the production of GABAergic neurons³⁹. Another study revealed that inhibition of *Otx2* from 4th ventricle-CP resulted in increased proliferation caused by alterations in Wnt signaling¹⁴. This studies evidence that the CPs produce modulators of essential signaling involved in the regulation of embryonic NSCs and their progeny.

1.5.2. Choroid plexus-CSF impact in adult SVZ

The proximity of the aSVZ with the ventricular surface and the fact that NSCs project their apical process into the lateral ventricles makes the CP-CSF system a key component of the aSVZ neurogenic niche. Recent adult CP transcriptome analysis revealed the presence of molecules, such as IGF1, IGF2, EGF, that as mentioned before, are involved in signaling pathways that modulate cell cycle, cell survival and cell differentiation⁷¹. Adult CSF is capable of supporting the growth of adult rat neurospheres¹⁵. Alterations of CSF composition in a time dependent manner are also observed during aging, where heterochronic infusion of “old” CSF into young mice resulted in a decrease of NSCs at the aSVZ and conversely the injection of “young” CSF into old mice increases the number of NSCs at the aSVZ⁶⁵. Additionally, this study revealed that not all types of aSVZ cells are sensitive to aged CSF, with NSCs being affected but not TAPs. Interestingly, transcriptome analysis of young and adult mice lateral ventricle CPs revealed that BMP5 and IGF1 are enriched in young CP (2 months), suggesting that this factors might be involved in

the age dependent effects that CP-derived factors promote in the SVZ. Moreover, taking into account its location between blood and CSF, the CP is capable of altering its secretion pattern in response to local changes of the niche as well as peripheral alterations.

The maintenance of the aSVZ cytoarchitecture is fundamental for the proper production of NSCs and their progeny. CP-secreted interleukin-1 β (IL-1 β) has been proposed as being involved in the modulation of aSVZ cytoarchitecture and proliferation of quiescent NSCs. By binding to IL-1 receptors on the surface of B cells, IL-1 β regulates the expression of VCAM1⁵³. *In vivo* disruption of this adhesion molecule resulted in disturbed cytoarchitecture and proliferation of NSCs resulting in increased neurogenesis at the OBs. Being IL-1 β secreted by the CP, this study revealed the key role of the CP to act as an environmental sensor, responding to chemokines involved in tissue repair. One other example of CP-derived molecule is neurotrophin 3, which regulates quiescence and long term maintenance of aSVZ-NSCs, inducing the phosphorylation of nitric oxide synthase leading to the production of nitric oxide. Moreover, SLIT proteins, secreted by the CPs are chemorepulsive factors that repel C cells in the direction of the OBs⁷².

Based on a previous transcriptome analysis of the adult CP in this work we selected two proteins secreted by the CP to explore their impact, which is currently unknown, in SVZ neurogenic niche: Amphiregulin (AREG) and Insulin Growth Factor Binding Protein 2 (IGFBP2)⁷¹. AREG is an EGF family protein that binds to the EGFR activating signaling cascades of cell survival, proliferation and motility. Previous work reported that AREG is expressed in the CP and hippocampus of adult mice⁷³. IGFBP2 belongs to a family of proteins responsible for the bioavailability and transport of IGF proteins. Interestingly, IGFBP2 is the predominant IGF binding protein present in the CSF³⁴.

Altogether, the information summarized above provides some evidences of the role of CP-derived molecules in the modulation of the SVZ cellular dynamics. Nevertheless, several aspects are still unexplored. Namely, what proteins secreted by the CPs play a role in the regulation of SVZ? What is the impact in the SVZ caused by alterations in the CPs transcriptome due to aging or immune response? Can CPs transcriptome provide a possible source of endogenous therapy for neurodegenerative diseases?

2. Aims

Given the proximity between the SVZ neurogenic niche and the CP, the central hypothesis of the work developed under this thesis is that CP-derived molecules play a role in modulating SVZ dynamics. So, to gain further insights in SVZ cell population dynamics, the goal of this project is to understand how molecules secreted by the CP into the CSF influence the SVZ cell population.

Specifically, we aimed at:

i) determining the effects of candidate CP-derived proteins using *in vitro* cultures of neural progenitor cells. For this, we used neurospheres cultures exposed to different concentrations of selected molecules secreted by the CP and evaluated cell proliferation and differentiation.

ii) evaluating how candidate CP-derived proteins impact in the SVZ cell population dynamics *in vivo*. For this we performed ventricular injections of the selected proteins to determine its putative effects in SVZ cells, namely SVZ cells proliferation and differentiation.

iii) characterizing the ontogenic expression pattern of the CP, from early postnatal stages to early adulthood. For this we determined the transcriptome of the CP by using high throughput sequencing RNA-seq. This will potentially enable the identification of key molecules that contribute to structural and functional temporal changes occurring in the SVZ.

3. Materials and methods

3.1. Ethics statement

This project was part of a study approved by the Ethics Commission of the University of Minho (SECVS-001/2013) and by the Portuguese national authority for animal experimentation, Direcção Geral de Veterinária (DGV9457). Animals were kept and handled in accordance with the guidelines for the care and handling of laboratory animals in the Directive 2010/63/EU of the European Parliament and of the Council.

3.2. Animals

For this project we used Wistar Han rats. Due to previously described specificities related to hormonal fluctuation, namely at gene expression level, females were not used. Animals were maintained in 12h light/dark cycles at 22 to 24°C and 55% humidity and fed with regular rodent's chow and tap water ad libitum.

3.3. Study the impact of CP-derived proteins in human neural progenitor cells.

To study the impact of CP-derived proteins in neural progenitor cells (NPCs) *in vitro* we used human NPCs (hNPCs), a kind gift from Prof. Leo A. Behie (University of Calgary, Canada). The cells were isolated, in the lab of Prof. Behie, from the telencephalon region of a 10 week post-conception fetus according with the protocols and strict ethical guidelines previously established and approved by the Conjoint Health Research Ethics Board (CHREB, University of Calgary, Canada; ID:E-18786)⁷⁴. In all the experiments, cells were maintained at 37°C in a humidified atmosphere containing 5% CO₂.

hNPCs were thawed and the content placed in T-75 culture flasks containing 15mL of serum-free medium PPRF-h2⁷⁴. After three days, cells were mechanically dissociated (25-30 times) into a single cell suspension and cultured in fresh PPRF-h2 medium. After 10 days of growth, cells were collected and enzymatically dissociated with 0.05% Trypsin-EDTA (Invitrogen, Carlsbad, California, USA) during 10min at 37°C followed by mechanic dissociation. At this point, cells were plated under specific conditions to perform clonal and differentiation assays that will be explained bellow in detail.

3.3.1. Clonal assay

Dissociated cells were plated under non-adherent conditions in serum-free medium (PPRF-h2), at a density of 10cells/ μL ^{75,76}. At the second day of culture, cells were exposed to one of the following concentrations of either AREG (Biolegend, San Diego, California, USA) or IGFBP2 (Biolegend): 25ng/mL, 100ng/mL or 200ng/mL. After 10 days in culture, we evaluated the effects of the exposure to the different concentrations of each protein by counting the number of formed neurospheres (Figure 5).

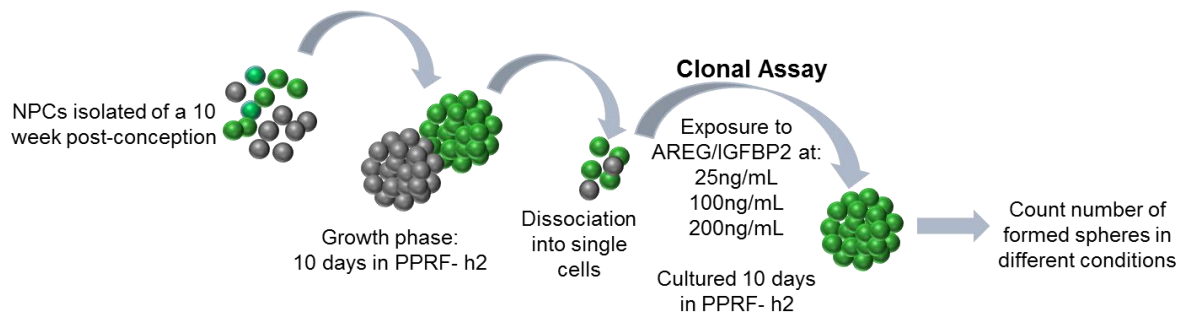


Figure 5: Schematic representation of clonal assay.

3.3.2. Differentiation assay

Dissociated hNPCs were plated on pre-coated coverslips [poly-D-lysine (100 $\mu\text{g}/\text{mL}$, Sigma-Aldrich, St Louis, Missouri, USA) and laminin (10 $\mu\text{g}/\text{mL}$, Sigma-Aldrich)] in 24-well plates at a density of 50.000cells/well⁷⁷. At the second day of culture cells were exposed to the same three concentrations of AREG or IGFBP2 as for the clonal assay. Simultaneously, cells were also exposed to BrdU, a thymidine analogue that incorporates newly generated DNA during the S-phase of the cell cycle, to also evaluate cell proliferation (10 μM , Sigma-Aldrich)⁷⁸. After 5 days in culture, cells were fixed during 30 minutes with 4% paraformaldehyde (PFA) for posterior immunocytochemistry for BrdU and β III-Tubulin (Figure 6).

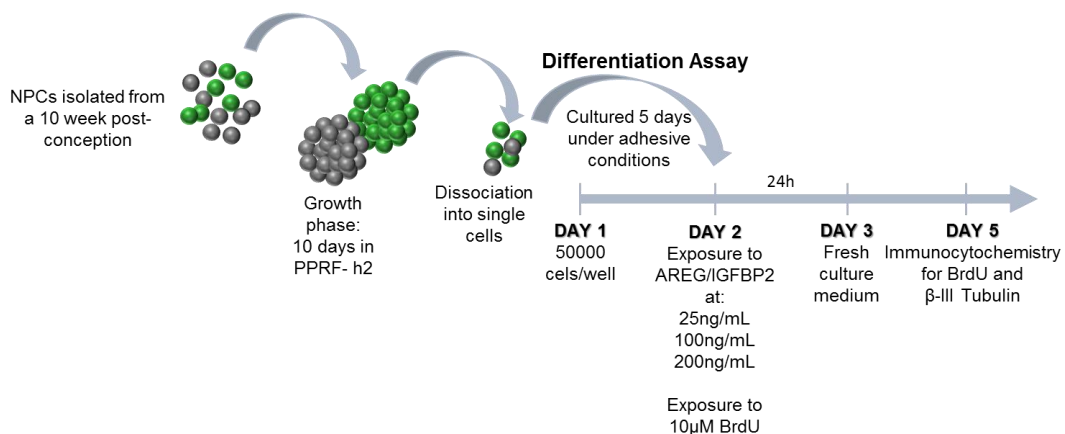


Figure 6: Schematic representation of differentiation assay.

3.3.3. Immunocytochemistry for BrdU and β III-Tubulin

Fixed cells were permeabilized in phosphate buffered saline (PBS) with 0.1% Triton X-100 (PBS-T; Sigma-Aldrich) for 5min at room temperature (RT). The acidification, required for the denaturation of DNA strands allowing the binding of the antibody against BrdU, was achieved immersing cells in 1M hydrochlorid acid (HCl) during 30min. Blockage of non-specific binding was performed using 10% fetal bovine serum (FBS, Invitrogen, Carlsbad, USA) for 1h at RT. Cells were then incubated with the primary antibodies (Table 4) diluted in 10% FBS for 1h at RT and then with the appropriate secondary antibodies (Table 4) diluted in 10% FBS for 1h at RT. The cells were counterstained with 4',6-diamidino-2-phenylindole (DAPI, 1:1000, Sigma-Aldrich), a compound that labels the nucleus, for 10min at RT. Coverslips were mounted on slides using immu-mount (Thermo Scientific, Waltham, Massachusetts, USA)⁷⁷. For quantification analysis, samples were observed using a fluorescence microscope (BX61, Olympus, Tokyo, Japan), and for this purpose, three coverslips per condition and 20-25 representative fields were chosen and analyzed. The results are presented as the number of positive cells for the respective markers (Table 4), divided the total number of cells in the field (DAPI-positive cells)⁷⁷.

Table 4: List of primary and secondary antibodies used for the immunocytochemistry.

Primary Antibody	Dilution	Company
BrdU – Rat	1:20	Abcam
β III-Tubulin – Mouse	1:500	Millipore
Secondary Antibody	Dilution	Company
Alexa Fluor 594 – Goat α -Rat	1:1000	Invitrogen
Alexa Fluor 488 – Goat α -Mouse	1:1000	Invitrogen

3.4. Study the impact of CP-derived proteins in the SVZ cell population

All experiments were conducted in 8-weeks-old Wistar Han rats. To reduce stress-induced changes in the hypothalamus-pituitary axis associated with the surgery procedure, animals submitted to intraperitoneal and cannula injections were handled daily during 1 week prior to surgery.

3.4.1. Surgeries

Animals were anesthetized with medetomidine (0.5mg/kg) and ketamine (75mg/kg). Once animals were anesthetized the skin over the implantation site was shaved and animals were immobilized in a stereotaxic apparatus. A small incision was made from between the eyes to the base of the neck to expose the scalp. A sterilized stainless-steel guide cannula (26gauge; Plastics One, Virginia, USA) was implanted in the right lateral ventricle (0.24 posterior, 1.5 lateral and 4 depth), through a burr-hole. The cannula was fixed to the scalp with four screws and dental acrylic cement and the skin sutured around it. To prevent contamination, it was inserted a dummy cannula into the guide cannula. At the end of the surgical procedures, the anesthesia was reverted with atipamezole hydrochloride (1mg/kg) and animals were monitored until they were fully recovered. After surgery animals were treated with anti-inflammatory (Carprofen, 5mg/kg) and antibiotic (Enrofloxacin, 5mg/kg) and were allowed to recover for one week⁷⁹ (Figure 7).

3.4.2. BrdU and proteins administration

For the analysis of AREG (Biolegend) and IGFBP2 (Biolegend) impact in the SVZ cell population, four groups of animals were compared (n= 5/group). To evaluate the effects of protein administration in cells proliferation, all animals received a single injection of BrdU (50mg/kg), 30min before the first administration of the protein. Three groups of animals received 4 injections (6h interval), during a 24h period, of protein at 25ng/mL, 100ng/mL or 200ng/mL of concentration. A sham control group was injected with the vehicle solution, artificial CSF (Figure 7).

For the protein injection animals were anesthetized with 4% sevoflurane in 100% oxygen. The proteins were administered through a 33gauge injection cannula (Plastics One), using a 5.0 μ L Hamilton syringe connected to the injection cannula through a polyethylene catheter (PE-10; Plastics One). The injection volume was 4 μ L injected at a velocity of 2 μ L/min. To prevent reflux of the protein back to the injection cannula, the injection cannula was left in place for one additional minute. Animals were sacrificed 24h after the first injection of the protein.

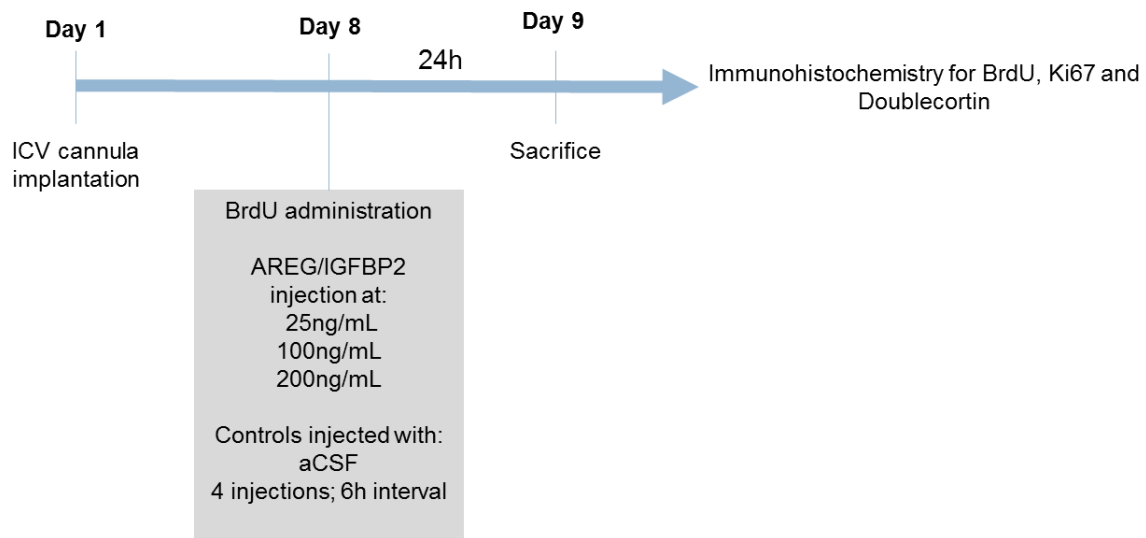


Figure 7: Schematic representation of protein administration procedure and postmortem analysis. aCSF, artificial cerebrospinal fluid; ICV, intracerebroventricular injection.

3.4.3. BrdU, Ki67 and Doublecortin immunohistochemistry

At time of sacrifice, animals were anesthetized with pentobarbital (80mg/kg, CEVA, Algés, Portugal), and transcardially perfused with 0.9% NaCl followed by perfusion with 4% PFA. Brains were carefully removed and immersed in 4% PFA during 24h followed by immersion in 30% saccharose for brain preservation for 24h. Brains were embedded in O.C.T compound (Sakura, Leiden, Holland) and snap frozen in liquid nitrogen. Coronal sections of 20 μ m were cut in a cryostat and collected to slides for immunohistochemistry⁸⁰.

Fluorescence immunohistochemistry was performed to label proliferating cells (using BrdU, an exogenous marker and Ki67, an endogenous proliferation marker), newborn neuroblasts (BrdU/DCX positive cells) and to perform a cell cycle index (Ki67/BrdU positive cell). The immunohistochemistry protocol is briefly described below.

Antigen retrieval, required to break protein cross-links established by PFA fixation revealing hidden antigen sites (epitopes), was performed immersing brain section in heated citrate buffer (pH 6) during 20min, followed by tissue permeabilization in 0.3% PBS-T (Sigma-Aldrich) during 15min. The acidification was achieved immersing slices in 2M HCl during 30min. Blockage of unspecific binding was accomplished by 30min incubation with 10% FBS (Invitrogen). Primary antibodies, were incubated overnight (Table 5).

Fluorescent secondary antibodies were incubated during at RT for 2h (Table 5). Slides were counterstained with DAPI (1:1000, Sigma-Aldrich) for 10min⁸⁰.

Table 5: List of primary and secondary antibodies used for the immunohistochemistry.

Primary antibody	Dilution	Company
BrdU – Rat	1:100	Abcam
Ki67 – Rabbit	1:300	Millipore
Doublecortin – Rabbit	1:500	Millipore
Antibody – Specie	Dilution	Company
Alexa Fluor 594 – Goat α -Rat	1:500	Invitrogen
Alexa Fluor 488 – Goat α -Rabbit	1:500	Invitrogen

3.4.4. Confocal imaging and quantitative analysis

Proliferation in the SVZ was assessed by the exogenous marker BrdU, and by Ki67, an internal marker expressed during G₁, S, G₂ and M phase; Ki67 is not expressed during G₀ phase⁸⁰. The number of BrdU and Ki67 positive cells was counted and the results expressed per area (mm²). Cell cycle index was performed determining the number of cell exiting and reentering the cell cycle according to the following equations.

$$\text{Reentry} = \frac{\text{Ki67}^+ \text{BrdU}^+}{\text{BrdU}^+} \qquad \text{Exit} = \frac{\text{Ki67}^- \text{BrdU}^+}{\text{BrdU}^+}$$

Newly generated neuroblasts were assessed by double staining with DCX (a marker of neuroblasts) and BrdU. The number of double positive cells (DCX/BrdU) was counted and the results expressed per area (mm²)⁸⁰.

Each analysis was performed along the dorsal-ventral axes of SVZ, divided in three different areas, RMS, dorsolateral and ventral⁸⁰ (Figure 8). For each section (3 per animal), images were taken for the entire lateral wall of the SVZ using a confocal microscope (FV1000; Olympus). Each area was determined using the Stereo Investigator (MBF Bioscience, Williston, North Dakota, USA).

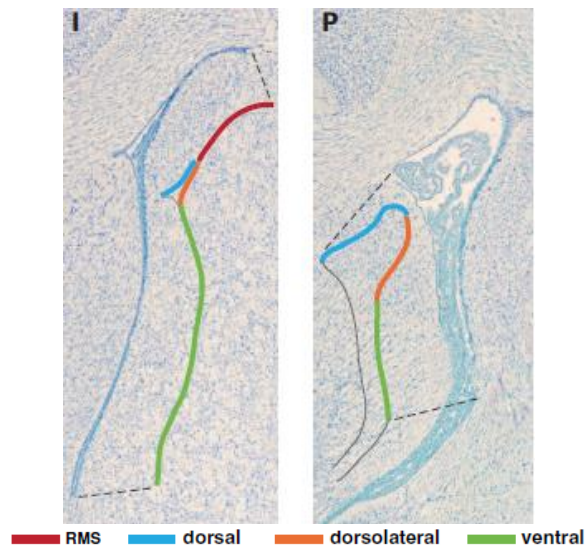


Figure 8: Division of the subventricular zone along the dorsal-ventral axes. For the purpose of this work we analyzed three of the established divisions: rostral migratory stream (RMS; red trace), dorsolateral (orange trace), and ventral (green trace). Adapted from Falcão et al. 2012⁸⁰.

3.5. Transcriptome analysis of CP in different stages of development

3.5.1. CP collection

The transcriptome analysis of the CP was performed in specific milestones of development (P1, P4, P7, P10 and P60). To collect CPs from the lateral ventricles, animals were anesthetized with pentobarbital (200mg/kg) and were transcardially perfused with sterile RNase free cold saline (0.9% NaCl). Brains were removed and CP isolated under a stereomicroscope (SZX7; Olympus), frozen in dry ice, and stored at -80°C.

3.5.2. RNA extraction and quality analysis

Total RNA extraction was performed using SPLIT RNA Extraction Kit (Lexogen, Viena, Austria) (Figure 9). Briefly, the CPs were homogenized in an isolation buffer highly chaotropic. Samples, were then transferred to a phase lock gel column, which contains a gel matrix that, based on the density differences, acts as a barrier between the organic and aqueous phase. Acidic phenol and acidic buffer were added to create a monophasic solution, which allows the separation of genomic DNA into the organic phase. Chloroform was added and the phases were separated by centrifugation for 2min at 12.000xg at 18°C. The RNA, contained in the aqueous phase, was decanted into a new micro tube. The RNA was then precipitated

onto a silica column by addition of 1.75x volume of isopropanol. The RNA was further purified by washing the column. Finally, RNA was eluted in 20 μ L of Elution Buffer.

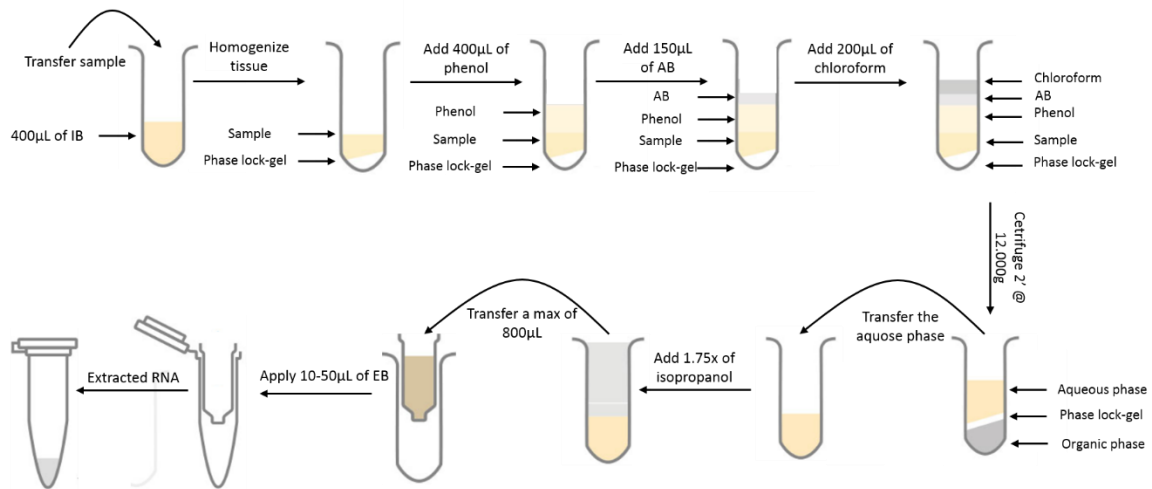


Figure 9: Schematic representation of total RNA extraction protocol using SPLIT RNA Extraction Kit (Lexogen). IB, Isolation Buffer; AB, Acidic Buffer; EB, Elution Buffer.

Quality of total RNA extracted was evaluated using Experion RNA StdSenses Analysis Kit (Bio-Rad, Hercules, California, USA). Briefly, heat denatured RNA was loaded into an electrophoresis system and detected measuring fluorescence of a fluorophore that binds to RNA. RNA quality is measured by the RNA quality index (RQI). Using an algorithm, RQI measures RNA integrity comparing the electropherogram of RNA samples to a series of standardized degraded RNA samples. The RQI method returns a number between 10 (intact RNA) and 1 (highly degraded RNA).

3.5.3. Library preparation

Complementary deoxyribonucleic acid (cDNA) library construction was performed using 3' mRNA-Seq Library Prep Kit (Lexogen). Library construction was initiated by the generation of the first cDNA strand using oligodT primer, containing Illumina-compatible linker sequence. After first strand synthesis RNA was removed and second strand synthesis was initiated by random priming, that also contained Illumina-compatible linker sequence, and a DNA polymerase. The double stranded library was purified using a magnetic bead-based purification. cDNA library was amplified to generate enough material for quality control and sequencing and to add the adapter sequences required for cluster generation. Finally, the

amplified library was purified using a magnetic bead-based purification to remove PCR components that might interfere with quantification.

3.5.4. RNA sequencing

The 15 samples were multiplexed resulting in 40µL of 15.5nM lane mix. Quality of the multiplexed library was evaluated using Agilent Bioanalyzer 2100, which ensures that the libraries are of proper size, free from primer dimer and that each library yields sufficient material for sequencing. RNA sequencing was performed at the Vienna Biocenter Core Facilities (Vienna, Austria). The library was subjected to 100bp single end read cycles of sequencing on an Illumina HiSeq 2500 sequencer according to the manufacturer's protocol.

3.5.5. Data analysis and interpretation

Quality control of the sequencing data was performed using MultiQC platform⁸¹. Currently we are performing the sequences alignment and gene expression analysis.

3.6. **Statistical analysis**

Statistical analysis was performed using IBM SPSS Statistics ver.22 (IBM, Armonk, New York, USA) and graph's representation using GraphPad Prism ver.6 (GraphPad Software, La Jolla, San Diego, USA).

For the statistical evaluation of the *in vitro* assay a one-way ANOVA was applied to compare the mean values for the four groups. In the *in vivo* assays, for the number of Ki67 and cell cycle index, since we only compared the control group and the 200ng/mL, we performed an independent sample t-test, or the Mann-Whitney test in case normality was not assumed. BrdU positive cells and the number of newborn neuroblasts was analyzed using one-way ANOVA to compare the mean values for the four groups, or the Kruskal-Wallis test in case of normality requirements were not achieved.

Normality was measured using the Shapiro-Wilk statistical tests. Equality of variances was measured using the Levene's test, and was assumed when $p_{\text{Levene's}} > 0.05$. Multiple comparisons between groups were accomplished through the Bonferroni statistical test.

Values were accepted as significant if the p-value was lower than 0.05 and results were expressed as group mean±SEM (standard error of the mean).

4. Results

4.1. Impact of AREG in neurogenesis

As mentioned previously (section 1.5.2), AREG belongs to the EGF protein family and it is secreted by the CP into the CSF. In order to evaluate if this protein might have an impact on neurogenesis we performed both *in vitro* and *in vivo* assays. Results from these experiments are next presented.

4.1.1. Does AREG impact the growth of hNPCs?

4.1.1.1. Clonal assay

hNPCs were cultured *in vitro* and exposed to one of the following concentrations of AREG: 25ng/mL, 100ng/mL and 200ng/mL. For all concentrations tested a significant 3-fold increase in the number of formed neurospheres was observed when compared with the control group. Despite the fact that no significant differences were observed between the protein concentrations tested, cells that were exposed to 100 and 200ng/mL of AREG formed a slightly superior number of neurospheres in comparison with cells exposed to 25ng/mL of the protein (Figure 10, Table 6, for post hoc tests see Table S1).

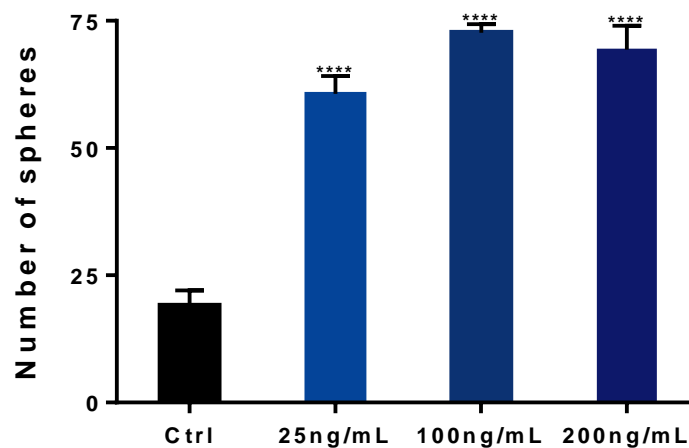


Figure 10: Clonal assay in hNPCs exposed to AREG. Quantification of the number of formed neurospheres when cells were exposed to 25, 100 and 200ng/mL of AREG. Results correspond to a representation of 3 independent assays. Data represent the mean number of neurospheres \pm SEM (n=3, **** p<0.0001, ANOVA).

Table 6: Statistical analysis of the clonal assay with AREG. Data presented as mean±SEM.

Group	Mean±SEM	Normality test	Homogeneity test	Statistical test
Ctrl	19.00±3.06	0.363		
25ng/mL	60.67±3.48	0.817	0.272	F _(3,8) =53.944; p<0.0001;
100ng/mL	73.00±1.53	0.363		
200ng/mL	69.33±4.70	0.235		

4.1.1.2. Differentiation assay

We next performed a differentiation assay. hNPCs grown *in vitro* in conditions that promoted their differentiation, presented a 2-fold increase in the proliferation rate when exposed to 25 and 100ng/mL of AREG, with 25ng/mL of the protein having the highest effect on proliferation (Figure 11A, B, Table 7, for post hoc tests see Table S2). Surprisingly, cells exposed to 200ng/mL of AREG did not present alterations in the proliferation rate when compared to the control group.

When evaluating cell differentiation, cells exposed to 25ng/mL of AREG significantly increased the number of newborn neurons. Although not statistically significant ($p=0.056$), cells exposed to 100ng/mL also presented an increase in the number of new neurons when compared with the control group. Similar to the observed in the proliferation rate, cells exposed to 200ng/mL of AREG did not show alterations in the formation of new neurons when compared with controls (Figure 11A, C, Table 7, for post hoc tests see Table S2).

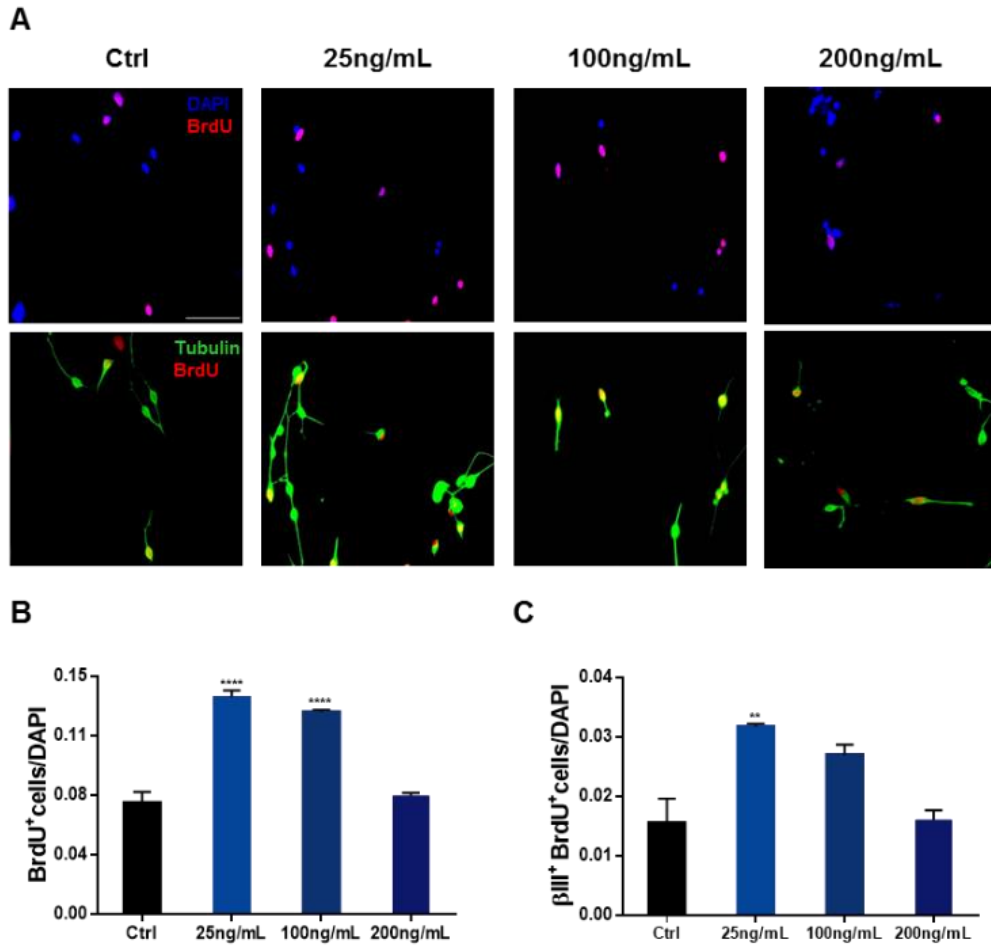


Figure 11: Differentiation assay in hNPCs exposed to AREG. A) Representative images of BrdU⁺ and β III-Tubulin⁺BrdU⁺ cells in the upper and lower panels, respectively, of hNPCs exposed to 25, 100 and 200ng/mL of AREG. Scale bar 50 μ m. B) Quantification of BrdU⁺ cells after exposure to different concentrations of AREG. Results correspond to a representation of 3 independent assays. Data represents mean percentage of BrdU⁺ cells divided by the total number of cells \pm SEM (n=3, **** p<0.0001, ANOVA). C) Quantification of β III-Tubulin⁺BrdU⁺ cells exposed to different AREG concentrations. Results correspond to a representation of 3 independent assays. Data represent the mean of β III-Tubulin⁺BrdU⁺ cells divided by the total number of cells \pm SEM (n=3, ** p<0.01, ANOVA).

Table 7: Statistical analysis of the differentiation assay of cells exposed to AREG. Data presented as mean±SEM.

	Group	Mean±SEM	Normality test	Homogeneity test	Statistical test
BrdU ⁺ cells	Ctrl	0.070±0.007	1.000	0.303	F _(3,8) =69.495; p<0.0001;
	25ng/mL	0.137±0.004	1.000		
	100ng/mL	0.128±0.001	1.000		
	200ng/mL	0.075±0.002	1.000		
βIII-Tubulin ⁺ BrdU ⁺ cells	Ctrl	0.016±0.004	1.000	0.259	F _(3,8) =11.642; p<0.01;
	25ng/mL	0.032±0.001	1.000		
	100ng/mL	0.027±0.002	1.000		
	200ng/mL	0.016±0.002	1.000		

4.1.2. Does AREG have an effect in the adult rat SVZ?

As described in detail in section 3.4, and to assess the effect of AREG *in vivo*, adult rats were injected (4 times with a 6h interval during 24h) with one of the following concentrations of AREG: 25ng/mL, 100ng/mL or 200ng/mL. The effects of protein administration in cell proliferation, cell cycle and number of new neuroblasts are presented below.

4.1.2.1. Analysis of cell proliferation rates along the SVZ

The proliferation rate assessed by BrdU labeling revealed that animals injected with 200ng/mL of AREG significantly increased the number of BrdU⁺ cells at the RMS, dorsolateral and ventral area of the SVZ. This alteration was most evident in the dorsolateral and ventral areas, where the number of cells increased approximately 2.5-fold when compared with the control group. Animals that received 25 and 100ng/mL of AREG did not show a significant increase in the number of BrdU⁺ cells in any of the SVZ areas analyzed when compared to vehicle injected animals (Figure 12A, B, Table 8, for post-hoc testes see Table S3). Considering the fact that animals that received 200ng/mL of AREG significantly increased the number of BrdU⁺ cells we next performed another analysis of the proliferation rate using an endogenous maker of proliferation, Ki67. Labelling with this marker revealed a 2-fold increase of proliferation in the dorsolateral area of animals injected with the 200ng/mL of AREG. However, no major differences were observed between controls and injected animals concerning proliferation at the RMS and ventral areas (Figure 13 A, B, Table 9).

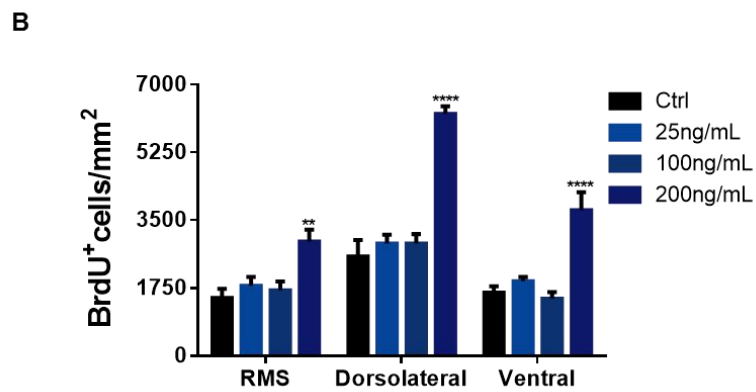
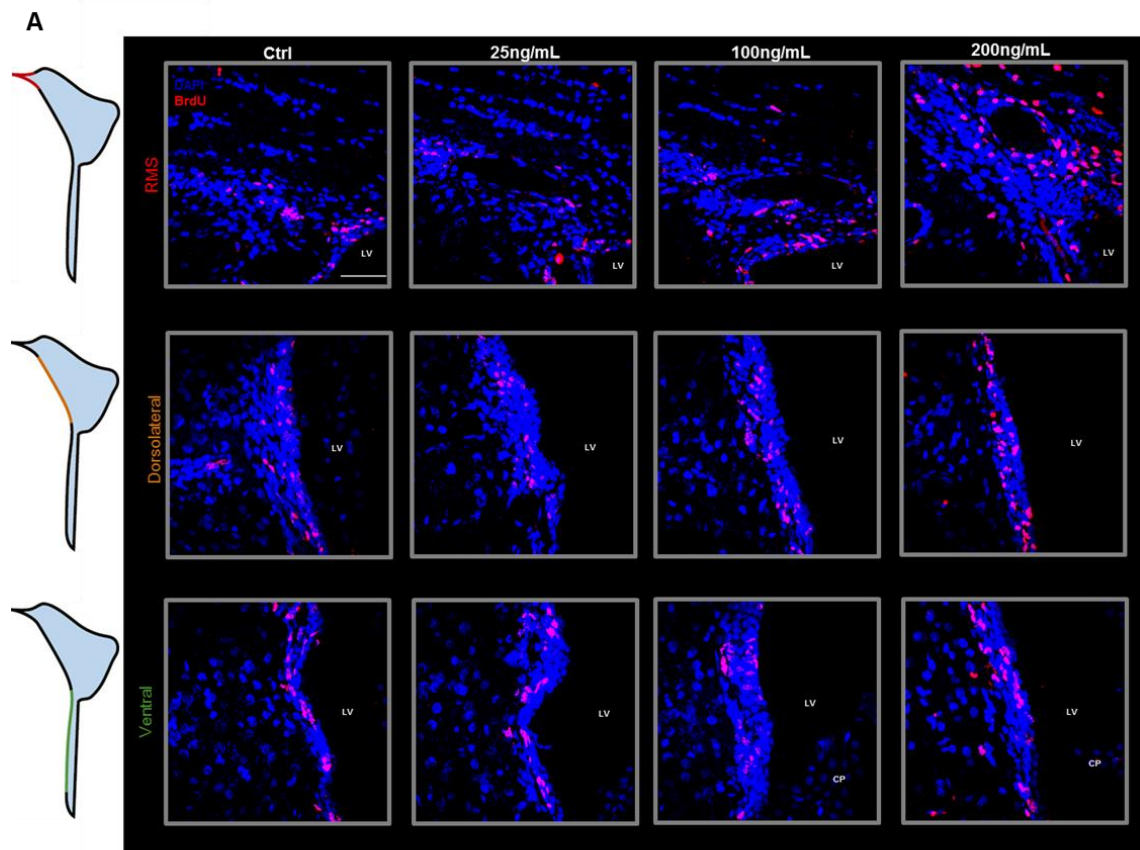


Figure 12: BrdU⁺ cells in the rostral migratory stream (RMS), dorsolateral and ventral areas of the subventricular zone of animals injected with 25, 100 or 200ng/mL of AREG. A) Representative images show BrdU⁺ cells along the 3 different areas of the subventricular zone. Scale bar 50µm. B) Quantification of the BrdU⁺ cells in the different experimental conditions. Data represent the mean of BrdU⁺ cells divided by the total area of each subventricular zone subdivision ± SEM (n=5, ** p<0.01; **** p<0.0001, ANOVA).

Table 8: Statistical analysis of BrdU⁺ cells in the subventricular zone of animals injected with AREG. Data presented as mean±SEM.

	Group	Mean±SEM	Normality test	Homogeneity test	Statistical test
RMS	Ctrl	1496.86±234.76	0.177	0.470	F _(3,16) =6.664; p<0.01;
	25ng/mL	1803.61±234.33	0.845		
	100ng/mL	1691.22±222.34	0.862		
	200ng/mL	2948.18±312.56	0.203		
Dorsolateral	Ctrl	2565.57±422.75	0.937	0.233	F _(3,16) =36.805; p<0.0001;
	25ng/mL	2895.68±226.27	0.973		
	100ng/mL	2894.05±244.99	0.262		
	200ng/mL	6241.46±193.05	0.136		
Ventral	Ctrl	1629.62±164.08	0.927	0.140	F _(3,16) =16.166; p<0.0001;
	25ng/mL	1925.00±108.74	0.547		
	100ng/mL	1473.65±165.98	0.997		
	200ng/mL	3761.89±459.88	0.754		

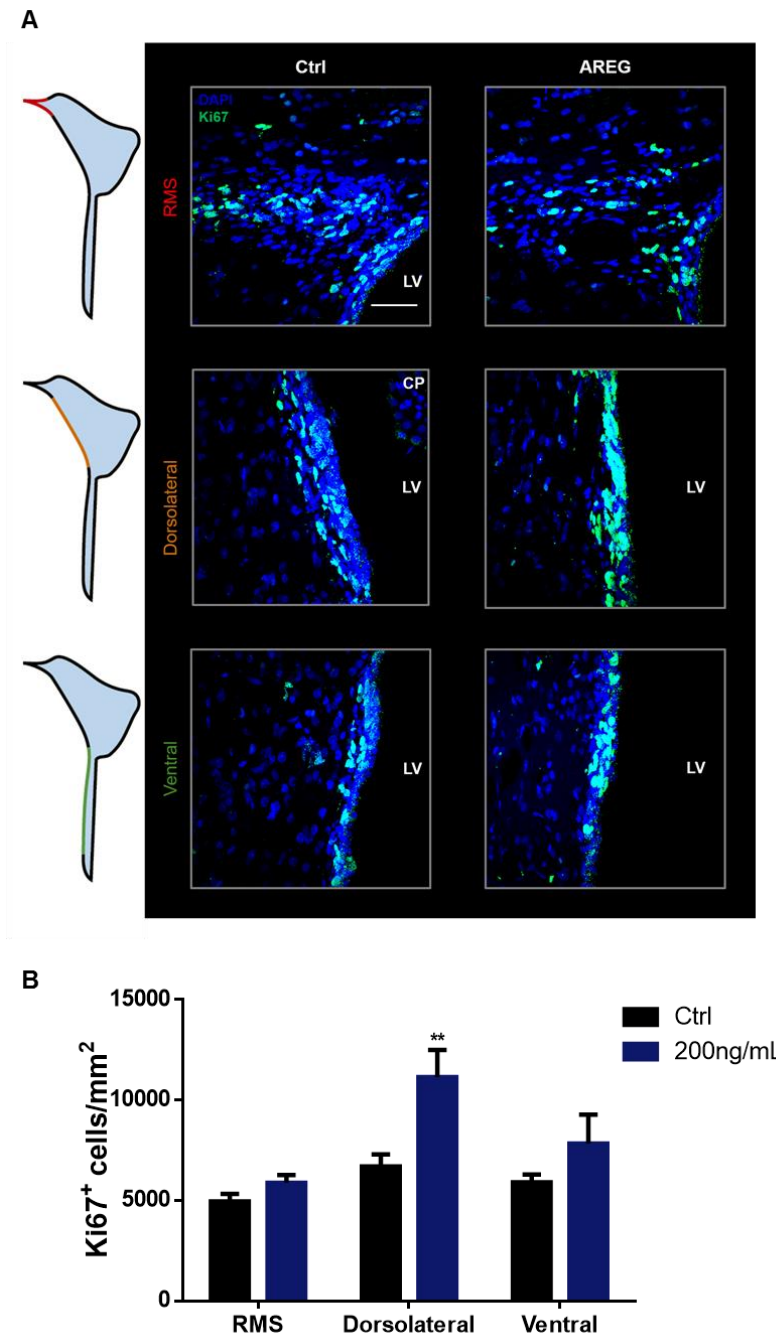


Figure 13: Ki67⁺ cells of animals injected with 200ng/mL of AREG in the rostral migratory stream (RMS), dorsolateral and ventral areas of the subventricular zone. A) Representative images show Ki67⁺ cells distribution in the three different areas of the subventricular zone. Scale bar 50 μ m. B) Quantification of the Ki67⁺ cells in the different experimental conditions. Data represents mean of Ki67⁺ cells divided by the total area of each subventricular zone subdivision \pm SEM (n=5, ** p<0.01, Student's t test).

Table 9: Statistical analysis of Ki67⁺ cells in the subventricular zone areas of animals injected with AREG. Data presented as mean±SEM.

	Group	Mean±SEM	Normality test	Statistical test
RMS	Ctrl	4961.42±371.34	0.900	$t_{(8)}=1.677$; $p>0.05$;
	200ng/mL	5875.47±399.14	0.745	
Dorsolateral	Ctrl	6689.00±599.08	0.76	U=0.000; P<0.01
	200ng/mL	11139.89±1354.55	0.046	
Ventral	Ctrl	5900.88±389.53	0.022	U=8.000; $p>0.05$
	200ng/mL	7833.68±1447.50	0.484	

4.1.2.2. Analysis of cell cycle index along the SVZ

The alterations observed in the number of BrdU positive cells of animals injected with 200ng/mL of AREG might be associated with an increase in the number of cells in S phase. Thus, considering this hypothesis, we then performed a cell cycle index based on the number of BrdU and Ki67 positive cells to evaluate if the injection of the protein might alter the number of cells reentering and exiting the cell cycle. Animals injected with 200ng/mL of AREG significantly increased the number of cells reentering the cell cycle, and consequently decreased the number of cells exiting the cycle in all analyzed areas (Figure 14, Table 10).

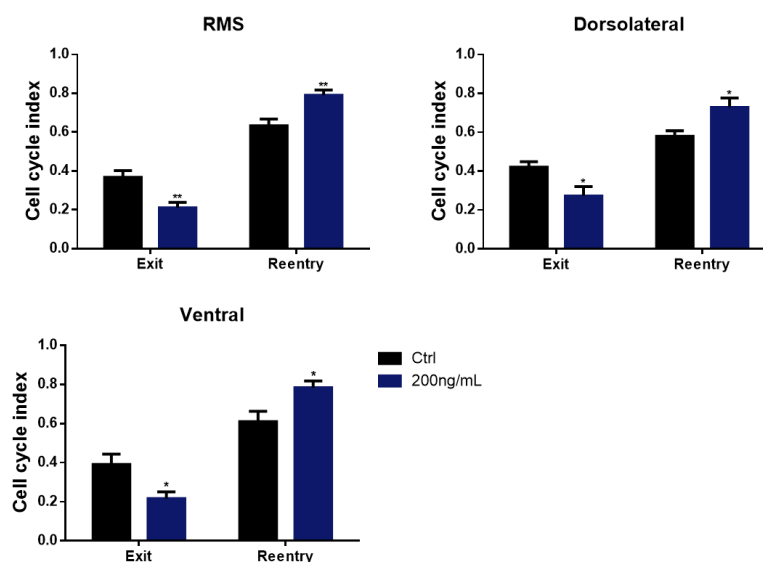


Figure 14: Cell cycle index analysis of animals injected with 200ng/mL of AREG in the rostral migratory stream (RMS), dorsolateral and ventral areas of the subventricular zone. Number of cells exiting the cell cycle are determined according to the ratio of Ki67⁺BrdU⁺/BrdU⁺, while cells reentering the cell cycle are determined according to the ratio of Ki67⁺BrdU⁺/BrdU⁺. Data represent mean of the cells reentering and exiting the cycle in each area of the subventricular zone ± SEM (n=5, * p<0.05; ** p<0.01, Student's t test).

Table 10: Statistical analysis of the cell cycle index in the subventricular zone of animals injected with AREG. Data presented as mean±SEM.

		Group	Mean±SEM	Normality test	Statistical test
RMS	Exit	Ctrl	0.367±0.035	0.552	$t_{(8)}=3.543$;
		200ng/mL	0.210±0.027	0.530	$p<0.01$;
	Reentry	Ctrl	0.633±0.035	0.552	$t_{(8)}=3.543$;
		200ng/mL	0.790±0.027	0.530	$p<0.01$;
Dorsolateral	Exit	Ctrl	0.421±0.028	0.851	$t_{(8)}=2.639$;
		200ng/mL	0.272±0.049	0.179	$p<0.05$;
	Reentry	Ctrl	0.579±0.028	0.851	$t_{(8)}=2.639$;
		200ng/mL	0.728±0.049	0.179	$p<0.05$;
Ventral	Exit	Ctrl	0.390±0.053	0.906	$t_{(8)}=2.749$;
		200ng/mL	0.216±0.034	0.637	$p<0.05$;
	Reentry	Ctrl	0.610±0.053	0.906	$t_{(8)}=2.749$;
		200ng/mL	0.784±0.034	0.637	$p<0.05$;

4.1.2.3. Analysis of new neuroblasts in the SVZ

Considering the results observed in cell proliferation analysis we next evaluated if this could alter the number of newly formed neuroblasts in the SVZ. To dissect this, we calculated the number of DCX/BrdU double positive cells. In this analysis, animals that were injected with 200ng/mL of AREG displayed a 2.6-fold increase in the number of double positive cells at the dorsolateral area of the SVZ. In the ventral area of AREG injected animals an increase of 1.7 in the number of new neuroblasts was observed. No differences were observed between controls and the 200ng/mL of AREG group at the RMS. Similar to what was observed in the proliferation rate determined by BrdU labelling, animals that were administered with 25 and 100ng/mL of AREG did not differ from controls (Figure 15 A, B, Table 11, for post hoc tests see Table S4).

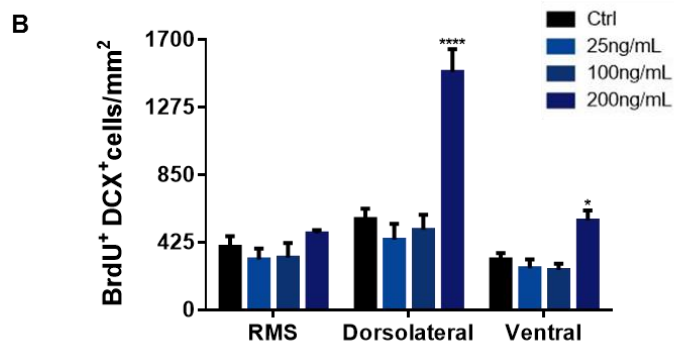
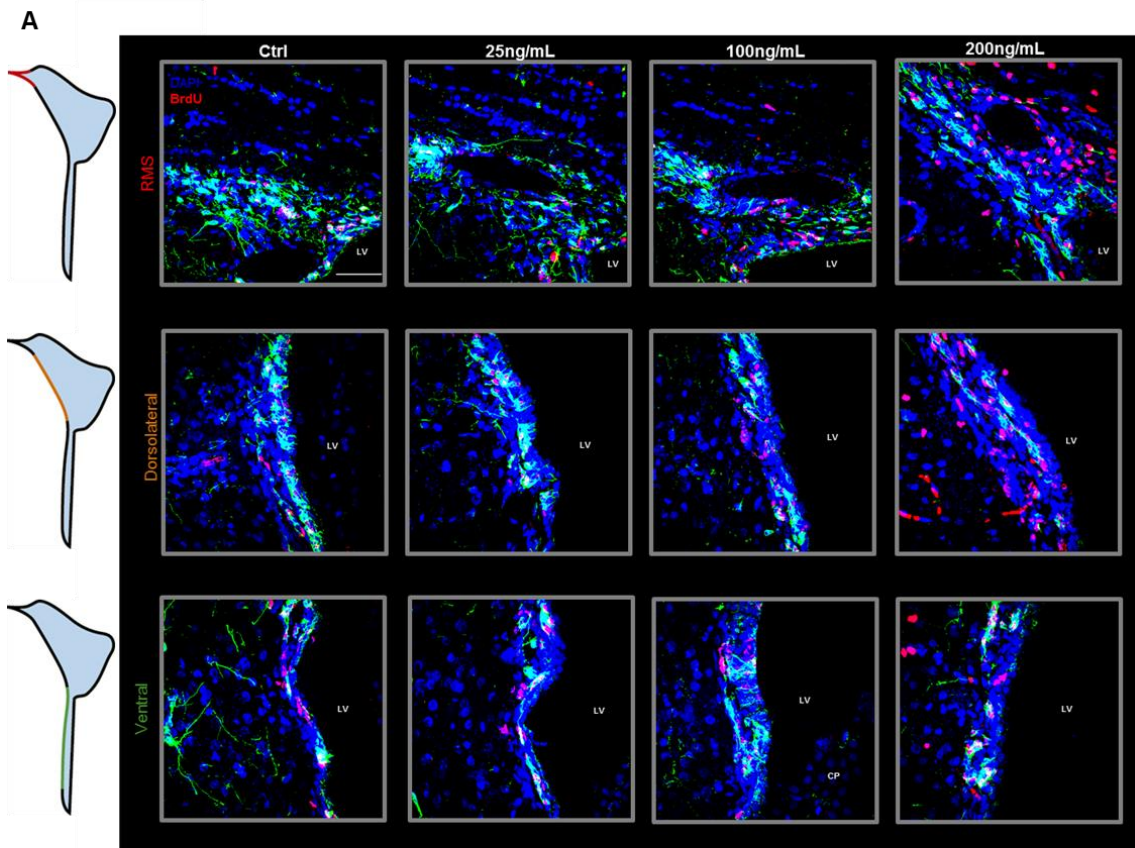


Figure 15: DCX⁺BrdU⁺ cells in the rostral migratory stream (RMS), dorsolateral and ventral areas of the subventricular zone of animals injected with 25, 100 or 200ng/mL of AREG. A) Representative images show DCX⁺BrdU⁺ cells distribution in the 3 different areas of the subventricular zone. Scale bar 50 μ m. B) Quantification of the DCX⁺BrdU⁺ cells in the different experimental conditions. Data represent mean of DCX⁺BrdU⁺ cells divided by the total area of each subventricular zone subdivision \pm SEM. (n=5, * p<0.05; **** p<0.0001, ANOVA).

Table 11: Statistical analysis of DCX⁺BrdU⁺ cells in the subventricular zone of animals injected with AREG. Data presented as mean±SEM.

	Group	Mean±SEM	Normality test	Homogeneity test	Statistical test
RMS	Ctrl	398.75±66.94	0.905	0.365	F _(3,16) =1.231; p>0.05;
	25ng/mL	319.90±68.19	0.454		
	100ng/mL	330.46±92.60	0.059		
	200ng/mL	482.03±21.98	0.541		
Dorsolateral	Ctrl	572.60±65.00	0.510	0.150	F _(3,16) =22.755; p<0.0001;
	25ng/mL	443.00±100.42	0.073		
	100ng/mL	504.51±95.03	0.146		
	200ng/mL	1498.70±142.83	0.719		
Ventral	Ctrl	319.45±39.75	0.767	0.801	F _(3,16) =8.187; p<0.01;
	25ng/mL	263.13±56.47	0.215		
	100ng/mL	252.99±39.76	0.365		
	200ng/mL	563.29±63.03	0.445		

4.2. Impact of IGFBP2 in neurogenesis

IGFBP2 is part of a protein family responsible for mediating the bioavailability and transport of IGFs. Given that this protein is secreted by the CP into the CSF, and the fact that it has been implicated in the modulation of other stem cell types, we evaluated if it impacts NSCs dynamics. For this, we used an experimental design similar to the described previously (sections 3.3 and 3.4) and the results are described in detail below.

4.2.1. IGFBP2 can impact growth of hNPCs?

4.2.1.1. Clonal assay

We cultured hNPCs under conditions that promoted their self-renewal and exposed them to one of the following concentrations of IGFBP2: 25, 100 and 200ng/mL. A significant increase in the number of formed neurospheres was observed when cells were exposed to 100 and 200ng/mL of the protein. The most significant effect was observed for the highest concentration, where the number of formed neurospheres increased 3.4 times when compared with the control group. Although it was not significant,

cells cultured in medium containing 25ng/mL of IGFBP2 also presented a slight increase in the number of formed neurospheres when compared with the control group (Figure 16, Table 12, for post-hoc testes see Table S5).

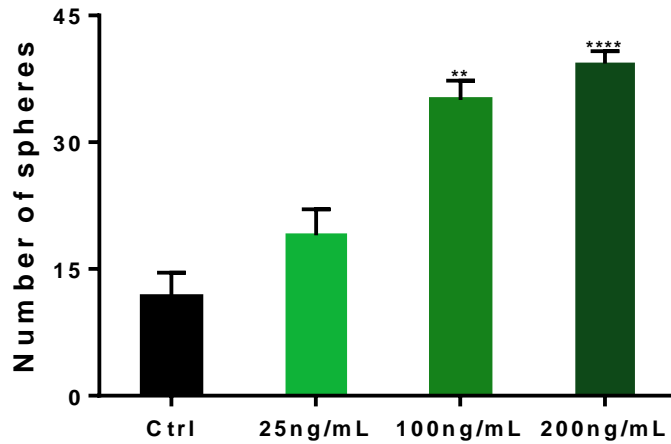


Figure 16: Clonal assay in hNPCs exposed to IGFBP2. Quantification of the number of formed neurospheres when cell were exposed to 25, 100 and 200ng/mL of IGFBP2. Results correspond to a representation of 3 independent assays. Data represent the mean number of neurospheres \pm SEM (n=3, ** p<0.01, **** p<0.0001, ANOVA).

Table 12: Statistical analysis of the clonal assay with IGFBP2. Data presented as meanSEM.

Group	Mean \pm SEM	Normality test	Homogeneity test	Statistical analysis
Ctrl	11.67 \pm 2.91	0.780		
25ng/mL	19.00 \pm 3.06	0.363	0.592	F _(3,8) =27.117; p<0.0001;
100ng/mL	35.00 \pm 2.31	1.000		
200ng/mL	39.33 \pm 1.45	0.780		

4.2.1.2. Differentiation assay

Using the same approach as before (section 3.3.2), we assessed if addition of different concentrations of IGFBP2 to the culture medium could impact the differentiation of hNPCs. Exposure to the two highest concentration of the protein caused a significant increase in the number of BrdU⁺ cells and the number of BrdU⁺ β III-Tubulin⁺ cells (newborn neurons). This increase was most notable for 200ng/mL of IGFBP2. No differences were observed between the control group and the cells exposed to 25ng/mL of IGFBP2 (Figure 17, Table 13, for post-hoc testes see Table S6).

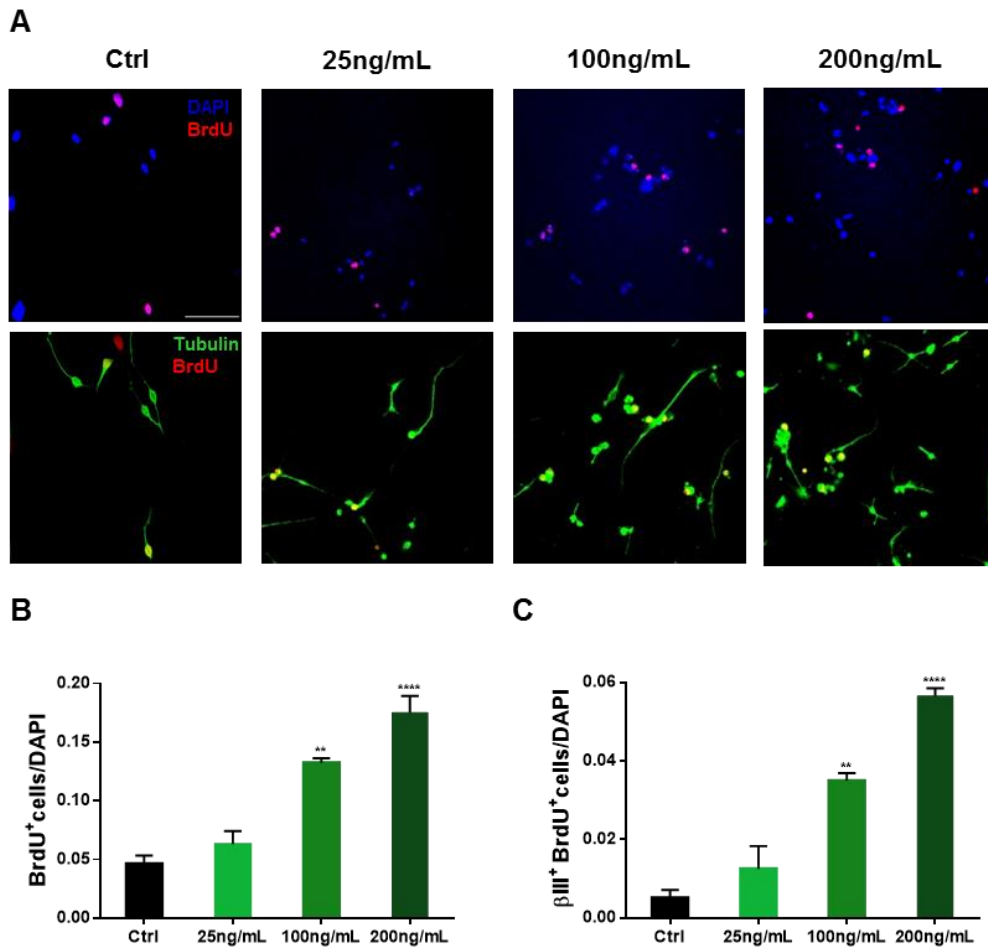


Figure 17: Differentiation assay in hNPCs exposed to IGFBP2. A) Representative images of BrdU⁺ and β III-Tubulin⁺BrdU⁺ cells in the upper and lower panels, respectively, of hNPCs exposed to 25, 100 and 200ng/mL of IGFBP2. Scale bar 50 μ m. B) Quantification of BrdU⁺ cells in the different experimental conditions. Results correspond to a representation of 3 independent assays. Data represent mean percentage of BrdU⁺ cells divided by the total number of cells \pm SEM (n=3, ** p<0.01, **** p<0.0001, ANOVA). C) Quantification of β III-Tubulin⁺BrdU⁺ cells exposed to increasing concentrations of IGFBP2. Results correspond to a representation of 3 independent assays. Data represent mean number of β III-Tubulin⁺BrdU⁺ cells divided by the total number of cells \pm SEM (n=3, ** p<0.01, **** p<0.0001, ANOVA).

Table 13: Statistical analysis of the differentiation assay with IGFBP2. Data presented as mean±SEM.

	Group	Mean±SEM	Normality test	Homogeneity test	Statistical test
BrdU ⁺ cells	Ctrl	0.046±0.007	1.000	0.485	F _(3,8) =36.825; p<0.0001;
	25ng/mL	0.063±0.011	1.000		
	100ng/mL	0.133±0.004	1.000		
	200ng/mL	0.175±0.014	1.000		
βIII-Tubulin ⁺ BrdU ⁺ cells	Ctrl	0.005±0.002	1.000	0.342	F _(3,8) =47.559; p<0.0001;
	25ng/mL	0.013±0.006	1.000		
	100ng/mL	0.035±0.002	1.000		
	200ng/mL	0.057±0.002	1.000		

4.2.2. IGFBP2 impact in SVZ neurogenesis

As explained in detail in section 3.4, adult rats received four injections (6h interval between injections) of one of the subsequent concentrations of IGFBP2: 25, 100 and 200ng/mL. The effects of these injections in cell proliferation and formation of new neuroblasts at the SVZ was then evaluated. Results will next be presented.

4.2.2.1. Effects of IGFBP2 in cell proliferation in the SVZ

When we determined the proliferation rate by BrdU labelling an increase in proliferation in the dorsolateral area of animals injected with 100 and 200ng/mL of IGFBP2 was observed. This increase was 2-fold in animals that received the highest dose of IGFBP2. Furthermore, animals receiving 200ng/mL of IGFBP2 increased 1.8-fold the number of BrdU⁺ cells in the ventral area. Even though it is not statistically significant, a slight increase in the number of BrdU⁺ cells at the dorsolateral area of animals injected with 25ng/mL and also an increase at the ventral area of animals injected with 100ng/mL was observed. No significant differences were observed in the RMS (Figure 18, Table 14, for post-hoc testes see Table S7). Given the fact that 200ng/mL was the concentration that had a more pronounced effect in the number of BrdU⁺ cells we decided to assess the proliferation rate of this group of animals using another proliferation marker, Ki67. Results show an increase of 1.2 times in cell proliferation, as evaluated by Ki67 staining at the dorsolateral area, while no differences were observed at the RMS and ventral areas (Figure 19, Table 15).

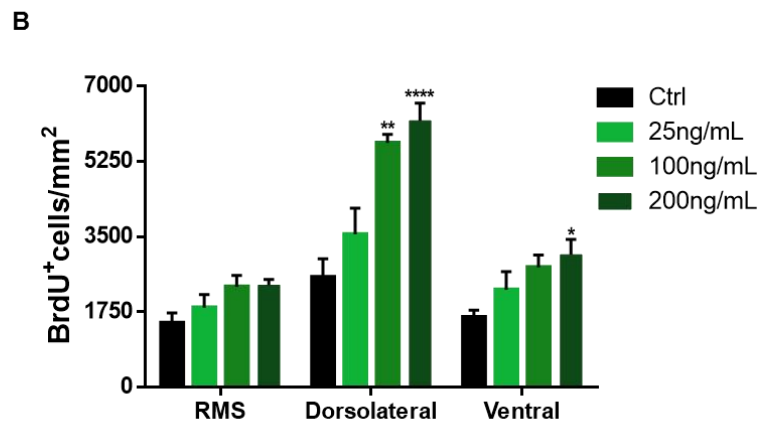
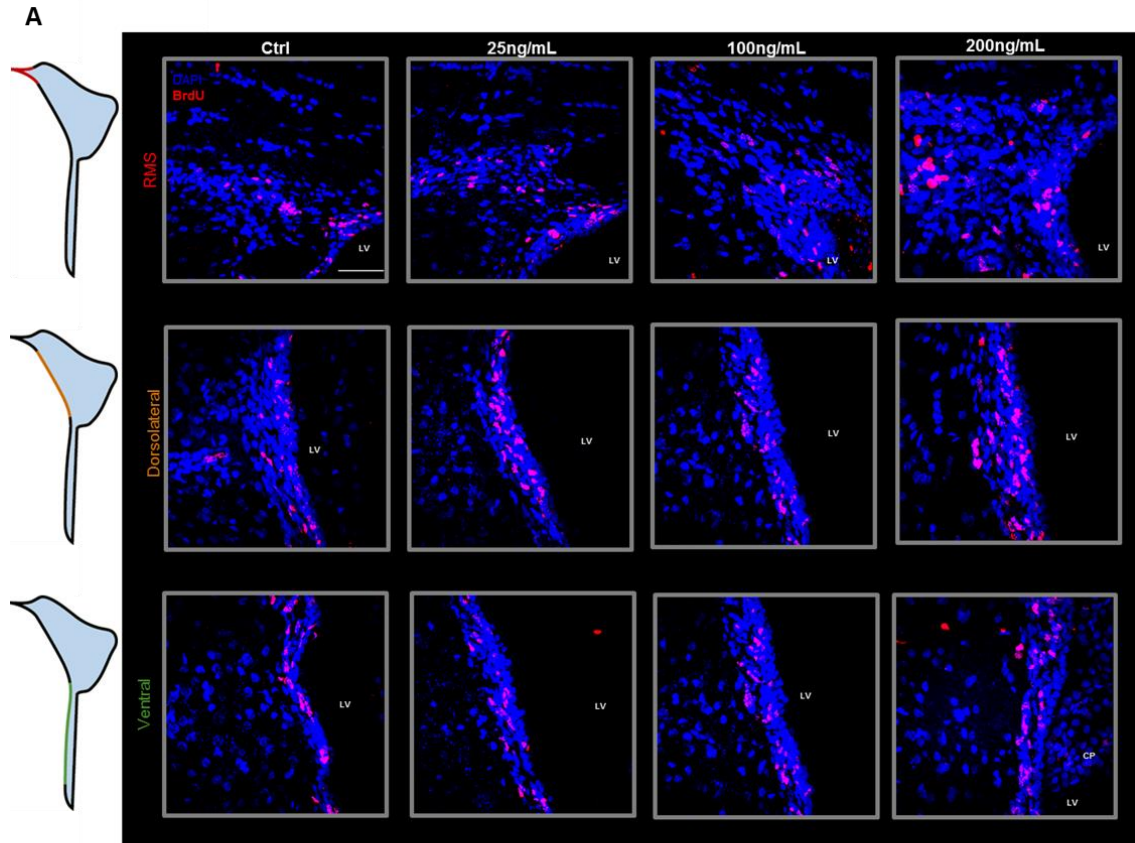


Figure 18: BrdU⁺ cells in the rostral migratory stream (RMS), dorsolateral and ventral areas of the subventricular zone of animals injected with 25, 100 or 200 ng/mL of IGFBP2. A) Representative images show BrdU⁺ cells distribution in the 3 different areas of the subventricular zone. Scale bar 50µm. B) Quantification of the number of BrdU⁺ cells in the different experimental conditions. Data represent mean of BrdU⁺ cells divided by the total area of each subventricular zone subdivision ± SEM (n=5, * p<0.05; ** p<0.01; **** p<0.0001, ANOVA).

Table 14: Statistical analysis of BrdU+ cells in the subventricular zone of animals injected with IGFBP2. Data presented as mean±SEM.

	Group	Mean±SEM	Normality test	Homogeneity test	ANOVA
RMS	Ctrl	1496.86±234.76	0.177	0.664	$F_{(3,16)}=3.037;$ $p>0.05;$
	25ng/mL	1852.59±303.39	0.460		
	100ng/mL	2339.59±262.66	0.169		
	200ng/mL	2379.83±134.12	0.483		
Dorsolateral	Ctrl	2565.57±422.75	0.937	0.268	$F_{(3,16)}=15.494;$ $p<0.0001;$
	25ng/mL	3553.05±614.17	0.540		
	100ng/mL	5683.32±200.27	0.088		
	200ng/mL	6196.01±413.73	0.636		
Ventral	Ctrl	1629.62±164.08	0.927	0.379	$F_{(3,16)}=3.949;$ $p<0.05;$
	25ng/mL	2272.75±417.25	0.983		
	100ng/mL	2790.32±286.53	0.224		
	200ng/mL	3082.66±359.01	0.722		

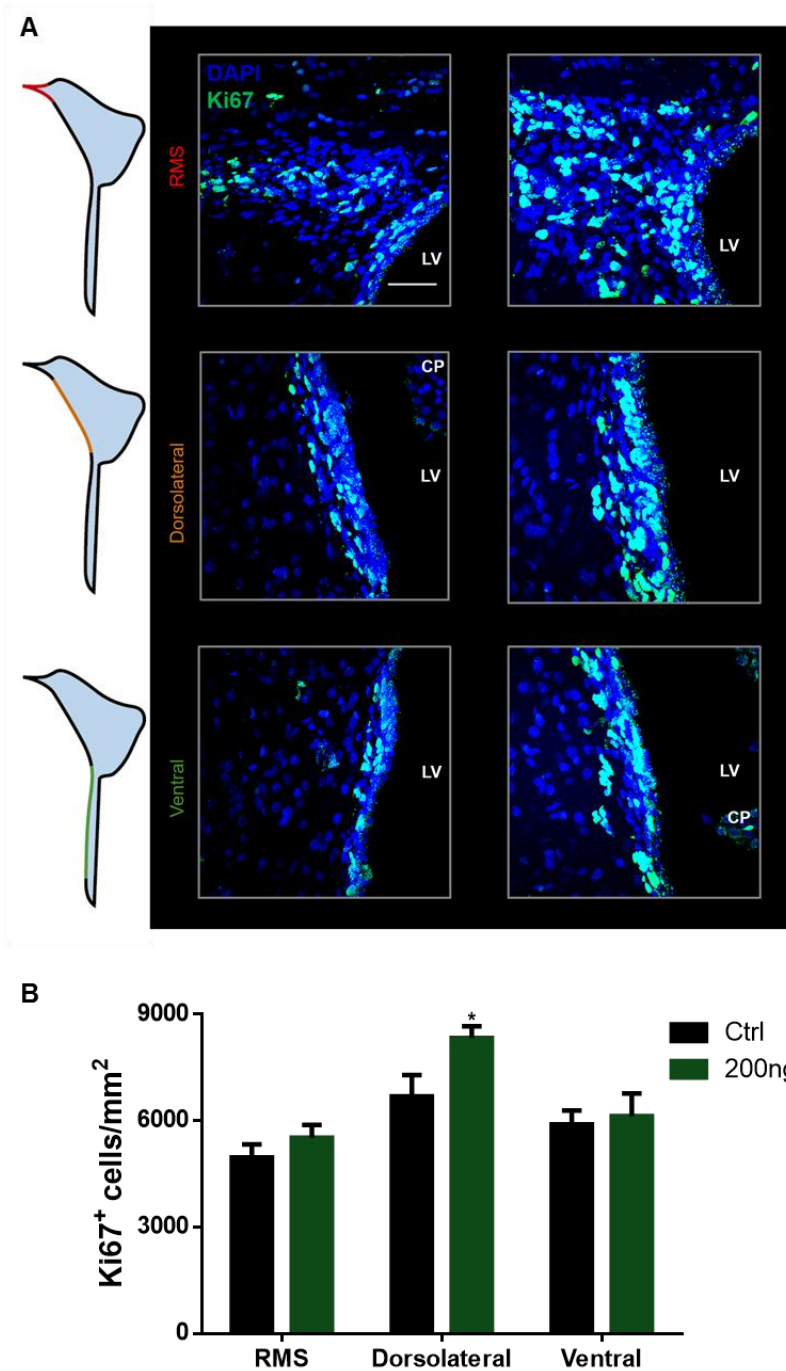


Figure 19: Ki67⁺ cells of animals injected with 200ng/mL of IGFBP2 in the rostral migratory stream (RMS), dorsolateral and ventral areas of the subventricular zone. A) Representative images show Ki67⁺ cells along the three different areas of the subventricular zone. Scale bar 50 μ m. B) Quantification of the Ki67⁺ cells in the different experimental conditions. Data represent mean percentage of Ki67⁺ cells divided by the total area of each subventricular zone subdivision \pm SEM (n=5, * p<0.05, Student's t test).

Table 15: Statistical analysis of Ki67⁺ cells in the subventricular zone of animals injected with IGFBP2. Data presented as mean±SEM.

	Group	Mean±SEM	Normality test	Statistical test
RMS	Ctrl	4961.42±371.34	0.900	$t_{(8)}=1.074$; $p>0.05$;
	200ng/mL	5520.36±364.62	0.529	
Dorsolateral	Ctrl	6689.00±599.08	0.758	$t_{(8)}=2.416$; $p<0.05$;
	200ng/mL	8339.60±328.62	0.272	
Ventral	Ctrl	5900.88±389.53	0.022	$U=10.000$; $p>0.05$
	200ng/mL	6129.35±636.76	0.330	

4.2.2.2. Effects of IGFBP2 in cell cycle index

Considering the increase in proliferation observed in animals injected with 200ng/mL of IGFBP2 we performed a cell cycle index to evaluate if these alterations affect the number of cells exiting and reentering the cell cycle. Animals injected with IGFBP2 presented a significant decrease in the number of cells exiting the cell cycle and an increase in the number of cells reentering the cycle at the dorsolateral and ventral areas. No differences were observed between controls and injected animals in the cell cycle index at the RMS (Figure 20, Table 16).

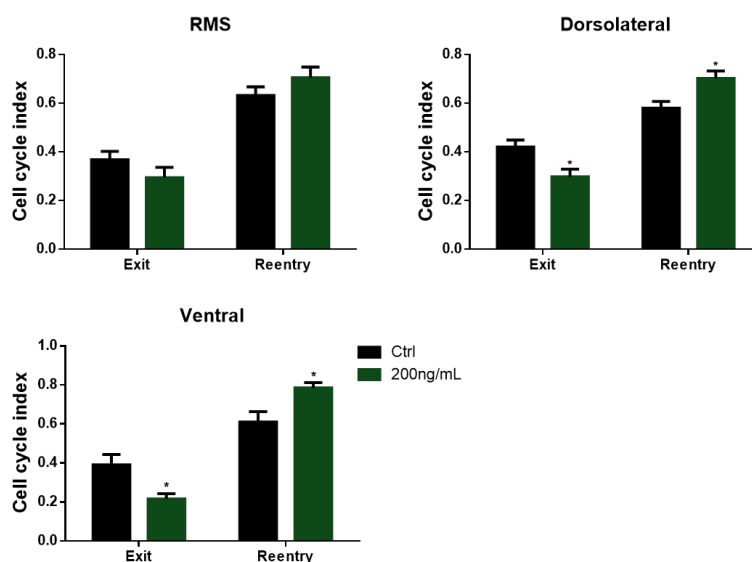


Figure 20: Cell cycle index of animals injected with 200ng/mL of IGFBP2 in rostral migratory stream (RMS), dorsolateral and ventral areas of the subventricular zone. Number of cells exiting the cell cycle are determined according to the ration of Ki67⁺BrdU⁺/BrdU⁺, while cells reentering the cell cycle are determined according to the ratio Ki67⁺BrdU⁺/BrdU⁺. Data represent the mean of cells reentering and exiting the cycle in each area of the subventricular zone ± SEM (n=5, * $p<0.05$, Student's t test).

Table 16: Statistical analysis of cell cycle index in the subventricular zone of animals injected with IGFBP2. Data presented as mean±SEM.

		Group	Mean±SEM	Normality test	Statistical test
RMS	Exit	Ctrl	0.367±0.035	0.552	$t_{(8)}=1.321$;
		200ng/mL	0.294±0.043	0.521	$p>0.05$;
	Reentry	Ctrl	0.633±0.035	0.552	$t_{(8)}=1.321$;
		200ng/mL	0.706±0.043	0.521	$p>0.05$
Dorsolateral	Exit	Ctrl	0.421±0.028	0.851	$t_{(8)}=2.926$;
		200ng/mL	0.298±0.031	0.424	$p<0.05$;
	Reentry	Ctrl	0.579±0.028	0.851	$t_{(8)}=2.926$;
		200ng/mL	0.702±0.031	0.424	$p<0.05$;
Ventral	Exit	Ctrl	0.390±0.053	0.906	$t_{(8)}=2.911$;
		200ng/mL	0.216±0.028	0.992	$p<0.05$;
	Reentry	Ctrl	0.610±0.053	0.906	$t_{(8)}=2.911$;
		200ng/mL	0.784±0.028	0.992	$p<0.05$;

4.2.2.3. Effects of IGFBP2 in the number of newly formed neuroblasts at the SVZ

Considering the increase in proliferation we next evaluated if this could impact the number of new neuroblasts (DCX⁺BrdU⁺ cells) at the SVZ. This analysis showed a 4-fold increase in the number of BrdU⁺DCX⁺ in the dorsolateral and a 2-fold increase in the ventral area of animals injected with 200ng/mL of IGFBP2. Animals injected with 100ng/mL of IGFBP2 presented almost 3 times more neuroblasts in the dorsolateral area. No differences were observed between control group and the animals injected with 25ng/mL of IGFBP2 (Figure 21, Table 17, for post-hoc testes see Table S8).

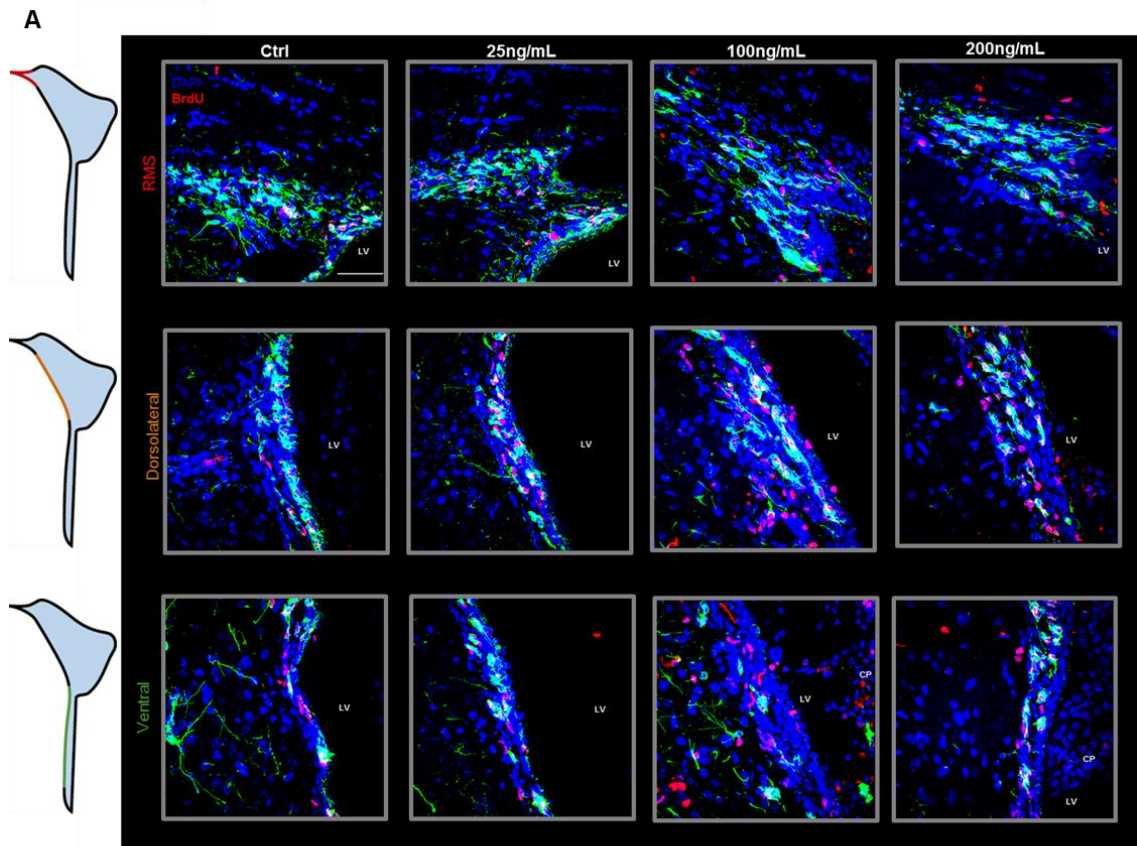


Figure 21: DCX⁺BrdU⁺ cells in the rostral migratory stream (RMS), dorsolateral and ventral areas of the subventricular zone of animals injected with 25, 100 or 200ng/mL of IGFBP2. A) Representative images show DCX⁺BrdU⁺ cells distribution in the 3 different areas of the subventricular zone. Scale bar 50µm. B) Quantification of the DCX⁺BrdU⁺ cells in the different experimental conditions. Data represent mean of DCX⁺BrdU⁺ cells divided by the total area of each subventricular zone subdivision ± SEM. (n=5, * p<0.05; ** p<0.01; **** p<0.0001, ANOVA).

Table 17: Statistical analysis of DCX+BrdU+ cells in the subventricular zone of animals injected with IGFBP2. Data presented as mean±SEM.

	Group	Mean±SEM	Normality test	Homogeneity test	Statistical test
RMS	Ctrl	398.75±66.94	0.905	0.848	$F_{3,16}=3.508;$ $p<0.05$
	25ng/mL	627.16±82.79	0.337		
	100ng/mL	673.75±54.53	0.212		
	200ng/mL	652.50±65.32	0.202		
Dorsolateral	Ctrl	572.60±65.00	0.510	0.387	$F_{(3,16)}=20.745;$ $p<0.0001;$
	25ng/mL	1194.55±163.08	0.567		
	100ng/mL	1497.85±162.19	0.164		
	200ng/mL	2240.79±188.41	0.539		
Ventral	Ctrl	319.45±39.75	0.767	0.036	Welch's $F_{(3,7.861)}=3.700;$ $p<0.05;$
	25ng/mL	691.26±138.66	0.418		
	100ng/mL	643.68±107.85	0.866		
	200ng/mL	761.83±95.04	0.377		

4.3. Analysis of CPs transcriptome in key developmental stages

4.3.1. RNA quality control

As explained in detail in section 3.5.2, the concentration and quality of the extracted RNA was assessed using the RNA StdSenses Analysis Kit (BioRad) that measures the RNA quality by the RQI. This method, returns a number between 1 (highly degraded) and 10 (intact RNA). Table 18 summarizes the results from the quality assessment. All samples presented a high RQI indicating that the extracted RNA was of high quality.

Table 18: Concentration and quality of the extracted RNA assessed with the RNA StdSenses Analysis Kit.

Age	Sample number	Concentration (ng/ μ L)	$\frac{28S}{18S}$	RQI
P1	1	140.9	1.64	9.9
	2	156.7	1.71	9.9
	3	56.3	1.65	9.9
P4	4	218.2	1.58	9.8
	5	321.9	1.48	9.7
	6	234.4	1.39	9.8
P7	7	189.0	1.70	9.9
	8	198.5	1.42	9.6
	9	437.7	1.63	9.9
P10	10	178.7	1.47	9.8
	11	381.4	1.45	9.6
	12	484.1	1.41	9.7
P60	13	395.9	1.23	9.5
	14	617.7	1.26	9.6
	15	457.8	1.23	9.4

4.3.2. cDNA library quality control

After assessment of RNA quality, we proceeded to the construction of cDNA library according to what is described in section 3.5.3. Samples were multiplexed and quality control of cDNA library was performed using an Agilent Bioanalyzer 2100. According to manufacturer instructions, the presence of a peak near 140bp indicates priming, while a second peak between 1000-9000bp is an indication of overcycling. Summary of the quality control indicate that the multiplexed library presented a good quality, thus indicating that samples were viable to perform the sequencing protocol (Figure 22).



Figure 22: Per base sequence quality. Provides an overview of the quality values of all sequenced bases in each sample file. Each line represents a sample. Samples quality is classified according to their score represented by the y-axis. The y-axis is divided into “very good quality samples” (green), “reasonable quality” (orange) and “poor quality” (red).

4.3.3. Quality control of RNA seq data: MultiQC report

As mentioned before (section 1.6) another goal of this work was to analyze the CP transcriptome in specific stages of development performing RNA-Seq (section 3.5.5). Quality control of raw data from the high throughput sequencing was performed using the MultiQC tool and the summary of the analysis will be presented next.

4.3.3.1. Per base sequence quality

The per base sequence quality score presents an overview of the range of quality values across all bases at each position in the raw data file. The y-axis on the graph contains the quality scores, the higher the score the better the quality. The background of the graph presents different colors, which divides the y-axis into “very good quality samples” (green), “reasonable quality” (orange) and “poor quality” (red). According to our MultiQC report, all samples are plotted in the green area of the graph, which indicates that all samples present a very good quality (Figure 23).

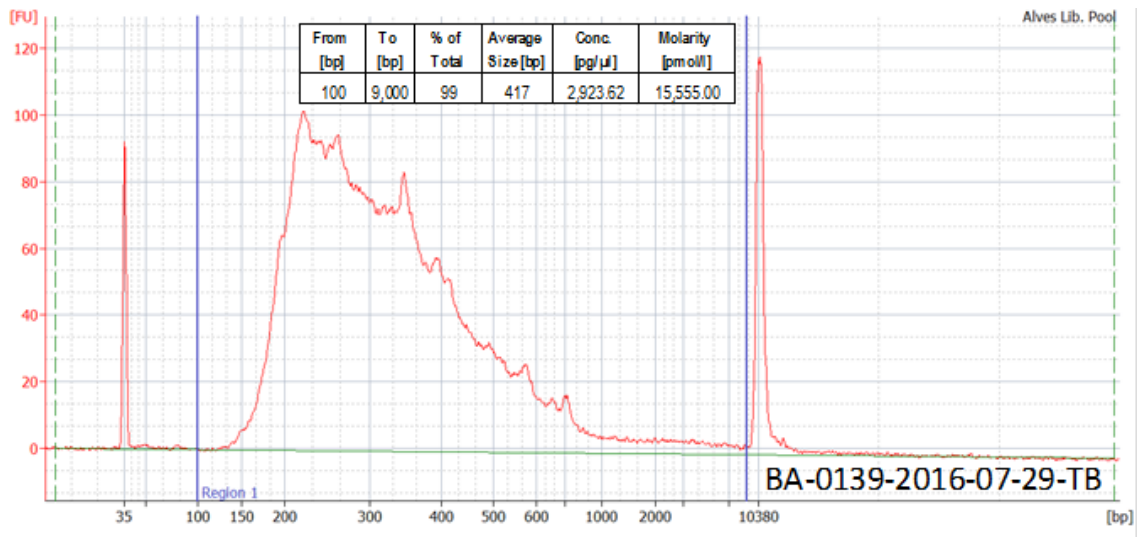


Figure 23: Summary of the quality control of the multiplexed cDNA library using Agilent Bioanalyzer 2100.

4.3.3.2. Per sequence quality score

This parameter allowed us to evaluate if a subset of our sequences has universally low quality, thus determining whether low quality bases are located in a specific region or distributed across all reads. X-axis represent the mean quality and y-axis shows the number of reads. According to the report, these low-quality samples should represent a small percentage, and the majority should have a score higher than 20 in the x-axis. Our quality control report, shows that only a small percentage of our sequences have a low-quality score located in a specific region, with the majority of the samples present a score higher than 20 (Figure 24).

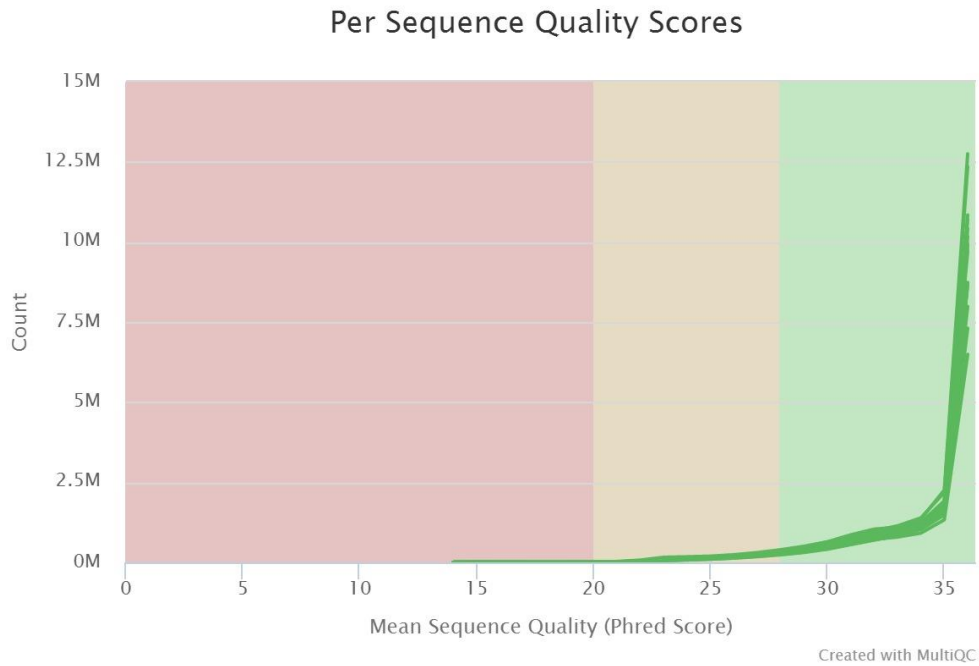


Figure 24: Per sequence quality score. Plot of the average quality of a read according to the distribution of this average quality. The X-axis represent the mean quality and y-axis shows the number of reads. X-axis is divided in three colored areas according: green- “very good quality samples”; orange- “reasonable quality”; red- “poor quality”.

4.3.3.3. Per base N content

If a sequencer is unable to identify a nucleotide with confidence, it will tag the sequenced nucleotide as an N instead of A, T, C or G. Per base N content represents the percentage of base identifications at each position for which an N was indicated. The x-axis represents the read position while the y-axis corresponds to the percentage of Ns among all reads. It is expected that high-quality samples present a low percentage of N content in each sample. Our quality control analysis revealed that all our samples display a very low percentage of N content, indicative of a high quality (Figure 25).

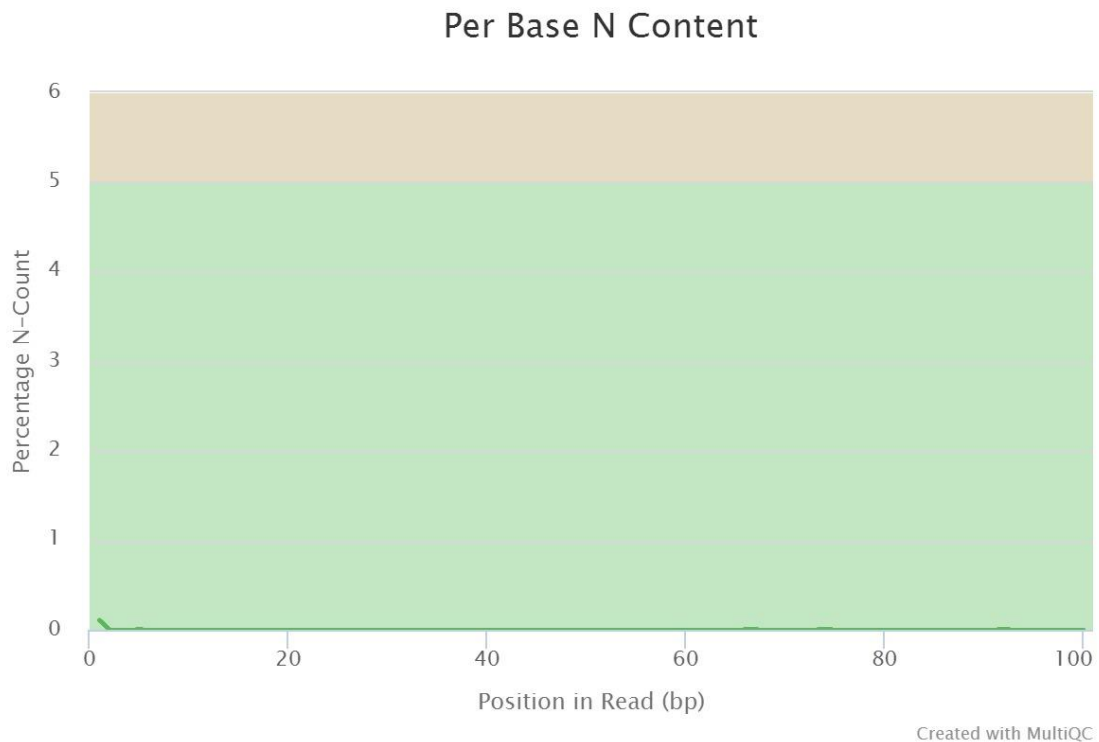


Figure 25: Per base N content. This graph represents the percentage of base calls at each position for which an N was identified. The x-axis represents the read position while the y-axis corresponds to the percentage of Ns among all reads.

Overall, this quality analysis indicates that all sequenced samples present a good quality allowing us to proceed with the data analysis.

Currently we are running the analysis which was not complete by the end of this work, so no further results will be presented regarding CPs transcriptome analysis.

5. Discussion

NSCs reside in specialized regions that promote their self-renewal or their differentiation into neuronal cells. During embryonic development, they exist through the developing brain whereas in the adult mammalian brain they are restricted to two major neurogenic niches, the SVZ and the subgranular zone of the dentate gyrus in the hippocampus⁸. The proper balance between intrinsic and extrinsic signaling is essential to modulate stem cells quiescence, self-renewal, activation and differentiation⁴⁰. Besides its essential role for the production of new neurons under physiological conditions, these neurogenic niches potentially constitute an endogenous source of therapies for several CNS disorders⁴⁰. Thus, there has been an increasing effort in uncovering the different players involved in the modulation of these niches. The SVZ, the major source of NSCs in the adult mammalian brain, is constituted by three different cells types⁸². Type B or progenitor cells divide and give rise to type C cells, which are rapid proliferating cells, that in turn divide to give rise to type A cells, or neuroblasts, the immature neurons that migrate towards the OBs to differentiate into mature neurons⁸². This layer of cells lines in the SVZ of the lateral brain ventricles, which are filled with CSF⁸². In fact, type B cells, project their apical process into the brain ventricles being under direct influence of the molecules that constitute the CSF⁸². Taking into account the fact that the CP is the major producer and modulator of the CSF composition, it is expected that its secretome has an impact in the NSCs of the SVZ and consequently in their progeny¹⁶. Despite its proximity with the SVZ and the fact that this is the major modulator of CSF composition, detailed information on how each CP derived molecule impacts neurogenesis is not completely available^{13,14,16,65,83}.

The work developed and presented here aimed at analyzing if CP transcribed and secreted proteins can impact the SVZ. To achieve this purpose, based on a previous transcriptome analysis of the adult CP under physiological conditions, we selected two proteins, AREG and IGFBP2⁷¹, for which there are no studies assessing its impact in SVZ cells. We then applied both *in vitro* and *in vivo* studies to evaluate if these proteins influence NSCs and their progeny. Using these two approaches, we were able to pinpoint some contributions of this proteins in cell proliferation, cell cycle and neuroblasts determination.

Overall, *in vitro*, we were able to show that both AREG and IGFBP2 modulate hNPCs proliferation and differentiation into immature neurons. Furthermore, *in vivo*, we provide the first insights of its participation in proliferation and cell cycle modulation at the SVZ of adult rats. We will next discuss in detail the significance of the data obtained for each protein.

5.1. Amphiregulin impact in the neural stem cells modulation

AREG binds to the EGFR promoting homo or heterodimerization of the receptor, which will result in self-phosphorylation of the intracellular tyrosine kinase domains and subsequent recruitment of several proteins that will activate downstream signaling pathways⁸⁴. Through its signaling, EGFR regulates cellular processes such as, proliferation, migration and also cell differentiation⁸⁵. Specifically, AREG signaling is described to modulate cell proliferation, apoptosis and migration of different cell types including epithelial cells, fibroblasts and immune cells⁸⁴. Furthermore, AREG was shown to be essential for the *in vitro* formation of floating mammospheres through activation of the mitogen activated protein kinase (MAPK) signaling pathway⁸⁶. AREG is also implicated in the *in vitro* proliferation of human keratinocytes⁸⁷. Moreover, it has also been shown as overexpressed in myeloma cells and as capable of promoting the growth and production of bone marrow stromal cells⁸⁸.

In the nervous system AREG is expressed in the CP^{71,73} and in the hippocampus of adult brain⁷³. Interestingly, in the SVZ, the AREG receptor EGFR is expressed in activated NSCs (type B cells), TAPs (type C cells) and neuroblasts (type A cells). Until now the only evidence regarding the impact of AREG in NSCs is from an *in vitro* experiment that demonstrates the normal growth of adult mouse neurospheres when EGF in the culture medium was replaced by AREG⁷³. This adds to other evidences, supporting the role of other EGF family members, that act via EGFR, in the modulation of NSCs. For example, EGF *in vitro* induces proliferation, self-renewal and expansion of both embryonic and adult NSCs⁵⁵. Furthermore, infusion of EGF in the lateral ventricle increases the proliferation at the SVZ with the majority of EGF responsive cells being type C cells⁵⁵. Finally, also TGF- α , another EGF family member, induced proliferation and differentiation of SVZ-NSCs *in vitro*⁸⁹. Thus, current evidence in the literature points that AREG, namely CP derived AREG, might potentially modulate NSCs dynamics, which we explored in this thesis and next discuss.

5.1.1. AREG enhances proliferation

To assess if AREG could influence the proliferation of NSCs we used both *in vitro* and *in vivo* approaches, and tested three different protein concentrations (25, 100 and 200ng/mL). Globally, both *in vitro* and *in vivo* results indicate that AREG increases cell proliferation when compared with control conditions. Specifically, *in vitro*, and regarding the clonal assay all tested concentrations induced an increase in the number of formed spheres, whereas in the differentiation assay only the two lowest concentrations

resulted in an increase of BrdU positive cells. The fact that cells exposed to the highest AREG concentration did not display an increased proliferation rate, when compared with controls, might be explained by a receptor internalization process. In fact, it has previously been reported that high concentrations of AREG (100nM) in the culture medium of HeLa cells lead to receptor internalization, which did not readily return to the surface, possibly due to a slowdown in its recycling⁹⁰. To further dissect if this hypothesis is occurring also in hNPCs, we could perform EGFR internalization analysis, determining the amount of the receptor present at the surface of the cell by labelling of the unpermeabilized and fixed cells with anti-EGFR antibody conjugated with FITC, followed by quantification of the amount of EGFR labeling through flow cytometry⁹⁰.

Concerning, the *in vivo* analysis of the cell proliferation rate using BrdU as an exogenous marker, the infusion of 200ng/mL of AREG significantly increased the proliferation at the three different areas of the SVZ (RMS, dorsolateral and ventral). Of notice, the highest increase was registered along the dorsolateral and ventral areas, which correspond to the areas that contain TAPs (type C cells), the cell type that presents the highest level of expression of EGFR⁵⁵.

Stemming from the data obtained in the proliferation assays *in vitro* and *in vivo* is the fact that for the highest AREG concentration used, the data obtained differ. In this sense, it should be noted that when performing *in vitro* and *in vivo* assays it is essential to be aware of the fact that the *in vitro* assay is not always translatable *in vivo*. Several critical conditions, such as the introduction of a saturating amount of exogenous factors or cell density, might bias the experiment⁷⁶. Nevertheless, *in vitro* assays can be seen as a complement of the *in vivo* studies, that despite the need of future technique improvement, allow us to identify functional properties of stem cells, self-renewal and differentiation⁷⁶. Therefore, even though our *in vivo* and *in vitro* results indicate that AREG has impact in NSCs (or their progeny), the differences observed between the effects of the different concentrations in the *in vitro* and *in vivo* approaches might be explained by technical specificities and limitations as mentioned above.

It should also be noted that, considering our experimental design, our first approach was to perform the *in vitro* studies by isolating NSCs from the SVZ of the animal model applied in the *in vivo* analysis. However, despite our efforts, some technical conditions, related with the high sensibility of these cells to alterations in the CO₂ and temperature, hampered establishing cultures of rat NSCs in our lab. So, considering the available options at our lab we decided to perform our *in vitro* analysis using hNPCs.

Since BrdU is incorporated during the S-phase of the cell cycle⁸⁰, the increase in proliferation of animals infused with the highest dose of AREG is probably associated with a higher number of cells in S-phase at

the SVZ. To further understand this, we used an endogenous proliferation marker, Ki67, that is expressed in all phases of the cell cycle except G₀⁸⁰. Assessment of the proliferation rate determined by this marker revealed a significant increase at the dorsolateral area of animals injected with 200ng/mL of AREG. In support of our results, betacelullin, a protein from the EGF family was shown to induce proliferation of NSC at the SVZ through the heterodimerization of EGFR and ERB4, activating MAPK and AKT signaling pathways⁹¹. To obtain insights into the signaling pathway triggered by AREG we should next assess phosphorylation of the AREG receptors through Western blot⁹¹ and perform RT-PCR targeting the activation of downstream signaling pathways⁹².

5.1.2. AREG induces cell cycle reentry in proliferating cells of the SVZ

Alterations in cell proliferation at the neurogenic niches might be associated with changes in the number of cells entering and exiting the cell cycle. In fact, it was recently reported that the decrease of neurogenesis with aging, at the SVZ, is related with a deregulation of the cell cycle machinery, where a decrease in activated NSCs proliferation is related with the lengthening of G₁ phase of the cell cycle⁹³. Another study, reported that dopamine, through the release of EGF increases proliferation of SVZ-derived cells, with a higher number of cells in the S-phase of the cell cycle⁹⁴. Thus, we hypothesized that the increase in proliferation promoted by the injection of 200ng/mL of AREG might cause a decrease in the number of cells exiting the cycle. Consistently our results, from the cell cycle index, indicate that there is an increase in the number of cells reentering the cell cycle and consequently a decrease in the number of cells exiting the cell cycle. As mentioned before phosphorylation of EGFR activates downstream signaling pathways, such as MAPK/ERK, that when activated regulate both cytosolic proteins and transcription factors involved in cell cycle progression⁹⁵. For example, sustained activation of ERK1/2 in normal cells is essential for efficient G₁-S phase progression⁹⁶.

5.1.3. AREG increase the number of immature neurons

Given the increase in proliferation observed in our experiments, we decided to evaluate if this increase could impact the number of newborn immature neurons. Both our *in vitro* and *in vivo* results suggest that there is an increase in the number of newly generated neurons. Specifically, in our *in vitro* assay, cells exposed to 25ng/mL of AREG significantly increased the number of new neurons: although not statistically significant, cells exposed to 100ng/mL also increased the number of new neurons.

Animals injected with 200ng/mL of AREG significantly increased the number of newborn neuroblasts at the dorsolateral and ventral areas. In support of this finding, the effect of betacellulin, an EGFR ligand, as referred above, in cell proliferation also revealed an increase in the number of neuroblasts at the SVZ⁹¹. Interestingly, the increase in proliferation at the RMS did not result in an increase in the number of neuroblasts in this area, which might be explained by the fact that a 24h interval is not sufficient to induce effects in the number of observable neuroblasts at the RMS⁹¹.

5.2. IGFBP2 impact in neural stem cells modulation

The members of the IGF family play key roles in the regulation of processes such as cell proliferation, differentiation and apoptosis⁹⁷. This system includes two ligands, IGF1 and IGF2, two receptors, IGF1R and IGF2R and six IGFbps⁹⁷. The biological actions of IGFs is mediated by the binding to cell surface tyrosine kinase receptors⁹⁸. Binding of IGFs induces self-phosphorylation of the receptor and of downstream adaptor proteins that activate downstream signaling pathways⁹⁸. One of the major signaling pathways activated by IGF signaling is PI3K/AKT, leading to the activation of forkheadbox transcription factors of the FOXO family as well as GSK-3 β or mTOR complex, promoting cellular growth, translation, transcription and autophagy. The other signaling pathway is the Ras/MAPK pathway, that promotes the activation of three different kinases, ERK, JNK and p38, that mediate processes involved in gene expression and cell proliferation⁹⁸. During development, IGF1 is highly expressed in the spinal cord, midbrain, cerebral cortex, OBs and hippocampus³⁴. Its expression is reduced postnatally in all of the named areas except the OBs, where it maintains its high expression profile³⁴. During embryonic development, IGF2 is highly expressed by the meninges and the CPs and is also detected in the hypothalamus³⁴. It continues to be highly expressed by the meninges and the CPs in adulthood³⁴. IGF2 is the IGF most abundantly expressed in the adult brain. Given the essential role of the IGF signaling in growth and development it is crucial to maintain a proper regulation of its availability. IGFbps are key players responsible for this regulation⁹⁸. They serve different functions, including stabilization and regulation of the concentration of diffusible IGFs, facilitation of IGFs binding to its receptors and modulation of IGFs bioavailability in the extracellular space⁹⁸. All six IGFbps are expressed in the brain, presenting higher levels of expression during embryonic development than in the adult. IGFBP2 is highly expressed by CPs epithelial cells in particular, but also in astroglia, and controls the availability of both

IGF1 and IGF2, either inhibiting or enhancing their effects³⁴. Until now there are no evidences of IGFBP2 impact in the SVZ, nevertheless, IGFBP2 *per se* was shown to be capable of regulating the expansion and proliferation of hematopoietic stem cells⁹⁹ and to promote proliferation and survival of glioma stem cells¹⁰⁰. Taking this into account we will next discuss the data collected with the work developed in this thesis.

5.2.1. IGFBP2 enhances cells proliferation

To evaluate if IGFBP2 could impact proliferation of hNPCs and of cells of the SVZ niche we performed both *in vitro* and *in vivo* assays where we tested the effects of the exposure to three different concentrations of IGFBP2 (25, 100 and 200ng/mL). When we evaluated the proliferation rate, using BrdU as an exogenous marker, both approaches show that exposure to 100 and 200ng/mL of IGFBP2 induced an increase in proliferation. Specifically, in the *in vivo* approach, the effects were observed in the dorsolateral area of the SVZ, where 100 and 200ng/mL concentrations increased the number of BrdU positive cells. A similar effect was observed in the ventral area, but only the 200ng/mL concentration increased proliferation. Given the fact that the highest concentration had the most pronounced effect both in the *in vitro* and *in vivo* analysis we evaluated the effect of this concentration in the proliferation rate at the SVZ using Ki67, as the endogenous marker of proliferation. Proliferation rate assessed with this marker revealed an increase in cell proliferation at the dorsolateral area of animals injected with 200ng/mL of IGFBP2. In support of these results, a previous report showed that IGFBP2-null mice present decreased survival of hematopoietic stem cell⁹⁹. Moreover, IGFBP2 promotes proliferation and survival of glioma stem cells¹⁰⁰. Furthermore, considering the role of IGFBP2 as a modulator of IGFs, previous studies reported that IGF1 increases proliferation of adult NSCs from the hippocampus¹⁰¹. Additionally, increase in the expression of IGF1 increased proliferation of neuronal precursors at E14 and E17³⁵. IGF2 signaling, has been reported to promote NSCs proliferation through the activation of IGF1R¹⁵. Taking this in consideration and given the fact that IGFBP2 can either bind to IGF1 or IGF2 to modulate their signaling, we could perform a co-immunoprecipitation of CSF samples, which would allow us to study the dynamics of protein-protein interaction, by western blot analysis¹⁰².

Most important is the fact that despite the IGF-dependent functions of IGFBP2 several studies demonstrated that this protein has IGF-independent functions that promote proliferation and differentiation of different cell types. One of the mechanisms proposed for these independent actions of IGFBP2 suggests that it binds to cell surface integrin supporting cell proliferation¹⁰³. Furthermore, other

IGFBP family members also present IGF-independent actions. For example, IGFBP4 was described to inhibit Wnt signaling in heart cells by binding to Frizzled 8 and LDL receptor-related protein 6¹⁰⁴. Thus, considering this evidences it would be of great interest to explore the IGF-independent effect of IGFBP2 in the SVZ cell population.

5.2.2. IGFBP2 alters cell cycle index at the SVZ

Considering the alterations observed in cell proliferation observed in our *in vitro* and *in vivo* analysis, we decided to perform a cell cycle index based in the number of BrdU and Ki67 positive cells at the SVZ. Our results indicate that injections of 200ng/mL of IGFBP2 resulted in an increase of cells reentering the cell cycle and consequently a decrease in the number of cells exiting the cell cycle. Supporting our results, IGFBP2-null mice presented reduced cycling and upregulated expression of cell cycle inhibitors in hematopoietic stem cells⁹⁹. Moreover, a previous study reported that IGF1 signaling accelerated the cell cycle at the embryonic SVZ, by increasing the cell cycle reentry and decreasing the length of G₁ phase without significant alteration in S, G₂ and M phases³⁵. Furthermore, it was reported that IGF1 promotes G₁-S cell cycle progression regulating cyclins and cyclin-dependent kinase inhibitors via Pi3K/AKT pathway⁶⁹.

5.2.3. IGFBP2 increases the number of newborn neurons

Since our results showed that IGFBP2 increases cell proliferation we decided to assess, using *in vitro* and *in vivo* tests, if this increase in proliferation could result in an increase in the numbers of new neuroblasts. Both approaches indicate that upon 24h of exposure to 100 and 200ng/mL of IGFBP2 there was an increase in the number of new immature neurons. At the SVZ, this increase was observed at the dorsolateral and ventral areas, with no significant effects found at the RMS. A recent study reported that a mutant for IGF2 presented reduced NSCs proliferation and consequently a reduction in the number of immature neurons, further adding to the involvement of IGF signaling in the control of proliferation and formation of new neuroblasts at the SVZ¹⁰⁵.

5.3. Choroid plexus transcriptome analysis in key milestones of development

As mentioned before in section 1.6 another objective of this work intended to analyze the CP transcriptome in key developmental stages to ascertain its temporal changes and posteriorly correlate this changes with developmental changes known to occur in the SVZ cellular composition. For this, we extracted RNA from rat CPs at several ages (P1, P4, P7, P10, P60) and sequenced it by RNA-Seq. Quality control analysis, presented in section 4.3, revealed that both, extracted RNA, cDNA library and sequencing data presented a good quality that allows us to proceed with the bioinformatics analysis of the sequencing data. At the end of this thesis the bioinformatic analysis was not concluded, but we will further discuss the potential outcome of this experiment in section 6.

6. Conclusion and future perspectives

The CP has been increasingly recognized over the past years as a key modulator of neurogenesis both during embryonic development¹³ as well as in adulthood¹⁶. Since it acts as the principal modulator of CSF composition and the NSCs from embryonic SVZ and aSVZ project their apical processes into the lateral ventricles, we can speculate that the CP transcriptome/secretome provide a milieu of molecules that might have an impact in the SVZ⁸².

The low number of studies that correlate the effects of CPs derived factors in the SVZ lead us to investigate the putative effect of two CP derived proteins in this neurogenic niche: AREG and IGFBP2. The results presented here indicate that AREG affects cell proliferation, since exposure to this protein resulted in increased proliferation accompanied by an increase in the number of cells reentering the cell cycle. Moreover, upon exposure to AREG the number of newborn neuroblasts was increased.

Concerning IGFBP2 effects, our results indicate that it increases proliferation rate as well as the number of cells reentering the cell cycle. Furthermore, when we evaluated the number of new immature neurons we observed a significant increase in cells under the signaling of IGFBP2. Altogether, the data presented herein adds new players that must be considered in the modulation of neurogenesis in the SVZ neurogenic niche.

Although we were able to provide the first insights onto the role of these proteins in the SVZ neurogenic niche further work is required which we will next explore.

Considering the increase in cell proliferation and in the number of newborn neuroblasts, it would be interesting to assess if the exposure to the proteins affect other cell types of the SVZ, using, for example, GFAP as a marker for type B cells, and Mash1 or Dlx2 for type C cells⁴⁰. Additionally, to determine if the proteins can have a specific impact in each cell type of the SVZ, we should perform cell culture of FACS-sorted cells, which enables to distinguish quiescent NSC, activated NSCs, TAPs and neuroblasts and thus pinpoint the exact impact of the proteins in the different cells⁵⁴. Furthermore, taking into account the alterations observed in the cell cycle index, a more detailed analysis using flow cytometry would allow us to determine if the observed results are affecting a specific phase of the cell cycle¹⁰⁶. Finally, considering the results observed in the number of new immature neurons it would be worthy to explore the effects of a long-term exposure to the proteins in the formation and maturation of new neurons at the OBs. Since we tested three different protein concentrations and not all produced an effect, it would be interesting as a future perspective, to determine the protein levels in the CSF in physiological conditions. Moreover, to determine if the level of these proteins is affected under pathological conditions we should also measure

AREG and IGFBP2 levels at the CSF in the context of neurodegenerative diseases and inflammatory diseases.

Furthermore, to properly study the impact of these CP-derived proteins it would be of great interest to alter its expression only in the CP. Using a viral vector that specifically targets CP-epithelial cells we could perform overexpression of the proteins and evaluate the effects of these expression not only at the level of the SVZ but also in the OBs^{107,108}. Moreover, to further dissect the effects of these proteins we could also perform an inhibition of proteins secretion, either using shRNA^{109,110} or performing a targeted deletion using CRISPR technique¹¹¹.

Further dissecting, with the tools described above, the role of CP-derived proteins, such as AREG and IGFBP2 is also important since the dynamic of SVZ neurogenic niche is highly susceptible to alterations caused by challenging conditions, such as under pathological conditions like Alzheimer and Parkinson diseases, that have been reported to cause decrease of cell proliferation and reduced neurogenesis¹¹². One other example are the alterations in the CP transcriptome caused by aging, that result in reduced proliferation of NSCs⁶⁵. So, taking this into account, modulation of the SVZ presents a potential source of endogenous therapies to severe alterations in the CNS¹¹². Thus, after further dissection of the role of AREG and IGFBP2 in physiological conditions, it would be of great interest to study the impact of these proteins in disease models reported to cause alterations in the SVZ.

As discussed before in section 1.3, an alteration in the cellular phenotype of the SVZ between P0 and P6; it corresponds to the arise of NSCs (type B) and the disappearance of RGCs. The mechanisms involved in this shift are largely unknown. Therefore, as an additional objective of this work we intended to analyze the CP transcriptome at ages that target this structural shift and identify possible temporal changes in the transcriptome that might influence the alterations observed at the SVZ. By identifying the factors that suffer this (hypothetical) temporal alterations we could then explore if altering their expression by the CPs would affect the changes that take place in the SVZ at these ages. In support of our hypothesis, that alterations in the CPs transcriptome affect cell dynamics at the SVZ, a study reported that cortical cultures presented changes in the proliferation rate when exposed to CSF from E19 compared to CSF from E18 or E21⁶⁶. Moreover, rat neurospheres proliferated differently when cultured with E17 or E14, P6 and adult CSF¹⁵. Additionally, a recent study, reported that injection of “old” CSF in the ventricles of young mice

causes impairments at the SVZ⁶⁵. Together, this evidences indicate the need for studies that instead of targeting single molecules, provide evidences of the global effect that alterations in CPs transcriptome might have in the SVZ. With our approach, we expect to add some insights on how the signaling provided by the CP-derived molecules affect a specific developmental stage (Figure 26).

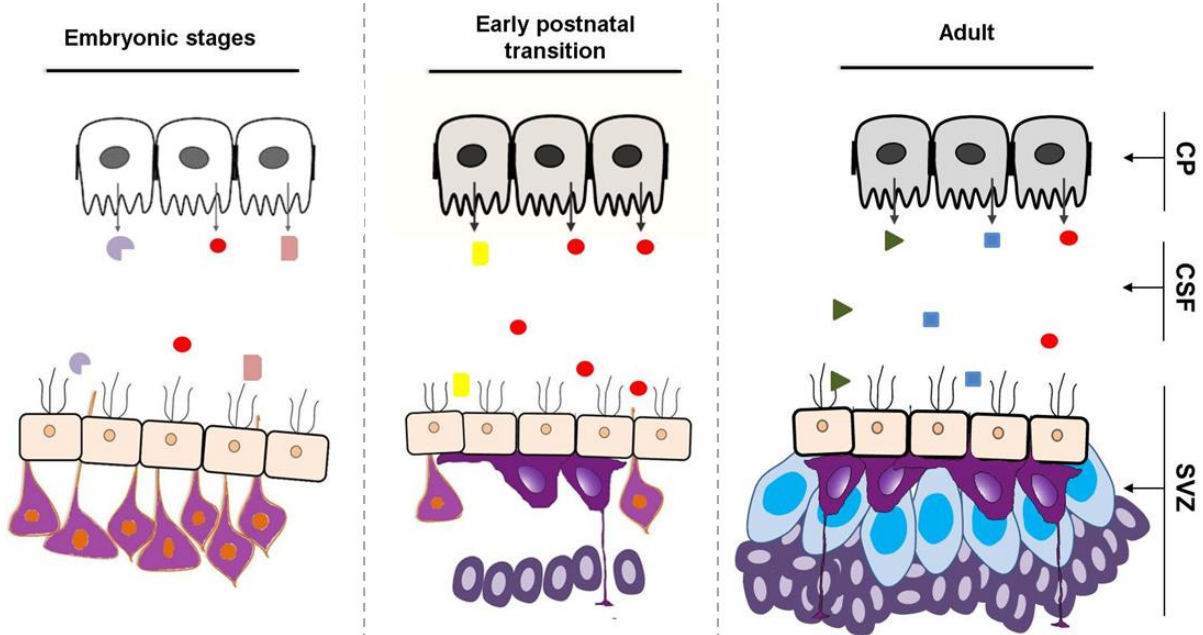


Figure 26: Representation of hypothetical temporal alterations of the CPs transcriptome and its effects in the SVZ cellular dynamics.

7. References

- 1 Ramon & Cajal, S., Degeneration and regeneration of the nervous system. *Oxford University Press*, (1913).
- 2 Allen, E., The cessation of the mitosis in the central nervous system of the albino rat. *Journal of Comparative Neurology*, **22**, 547-568, (1912).
- 3 Messier, B., Leblond, C. P. & Smart, I., Presence of DNA synthesis and mitosis in the brain of young adult mice. *Experimental Cell Research*, **14**, 224-226, (1958).
- 4 Ming, G.-L. & Song, H., Adult neurogenesis in the mammalian central nervous system. *Annual Review of Neuroscience*, **28**, 223-250, (2005).
- 5 Bond, A. M., Ming, G.-L. & Song, H., Adult mammalian neural stem cells and neurogenesis: Five decades later. *Cell Stem Cell*, **17**, 385-395, (2015).
- 6 Kazanis, I., Lathia, J., Moss, L. & French-Constant, C., The neural stem cell microenvironment, in *Stembook*, Harvard Stem Cell Institute
- 7 Pontious, A., Kowalczyk, T., Englund, C. & Hevner, R. F., Role of intermediate progenitor cells in cerebral cortex development. *Developmental neuroscience*, **30**, 24-32, (2008).
- 8 Bjornsson, C. S., Apostolopoulou, M., Tian, Y. & Temple, S., It takes a village: Constructing the neurogenic niche. *Developmental Cell*, **32**, 435-446, (2015).
- 9 Götz, M. & Huttner, W. B., The cell biology of neurogenesis. *Nature reviews. Molecular cell biology*, **6**, 777-788, (2005).
- 10 Paridaen, J. & Huttner, W. B., Neurogenesis during development of the vertebrate central nervous system. *EMBO reports*, **15**, 351-364, (2014).
- 11 Hatakeyama, J. *et al.*, Hes genes regulate size, shape and histogenesis of the nervous system by control of the timing of neural stem cell differentiation. *Development*, **131**, 5539-5550, (2004).
- 12 Sahara, S. & O'leary, D. D. M., Fgf10 regulates transition period of cortical stem cell differentiation to radial glia controlling generation of neurons and basal progenitors. *Neuron*, **63**, 48-62, (2009).
- 13 Johansson, P. A., The choroid plexuses and their impact on developmental neurogenesis. *Frontiers in neuroscience*, **8**, 340, (2014).
- 14 Johansson, P. A. *et al.*, The transcription factor otx2 regulates choroid plexus development and function. *Development*, **140**, 1055-1066, (2013).
- 15 Lehtinen, M. K. *et al.*, The cerebrospinal fluid provides a proliferative niche for neural progenitor cells. *Neuron*, **69**, 893-905, (2011).

- 16 Falcão, A. *et al.*, The path from the choroid plexus to the subventricular zone: Go with the flow! *Frontiers in Cellular Neuroscience*, **6**, 34, (2012).
- 17 Lehtinen, M. K. & Walsh, C. A., Neurogenesis at the brain-cerebrospinal fluid interface. *Annual review of cell and developmental biology*, **27**, 653-679, (2011).
- 18 Higginbotham, H. *et al.*, Arl13b-regulated cilia activities are essential for polarized radial glial scaffold formation. *Nature Neuroscience*, **16**, 1000-1007, (2013).
- 19 Tsunekawa, Y. *et al.*, Cyclin Dd2 in the basal process of neural progenitors is linked to non-equivalent cell fates. *The EMBO Journal*, **31**, 1879-1892, (2012).
- 20 Taverna, E., Götz, M. & Huttner, W. B., The cell biology of neurogenesis: Toward an understanding of the development and evolution of the neocortex. *Annual Review of Cell and Developmental Biology*, **30**, 1-38, (2014).
- 21 Gaiano, N. & Fishell, G., The role of Notch in promoting glial and neural stem cell fates. *Annual Review of Neuroscience*, **25**, 471-490, (2002).
- 22 Silva, A. O., Ercole, C. E. & Mclooney, S. C., Regulation of ganglion cell production by notch signaling during retinal development. *Journal of Neurobiology*, **54**, 511-524, (2003).
- 23 Gaiano, N., Nye, J. S. & Fishell, G., Radial glial identity is promoted by Notch1 signaling in the murine forebrain. *Neuron*, **26**, 395-404, (2000).
- 24 Kriegstein, A. & Alvarez-Buylla, A., The glial nature of embryonic and adult neural stem cells. *Annual Review of Neuroscience*, **32**, 149-184, (2009).
- 25 Noctor, S. C., Martínez-Cerdeño, V., Ivic, L. & Kriegstein, A. R., Cortical neurons arise in symmetric and asymmetric division zones and migrate through specific phases. *Nature Neuroscience*, **7**, 136-144, (2004).
- 26 Florio, M. & Huttner, W. B., Neural progenitors, neurogenesis and the evolution of the neocortex. *Development*, **141**, 2182-2194, (2014).
- 27 Anthony, T. E., Klein, C., Fishell, G. & Heintz, N., Radial glia serve as neuronal progenitors in all regions of the central nervous system. *Neuron*, **41**, 881-890, (2004).
- 28 Li, W., Cogswell, C. A. & Loturco, J. J., Neuronal differentiation of precursors in the neocortical ventricular zone is triggered by BMP. *The Journal of Neuroscience*, **18**, 8853-8862, (1998).
- 29 Segkilia, A. *et al.*, BMP7 regulates the survival, proliferation, and neurogenic properties of neural progenitor cells during corticogenesis in the mouse. *PLoS ONE*, **7**, e34088, (2012).

- 30 Rash, B. G., Lim, H. D., Breunig, J. J. & Vaccarino, F. M., FGF signaling expands embryonic cortical surface area by regulating notch-dependent neurogenesis. *The Journal of Neuroscience*, **31**, 15604-15617, (2011).
- 31 Raballo, R. *et al.*, Basic fibroblast growth factor (FGF2) is necessary for cell proliferation and neurogenesis in the developing cerebral cortex. *The Journal of Neuroscience*, **20**, 5012-5023, (2000).
- 32 Shimojo, H., Ohtsuka, T. & Kageyama, R., Oscillations in notch signaling regulate maintenance of neural progenitors. *Neuron*, **58**, 52-64, (2008).
- 33 Hitoshi, S. *et al.*, Notch pathway molecules are essential for the maintenance, but not the generation, of mammalian neural stem cells. *Genes & Development*, **16**, 846-858, (2002).
- 34 Ziegler, A. N., Levison, S. W. & Wood, T. L., Insulin and IGF receptor signalling in neural-stem-cell homeostasis. *Nature Reviews Endocrinology*, **11**, 161-170, (2015).
- 35 Hodge, R. D., D'ercole, J. A. & O'kusky, J. R., Insulin-like growth factor-1 accelerates the cell cycle by decreasing G1 phase length and increases cell cycle reentry in the embryonic cerebral cortex. *The Journal of Neuroscience*, **24**, 10201-10210, (2004).
- 36 Kuwahara, A. *et al.*, Wnt signaling and its downstream target n-myc regulate basal progenitors in the developing neocortex. *Development*, **137**, 1035-1044, (2010).
- 37 Munji, R. N., Choe, Y., Li, G., Siegenthaler, J. A. & Pleasure, S. J., Wnt signaling regulates neuronal differentiation of cortical intermediate progenitors. *The Journal of Neuroscience*, **31**, 1676-1687, (2011).
- 38 Dave, R. K. *et al.*, Sonic hedgehog and Notch signaling can cooperate to regulate neurogenic divisions of neocortical progenitors. *PLoS ONE*, **6**, e14680, (2011).
- 39 Huang, X. *et al.*, Transventricular delivery of sonic hedgehog is essential to cerebellar ventricular zone development. *Proceedings of the National Academy of Sciences*, **107**, 8422-8427, (2010).
- 40 Lim, D. A. & Alvarez-Buylla, A., The adult ventricular-subventricular zone (V-SVZ) and olfactory bulb (OB) neurogenesis. *Cold Spring Harbor Perspectives in Biology*, **8**, 1-33, (2016).
- 41 Merkle, F. T., Tramontin, A. D., Garcia-Verdugo, J. M. M. & Alvarez-Buylla, A., Radial glia give rise to adult neural stem cells in the subventricular zone. *Proceedings of the National Academy of Sciences of the United States of America*, **101**, 17528-17532, (2004).
- 42 Gritti, A. *et al.*, Multipotent neural stem cells reside into the rostral extension and olfactory bulb of adult rodents. *The Journal of Neuroscience*, **22**, 437-445, (2002).

- 43 Seri, B. *et al.*, Composition and organization of the SCZ: A large germinal layer containing neural stem cells in the adult mammalian brain. *Cerebral Cortex*, **16**, 104-111, (2006).
- 44 Robins, S. C. *et al.*, α -tanyocytes of the adult hypothalamic third ventricle include distinct populations of fgf-responsive neural progenitors. *Nature Communications*, **4**,1-13 (2013).
- 45 Young, K. M., Fogarty, M., Kessar, N. & Richardson, W. D., Subventricular zone stem cells are heterogeneous with respect to their embryonic origins and neurogenic fates in the adult olfactory bulb. *The Journal of Neuroscience*, **27**, 8286-8296, (2007).
- 46 Mirzadeh, Z., Merkle, F. T., Soriano-Navarro, M., Garcia-Verdugo, J. M. & Alvarez-Buylla, A., Neural stem cells confer unique pinwheel architecture to the ventricular surface in neurogenic regions of the adult brain. *Cell Stem Cell*, **3**, 265-278, (2008).
- 47 Carlen, M. *et al.*, Forebrain ependymal cells are notch-dependent and generate neuroblasts and astrocytes after stroke. *Nature Neuroscience*, **12**, 259-267, (2009).
- 48 Doetsch, F., Verdugo, J.-A. & Alvarez-Buylla, A., Cellular composition and three-dimensional organization of the subventricular germinal zone in the adult mammalian brain. *The Journal of Neuroscience*, **17**, 5046-5061, (1997).
- 49 Silva-Vargas, V., Crouch, E. E. & Doetsch, F., Adult neural stem cells and their niche: A dynamic duo during homeostasis, regeneration, and aging. *Current Opinion in Neurobiology*, **23**, 935-942, (2013).
- 50 Giachino, C. *et al.*, Molecular diversity subdivides the adult forebrain neural stem cell population. *Stem Cells*, **32**, 70-84, (2014).
- 51 Nam, H.-S. & Benezra, R., High levels of Id1 expression define B1 type adult neural stem cells. *Cell Stem Cell*, **5**, 515-526, (2009).
- 52 Beckervordersandforth, R. *et al.*, In vivo fate mapping and expression analysis reveals molecular hallmarks of prospectively isolated adult neural stem cells. *Cell Stem Cell*, **7**, 744-758, (2010).
- 53 Kokovay, E. *et al.*, Vcam1 is essential to maintain the structure of the SVZ niche and acts as an environmental sensor to regulate SVZ lineage progression. *Cell Stem Cell*, **11**, 220-230, (2012).
- 54 Codega, P. *et al.*, Prospective identification and purification of quiescent adult neural stem cells from their in vivo niche. *Neuron*, **82**, 545-559, (2014).
- 55 Doetsch, F., Petreanu, L., Caille, I., Garcia-Verdugo, J.-M. & Alvarez-Buylla, A., EGF converts transit-amplifying neurogenic precursors in the adult brain into multipotent stem cells. *Neuron*, **36**, 1021-1034, (2002).

- 56 Ming, G.-L. & Song, H., Adult neurogenesis in the mammalian brain: Significant answers and significant questions. *Neuron*, **70**, 687-702, (2011).
- 57 Kuhn, H. G., Winkler, J., Kempermann, G., Thal, L. J. & Gage, F. H., Epidermal growth factor and fibroblast growth factor-2 have different effects on neural progenitors in the adult rat brain. *The Journal of Neuroscience*, **17**, 5820-5829, (1997).
- 58 Merkle, F. T., Mirzadeh, Z. & Alvarez-Buylla, A., Mosaic organization of neural stem cells in the adult brain. *Science*, **317**, 381-384, (2007).
- 59 Kempermann, G., Neurogenesis in the adult subventricular zone and olfactory bulb, in *Adult neurogenesis 2*, 158-184 Oxford University Press, (2011).
- 60 Kempermann, G., Regulation, in *Adult neurogenesis 2*, 327-438 Oxford University Press, (2011).
- 61 Sahay, A., Wilson, D. A. & Hen, R., Pattern separation: A common function for new neurons in hippocampus and olfactory bulb. *Neuron*, **70**, 582-588, (2011).
- 62 Zhao, C., Deng, W. & Gage, F. H., Mechanisms and functional implications of adult neurogenesis. *Cell*, **132**, 645-660, (2008).
- 63 Lun, M. P., Monuki, E. S. & Lehtinen, M. K., Development and functions of the choroid plexus-cerebrospinal fluid system. *Nature reviews, Neuroscience*, **16**, 445-457, (2015).
- 64 Liddelow, S. A. *et al.*, Modification of protein transfer across blood/cerebrospinal fluid barrier in response to altered plasma protein composition during development. *European Journal of Neuroscience*, **33**, 391-400, (2011).
- 65 Silva-Vargas, V., Maldonado-Soto, A. R., Mizrak, D., Codega, P. & Doetsch, F., Age-dependent niche signals from the choroid plexus regulate adult neural stem cells. *Cell Stem Cell*, **1**, 1-10, (2016).
- 66 Miyan, J. A., Zendah, M., Mashayekhi, F. & Owen-Lynch, P. J., Cerebrospinal fluid supports viability and proliferation of cortical cells *in vitro*, mirroring *in vivo* development. *Cerebrospinal Fluid Research*, **3**, 1-7, (2006).
- 67 Zappaterra, M. D. *et al.*, A comparative proteomic analysis of human and rat embryonic cerebrospinal fluid. *Journal of Proteome Research*, **6**, 3537-3548, (2007).
- 68 Feliciano, D. M., Zhang, S., Nasrallah, C. M., Lisgo, S. N. & Bordey, A., Embryonic cerebrospinal fluid nanovesicles carry evolutionarily conserved molecules and promote neural stem cell amplification. *PLoS ONE*, **9**, e88810, (2014).

- 69 Mairet-Coello, G., Tury, A. & Diccico-Bloom, E., Insulin-like growth factor-1 promotes G1/s cell cycle progression through bidirectional regulation of cyclins and cyclin-dependent kinase inhibitors via the phosphatidylinositol 3-kinase/AKT pathway in developing rat cerebral cortex. *The Journal of Neuroscience*, **29**, 775-788, (2009).
- 70 Martin, C. *et al.*, FGF2 plays a key role in embryonic cerebrospinal fluid trophic properties over chick embryo neuroepithelial stem cells. *Developmental Biology*, **297**, 402-416, (2006).
- 71 Marques, F. *et al.*, Transcriptome signature of the adult mouse choroid plexus. *Fluids and Barriers of the CNS*, **8**, 1-11, (2011).
- 72 Nguyen-Ba-Charvet, K. T. *et al.*, Multiple roles for slits in the control of cell migration in the rostral migratory stream. *The Journal of Neuroscience*, **24**, 1497-1506, (2004).
- 73 Falk, A. & Frisén, J., Amphiregulin is a mitogen for adult neural stem cells. *Journal of Neuroscience Research*, **69**, 757-762, (2002).
- 74 Baghbaderani, B. A. *et al.*, Bioreactor expansion of human neural precursor cells in serum-free media retains neurogenic potential. *Biotechnology and Bioengineering*, **105**, 823-833, (2010).
- 75 Coles-Takabe, B. *et al.*, Don't look: Growing clonal versus nonclonal neural stem cell colonies. *Stem Cells*, **26**, 2938-2944, (2008).
- 76 Pastrana, E., Silva-Vargas, V. & Doetsch, F., Eyes wide open: A critical review of sphere-formation as an assay for stem cells. *Cell Stem Cell*, **8**, 486-498, (2011).
- 77 Teixeira, F. G. *et al.*, Secretome of mesenchymal progenitors from the umbilical cord acts as modulator of neural/glial proliferation and differentiation. *Stem Cell Reviews and Reports*, **11**, 288-297, (2015).
- 78 Ferreira, R. *et al.*, Retinoic acid-loaded polymeric nanoparticles enhance vascular regulation of neural stem cell survival and differentiation after ischaemia. *Nanoscale*, **8**, 8126-8137, (2016).
- 79 David-Pereira, A. *et al.*, Metabotropic glutamate 5 receptor in the infralimbic cortex contributes to descending pain facilitation in healthy and arthritic animals. *Neuroscience*, **312**, 108-119, (2016).
- 80 Falcão, A. *et al.*, Topographical analysis of the subependymal zone neurogenic niche. *PLoS ONE*, **7**, e38647, (2012).
- 81 Ewels, P., Magnusson, M., Lundin, S. & Käller, M., Multiqc: Summarize analysis results for multiple tools and samples in a single report. *Bioinformatics*, (2016).

- 82 Chaker, Z., Codega, P. & Doetsch, F., A mosaic world: Puzzles revealed by adult neural stem cell heterogeneity. *Wiley Interdisciplinary Reviews: Developmental Biology*, **5**, 640-658, (2016).
- 83 Lun, M. P., Monuki, E. S. & Lehtinen, M. K., Development and functions of the choroid plexus-cerebrospinal fluid system. *Nature Reviews Neuroscience*, **16**, 445-457, (2015).
- 84 Berasain, C. & Avila, M. A., Amphiregulin. *Seminars in Cell & Developmental Biology*, **28**, 31-41, (2014).
- 85 Galvez-Contreras, A. Y., Quiñones-Hinojosa, A. & Gonzalez-Perez, O., The role of EGFR and ERBB family related proteins in the oligodendrocyte specification in germinal niches of the adult mammalian brain. *Frontiers in Cellular Neuroscience*, **7**, 258, (2013).
- 86 Booth, B. W. *et al.*, Amphiregulin mediates self-renewal in an immortal mammary epithelial cell line with stem cell characteristics. *Experimental Cell Research*, **316**, 422-432, (2010).
- 87 Piepkorn, M., Lo, C. & Plowman, G., Amphiregulin-dependent proliferation of cultured human keratinocytes: Autocrine growth, the effects of exogenous recombinant cytokine, and apparent requirement for heparin-like glycosaminoglycans. *Journal of Cellular Physiology*, **159**, 114-120, (1994).
- 88 Mahtouk, K. *et al.*, Expression of EGF-family receptors and amphiregulin in multiple myeloma. Amphiregulin is a growth factor for myeloma cells. *Oncogene*, **24**, 3512-3524, (2005).
- 89 Bernardino, L. *et al.*, Tumor necrosis factor- α modulates survival, proliferation, and neuronal differentiation in neonatal subventricular zone cell cultures. *Stem Cells*, **26**, 2361-2371, (2008).
- 90 Henriksen, L., Grandal, M., Knudsen, S., Van Deurs, B. & Grøvdal, L., Internalization mechanisms of the epidermal growth factor receptor after activation with different ligands. *PLoS ONE*, **8**, e58148, (2013).
- 91 Gómez-Gaviro, M. V. *et al.*, Betacellulin promotes cell proliferation in the neural stem cell niche and stimulates neurogenesis. *Proceedings of the National Academy of Sciences*, **109**, 1317-1322, (2012).
- 92 Chiaramello, S. *et al.*, BDNF/ TRKB interaction regulates migration of SVZ precursor cells via Pi3-K and MAP-K signalling pathways. *European Journal of Neuroscience*, **26**, 1780-1790, (2007).
- 93 Daynac, M., Morizur, L., Chicheportiche, A., Mouthon, M.-A. & Boussin, F. D., Age-related neurogenesis decline in the subventricular zone is associated with specific cell cycle regulation changes in activated neural stem cells. *Scientific Reports*, **6**, 21505, (2016).

- 94 O'keeffe, G. C. *et al.*, Dopamine-induced proliferation of adult neural precursor cells in the mammalian subventricular zone is mediated through egf. *PNAS*, **106**, 8754-8759, (2009).
- 95 De Luca, A., Maiello, M. R., D'alessio, A., Pergameno, M. & Normanno, N., The RAS/RAF/MEK/ERK and the Pi3K/AKT signalling pathways: Role in cancer pathogenesis and implications for therapeutic approaches. *Expert Opinion on Therapeutic Targets*, **16**, S17-S27, (2012).
- 96 Cargnello, M. & Roux, P. P., Activation and function of the MAPKs and their substrates, the MAPK-activated protein kinases. *Microbiology and Molecular Biology Reviews*, **75**, 50-83, (2011).
- 97 Yao, X., Sun, S., Zhou, X., Guo, W. & Zhang, L., IGF-binding protein 2 is a candidate target of therapeutic potential in cancer. *Tumour biology : the journal of the International Society for Oncodevelopmental Biology and Medicine*, **37**, 1451-1459, (2016).
- 98 Vogel, T., Insulin/igf-signalling in embryonic and adult neural proliferation and differentiation in the mammalian central nervous system, in *Trends in cell signaling pathways in neuronal fate decision*, (2013).
- 99 Huynh, H. *et al.*, IGF binding protein 2 supports the survival and cycling of hematopoietic stem cells. *Blood*, **118**, 3236-3243, (2011).
- 100 Hsieh, D., Hsieh, A., Stea, B. & Ellsworth, R., IGFBP2 promotes glioma tumor stem cell expansion and survival. *Biochemical and biophysical research communications*, **397**, 367-372, (2010).
- 101 Åberg, M. a. I., Åberg, N. D., Hedbäcker, H., Oscarsson, J. & Eriksson, P. S., Peripheral infusion of IGF-i selectively induces neurogenesis in the adult rat hippocampus. *The Journal of Neuroscience*, **20**, 2896-2903, (2000).
- 102 Lee, C., Coimmunoprecipitation assay, in *Circadian rhythms: Methods and protocols*, 401-406 Humana Press, (2007).
- 103 Schutt, B. S., Langkamp, M., Rauschnabel, U., Ranke & Elmlinger, M. W., Integrin-mediated action of insulin-like growth factor binding protein-2 in tumor cells. *Journal of molecular endocrinology*, **32**, 859-868, (2004).
- 104 Zhu, W. *et al.*, IGFBP-4 is an inhibitor of canonical wnt signalling required for cardiogenesis. *Nature*, **454**, 345-349, (2008).
- 105 Ferrón, S. R. *et al.*, Differential genomic imprinting regulates paracrine and autocrine roles of IGF2 in mouse adult neurogenesis. *Nature communications*, **6**, 8265, (2015).

- 106 Morte, M. I. *et al.*, Evaluation of proliferation of neural stem cells in vitro and in vivo, in *Current protocols in stem cell biology*, John Wiley & Sons, (2007).
- 107 Haddad, M. R., Donsante, A., Zervas, P. & Kaler, S. G., Fetal brain-directed AAV gene therapy results in rapid, robust, and persistent transduction of mouse choroid plexus epithelia. *Molecular therapy. Nucleic acids*, **2**, e101, (2013).
- 108 Regev, L., Ezrielev, E., Gershon, E., Gil, S. & Chen, A., Genetic approach for intracerebroventricular delivery. *Proceedings of the National Academy of Sciences*, **107**, 4424-4429, (2010).
- 109 Taxman, D. J., Moore, C. B., Guthrie, E. H. & Huang, M. T.-H., Short hairpin rna (shRNA): Design, delivery, and assessment of gene knockdown, in *RNA therapeutics: Function, design, and delivery*, 139-156 Humana Press, (2010).
- 110 Carro, E., Spuch, C., Trejo, J. L., Antequera, D. & Torres-Aleman, I., Choroid plexus megalin is involved in neuroprotection by serum insulin-like growth factor i. *Journal of Neuroscience*, **25**, 10884-10893, (2005).
- 111 Ran, F. A. *et al.*, Genome engineering using the CRISPR-CAS9 system. *Nature Protocols*, **8**, 2281-2308, (2013).
- 112 Winner, B., Kohl, Z. & Gage, F. H., Neurodegenerative disease and adult neurogenesis. *The European journal of neuroscience*, **33**, 1139-1151, (2011).

8. Supplementary information

Table S 1: Post hoc test for the statistical analysis of clonal assay with AREG

Group		Mean difference	SEM	Sig.	
Ctrl	25ng/mL	-41.667	4.790	0.000	****
	100ng/mL	-55.00	4.790	0.000	****
	200ng/mL	-50.333	4.790	0.000	****
25ng/mL	Ctrl	-41.667	4.790	0.000	****
	100ng/mL	-12.333	4.790	0.197	
	200ng/mL	-8.667	4.790	0.648	
100ng/mL	Ctrl	54.000	4.790	0.000	****
	25ng/mL	12.333	4.790	0.197	
	200ng/mL	3.667	4.790	1.000	
200ng/mL	Ctrl	50.333	4.790	0.000	****
	25ng/mL	8.667	4.790	0.648	
	100ng/mL	-3.667	4.790	1.000	

Table S 2: Post hoc test for the statistical analysis of differentiation assay with AREG.

		Group	Mean difference	SEM	Sig.	
BrdU ⁺ cells	Ctrl	25ng/mL	-0.067	0.006	0.000	****
		100ng/mL	-0.057	0.006	0.000	****
		200ng/mL	-0.004	0.006	10.000	
	25ng/mL	Ctrl	0.067	0.006	0.000	****
		100ng/mL	0.010	0.006	0.875	
		200ng/mL	0.062	0.006	0.000	****
	100ng/mL	Ctrl	0.057	0.006	0.000	****
		25ng/mL	-0.010	0.006	0.875	
		200ng/mL	0.053	0.006	0.000	****
	200ng/mL	Ctrl	0.004	0.006	1.000	
		25ng/mL	-0.062	0.006	0.000	****
		100ng/mL	-0.053	0.006	0.000	****
β III-Tubulin ⁺ BrdU ⁺ cells	Ctrl	25ng/mL	-0.016	0.003	0.008	**
		100ng/mL	-0.011	0.003	0.056	
		200ng/mL	0.000	0.003	1.000	
	25ng/mL	Ctrl	0.016	0.003	0.008	**
		100ng/mL	0.005	0.003	1.000	
		200ng/mL	0.016	0.003	0.009	**
	100ng/mL	Ctrl	0.011	0.003	0.056	
		25ng/mL	-0.005	0.003	1.000	
		200ng/mL	0.011	0.003	0.067	
	200ng/mL	Ctrl	0.000	0.003	1.000	
		25ng/mL	-0.016	0.003	0.009	
		100ng/mL	-0.011	0.003	0.067	

Table S 3: Post hoc tests for the Statistical analysis of BrdU⁺ cells in the subventricular zone of animals injected with AREG.

	Group	Mean difference	SEM	Sig.		
RMS	Ctrl	25ng/mL	-306.757	358.572	1.000	
		100ng/mL	-194.361	358.572	1.000	
		200ng/mL	-1451.329	358.572	0.006	**
	25ng/mL	Ctrl	306.757	358.572	1.000	
		100ng/mL	112.395	358.572	1.000	
		200ng/mL	-1144.572	358.572	0.034	*
	100ng/mL	Ctrl	194.361	358.572	1.000	
		25ng/mL	-112.395	358.572	1.000	
		200ng/mL	-1256.968	358.572	0.018	*
	200ng/mL	Ctrl	1451.329	358.572	0.006	**
		25ng/mL	1144.572	358.572	0.034	*
		100ng/mL	1256.968	358.572	0.018	*
Dorsolateral	Ctrl	25ng/mL	-330.108	404.477	1.000	
		100ng/mL	-328.481	404.477	1.000	
		200ng/mL	-3675.884	404.477	0.000	****
	25ng/mL	Ctrl	330.108	404.477	1.000	
		100ng/mL	1.627	404.477	1.000	
		200ng/mL	-3345.776	404.477	0.000	****
	100ng/mL	Ctrl	328.481	404.477	1.000	
		25ng/mL	-1.627	404.477	1.000	
		200ng/mL	-3347.403	404.477	0.000	****
	200ng/mL	Ctrl	3675.884	404.477	0.000	****
		25ng/mL	3345.776	404.477	0.000	****
		100ng/mL	3347.403	404.477	0.000	****
Ventral	Ctrl	25ng/mL	-295.377	372.681	1.000	
		100ng/mL	155.970	372.681	1.000	
		200ng/mL	-2132.264	372.681	0.000	****
	25ng/mL	Ctrl	295.377	372.681	1.000	
		100ng/mL	451.347	372.681	1.000	
		200ng/mL	-1836.886	372.681	0.001	**
	100ng/mL	Ctrl	-155.970	372.681	1.000	
		25ng/mL	-451.347	372.681	1.000	
		200ng/mL	-2288.234	372.681	0.000	****
	200ng/mL	Ctrl	2132.264	372.681	0.000	****
		25ng/mL	1836.886	372.681	0.001	**
		100ng/mL	2288.234	372.681	0.000	****

Table S 4: Post hoc tests for the Statistical analysis of DCX⁺BrdU⁺ cells in the subventricular zone of animals injected with AREG.

	Group	Mean difference	SEM	Sig.		
RMS	Ctrl	25ng/mL	78.851	95.361	1.000	
		100ng/mL	68.295	95.361	1.000	
		200ng/mL	-83.277	95.361	1.000	
	25ng/mL	Ctrl	-78.851	95.361	1.000	
		100ng/mL	-10.556	95.361	1.000	
		200ng/mL	-162.128	95.361	0.651	
	100ng/mL	Ctrl	-68.295	95.361	1.000	
		25ng/mL	10.556	95.361	1.000	
		200ng/mL	-151.572	95.361	0.789	
	200ng/mL	Ctrl	83.277	95.361	1.000	
		25ng/mL	162.128	95.361	0.651	
		100ng/mL	151.572	95.361	0.789	
Dorsolateral	Ctrl	25ng/mL	129.603	147.884	1.000	
		100ng/mL	68.097	147.884	1.000	
		200ng/mL	-926.101	147.884	0.000	
	25ng/mL	Ctrl	-129.603	147.884	1.000	
		100ng/mL	-61.506	147.884	1.000	
		200ng/mL	1055.704	147.884	0.000	****
	100ng/mL	Ctrl	-68.097	147.884	1.000	
		25ng/mL	61.506	147.884	1.000	
		200ng/mL	-994.198	147.884	0.000	****
	200ng/mL	Ctrl	926.101	147.884	0.000	****
		25ng/mL	1055.704	147.884	0.000	****
		100ng/mL	994.198	147.884	0.000	****
Ventral	Ctrl	25ng/mL	56.327	71.843	1.000	
		100ng/mL	66.467	71.843	1.000	
		200ng/mL	-243.832	71.843	0.022	*
	25ng/mL	Ctrl	-56.327	71.843	1.000	
		100ng/mL	10.140	71.843	1.000	
		200ng/mL	-300.159	71.843	0.004	**
	100ng/mL	Ctrl	-66.467	71.843	1.000	
		25ng/mL	-10.140	71.843	1.000	
		200ng/mL	-310.299	71.843	0.003	**
	200ng/mL	Ctrl	243.832	71.843	0.022	*
		25ng/mL	300.159	71.843	0.004	**
		100ng/mL	310.299	71.843	0.003	**

Table S 5: Post hoc test for the statistical analysis of clonal assay with IGFBP2.

Group		Mean difference	SEM	Sig.	
Ctrl	25ng/mL	-7.333	3.551	0.437	
	100ng/mL	-23.333	3.551	0.001	**
	200ng/mL	-27.667	3.551	0.000	****
25ng/mL	Ctrl	7.333	3.551	0.437	
	100ng/mL	-16.00	3.551	0.012	*
	200ng/mL	-20.333	3.551	0.003	**
100ng/mL	Ctrl	23.333	3.551	0.001	**
	25ng/mL	16.000	3.551	0.012	*
	200ng/mL	-4.333	3.551	1.000	
200ng/mL	Ctrl	27.667	3.551	0.000	****
	25ng/mL	20.333	3.551	0.003	**
	100ng/mL	4.333	3.551	1.000	

Table S 6: Post hoc test for the statistical analysis of differentiation assay with IGFBP2.

		Group	Mean difference	SEM	Sig.	
BrdU ⁺ cells	Ctrl	25ng/mL	-0.017	0.014	1.000	
		100ng/mL	-0.086	0.014	0.002	**
		200ng/mL	-0.129	0.014	0.000	****
	25ng/mL	Ctrl	0.017	0.014	1.000	
		100ng/mL	-0.069	0.014	0.007	**
		200ng/mL	-0.112	0.014	0.000	****
	100ng/mL	Ctrl	0.086	0.014	0.002	**
		25ng/mL	0.069	0.014	0.007	**
		200ng/mL	-0.043	0.014	0.097	
	200ng/mL	Ctrl	0.129	0.014	0.000	****
		25ng/mL	0.112	0.014	0.000	****
		100ng/mL	0.043	0.014	0.097	
βIII-Tubulin ⁺ BrdU ⁺ cells	Ctrl	25ng/mL	-0.007	0.005	0.952	
		100ng/mL	-0.030	0.005	0.001	**
		200ng/mL	-0.051	0.005	0.000	****
	25ng/mL	Ctrl	0.007	0.005	0.952	
		100ng/mL	-0.022	0.005	0.009	**
		200ng/mL	-0.044	0.005	0.000	****
	100ng/mL	Ctrl	0.030	0.005	0.001	**
		25ng/mL	0.022	0.005	0.009	**
		200ng/mL	-0.022	0.005	0.012	*
	200ng/mL	Ctrl	0.051	0.005	0.000	****
		25ng/mL	0.044	0.005	0.000	****
		100ng/mL	0.022	0.005	0.012	*

Table S 7: Post hoc tests for the Statistical analysis of BrdU⁺ cells in the subventricular zone of animals injected with IGFBP2.

	Group	Mean difference	SEM	Sig.		
RMS	Ctrl	25ng/mL	-355.732	3420.153	1.000	
		100ng/mL	-842.733	3420.153	0.153	
		200ng/mL	-882.973	3420.153	0.121	
	25ng/mL	Ctrl	355.732	3420.153	1.000	
		100ng/mL	-487.001	3420.153	1.000	
		200ng/mL	-527.241	3420.153	0.857	
	100ng/mL	Ctrl	842.733	3420.153	0.153	
		25ng/mL	487.001	3420.153	1.000	
		200ng/mL	-40.240	3420.153	1.000	
	200ng/mL	Ctrl	882.973	3420.153	0.121	
		25ng/mL	527.241	3420.153	0.857	
		100ng/mL	40.240	3420.153	1.000	
Dorsolateral	Ctrl	25ng/mL	-987.478	6190.357	0.782	
		100ng/mL	-3117.749	6190.357	0.001	**
		200ng/mL	-3630.443	6190.357	0.000	****
	25ng/mL	Ctrl	987.478	6190.357	0.782	
		100ng/mL	-2130.270	6190.357	0.020	*
		200ng/mL	-2642.964	6190.357	0.004	**
	100ng/mL	Ctrl	3117.749	6190.357	0.001	**
		25ng/mL	2130.270	6190.357	0.020	*
		200ng/mL	-512.694	6190.357	1.000	
	200ng/mL	Ctrl	3630.443	6190.357	0.000	****
		25ng/mL	2642.964	6190.357	0.004	**
		100ng/mL	512.694	6190.357	1.000	
Ventral	Ctrl	25ng/mL	-643.133	4530.873	1.000	
		100ng/mL	-1160.694	4530.873	0.127	
		200ng/mL	-1453.035	4530.873	0.033	*
	25ng/mL	Ctrl	643.133	4530.873	1.000	
		100ng/mL	-517.561	4530.873	1.000	
		200ng/mL	-809.902	4530.873	0.560	
	100ng/mL	Ctrl	1160.694	4530.873	0.127	
		25ng/mL	517.561	4530.873	1.000	
		200ng/mL	-292.341	4530.873	1.000	
	200ng/mL	Ctrl	1453.035	4530.873	0.033	*
		25ng/mL	809.902	4530.873	0.560	
		100ng/mL	292.341	4530.873	1.000	

Table S 8: Post hoc tests for the Statistical analysis of DCX⁺BrdU⁺ cells in the subventricular zone of animals injected with IGFBP2.

	Group	Mean difference	SEM	Sig.		
RMS	Ctrl	25ng/mL	-228.404	96.368	0.184	
		100ng/mL	-275.001	96.368	0.069	
		200ng/mL	-253.744	96.368	0.108	
	25ng/mL	Ctrl	228.404	96.368	0.184	
		100ng/mL	-46.596	96.368	1.000	
		200ng/mL	-25.339	96.368	1.000	
	100ng/mL	Ctrl	275.001	96.368	0.069	
		25ng/mL	46.596	96.368	1.000	
		200ng/mL	21.257	96.368	1.000	
	200ng/mL	Ctrl	253.744	96.368	0.108	
		25ng/mL	25.339	96.368	1.000	
		100ng/mL	-21.257	96.368	1.000	
Dorsolateral	Ctrl	25ng/mL	-621.950	215.201	0.064	
		100ng/mL	-925.246	215.201	0.003	**
		200ng/mL	-1668.188	215.201	0.000	****
	25ng/mL	Ctrl	621.950	215.201	0.064	
		100ng/mL	-303.296	215.201	1.000	
		200ng/mL	-1046.238	215.201	0.001	**
	100ng/mL	Ctrl	925.246	215.201	0.003	**
		25ng/mL	303.296	215.201	1.000	
		200ng/mL	-742.942	215.201	0.020	*
	200ng/mL	Ctrl	1668.188	215.201	0.000	****
		25ng/mL	1046.238	215.201	0.001	**
		100ng/mL	742.942	215.201	0.020	*
Ventral	Ctrl	25ng/mL	-371.809	143.998	0.120	
		100ng/mL	-324.224	143.998	0.233	
		200ng/mL	-442.379	143.998	0.044	*
	25ng/mL	Ctrl	371.809	143.998	0.120	
		100ng/mL	47.586	143.998	1.000	
		200ng/mL	-70.569	143.998	1.000	
	100ng/mL	Ctrl	324.224	143.998	0.233	
		25ng/mL	-47.586	143.998	1.000	
		200ng/mL	-118.155	143.998	1.000	
	200ng/mL	Ctrl	442.379	143.998	0.044	*
		25ng/mL	70.569	143.998	1.000	
		100ng/mL	118.155	143.998	1.000	